



UNIL | Université de Lausanne

Unicentre

CH-1015 Lausanne

<http://serval.unil.ch>

Year : 2018

The sleep-wake distribution contributes to clock gene expression: a descriptive and a mechanistic study in mice

Hoekstra Marieke

Hoekstra Marieke, 2018, The sleep-wake distribution contributes to clock gene expression: a descriptive and a mechanistic study in mice

Originally published at : Thesis, University of Lausanne

Posted at the University of Lausanne Open Archive <http://serval.unil.ch>

Document URN : urn:nbn:ch:serval-BIB_2FFBC89A3D007

Droits d'auteur

L'Université de Lausanne attire expressément l'attention des utilisateurs sur le fait que tous les documents publiés dans l'Archive SERVAL sont protégés par le droit d'auteur, conformément à la loi fédérale sur le droit d'auteur et les droits voisins (LDA). A ce titre, il est indispensable d'obtenir le consentement préalable de l'auteur et/ou de l'éditeur avant toute utilisation d'une oeuvre ou d'une partie d'une oeuvre ne relevant pas d'une utilisation à des fins personnelles au sens de la LDA (art. 19, al. 1 lettre a). A défaut, tout contrevenant s'expose aux sanctions prévues par cette loi. Nous déclinons toute responsabilité en la matière.

Copyright

The University of Lausanne expressly draws the attention of users to the fact that all documents published in the SERVAL Archive are protected by copyright in accordance with federal law on copyright and similar rights (LDA). Accordingly it is indispensable to obtain prior consent from the author and/or publisher before any use of a work or part of a work for purposes other than personal use within the meaning of LDA (art. 19, para. 1 letter a). Failure to do so will expose offenders to the sanctions laid down by this law. We accept no liability in this respect.



UNIL | Université de Lausanne

Faculté de biologie
et de médecine

Département de Centre Intégré de Génomique

**THE SLEEP-WAKE DISTRIBUTION CONTRIBUTES
TO CLOCK GENE EXPRESSION:
A DESCRIPTIVE AND A MECHANISTIC STUDY IN MICE**

Thèse de doctorat en Neurosciences

présentée à la
Faculté de Biologie et de Médecine
de l'Université de Lausanne
par

Marieke Hoekstra

Master en Neurosciences, l'Université de Groningen, Les Pays-Bas

Jury

Prof. Simon Archer, Expert
Prof. Paul Franken, Directeur
Prof. Jean-Pierre Hornung, Président
Prof. Markus Schmidt, Expert

Thèse n° 235

Lausanne 2018

*Programme doctoral interuniversitaire en Neurosciences des
Universités de Lausanne et Genève*



**UNIVERSITÉ
DE GENÈVE**



Imprimatur

Vu le rapport présenté par le jury d'examen, composé de

Président·e Monsieur Prof. Jean-Pierre **Hornung**
Directeur·trice de thèse Monsieur Prof. Paul **Franken**
Expert·e·s Monsieur Prof. Simon **Archer**
Monsieur Prof. Markus **Schmidt**

le Conseil de Faculté autorise l'impression de la thèse de
Madame Marieke Hoekstra

Master of Neuroscience, University of Groningen, Netherlands

intitulée

**The sleep-wake distribution contributes to
clock gene expression :
a descriptive and a mechanistic study**

Lausanne, le 5 octobre 2018


pour Le Doyen
de la Faculté de Biologie et de Médecine

Prof. Jean-Pierre Hornung

Table of Contents

OUTLINE	7
ACKNOWLEDGEMENTS	9
ABSTRACT	11
RÉSUMÉ	13
CHAPTER 1 CIRCADIAN AND SLEEP HOMEOSTATIC PROCESSES ORCHESTRATE THE NYCTHEMERAL SLEEP-WAKE DISTRIBUTION.....	15
ON THE STUDY, FUNCTION AND REGULATION OF SLEEP	15
CIRCADIAN RHYTHMS: FROM MOLECULAR TO OVERT BEHAVIOR	21
PROCESS S AND PROCESS C: INTERACTING PROCESSES.....	27
CHAPTER 2 THE CONTRIBUTION OF SLEEP-WAKE STATE TO PER2 BIOLUMINESCENCE IN UN-ANAESTHETIZED MICE	33
SUMMARY AND CONTRIBUTIONS	34
ABSTRACT.....	36
INTRODUCTION.....	36
RESULTS	37
DISCUSSION	49
MATERIAL AND METHODS.....	54
SUPPLEMENTARY DATA	59
CHAPTER 3 COLD INDUCIBLE RNA BINDING PROTEINS: REGULATIONS AND FUNCTIONS.....	69
CHAPTER 4 COLD-INDUCIBLE RNA-BINDING PROTEIN (CIRBP) ADJUSTS CORTICAL CLOCK GENE EXPRESSION AND REM SLEEP RECOVERY FOLLOWING SLEEP DEPRIVATION IN MICE	77
SUMMARY AND CONTRIBUTIONS	78
INTRODUCTION.....	80
RESULTS	82
DISCUSSION	99
MATERIAL AND METHODS.....	106
CHAPTER 5 GENERAL DISCUSSION	119
REFERENCES.....	129

Outline

In this thesis, I have i) investigated the influence of the sleep-wake distribution on the expression of a clock gene, period-2 and ii) explored a possible mechanism that accounts for the sleep-driven changes in clock gene expression. In Chapter 1, a brief literature overview on sleep regulation, function and homeostasis and on circadian rhythms is provided, after which the interaction between these two processes with a focus on clock genes is discussed. In Chapter 2, you will read that changes in spontaneous sleep-wake state contribute to PER2, as quantified by bioluminescence. Furthermore, imposing a sleep deprivation protocol that reduces the circadian amplitude of the sleep-wake distribution also affects PER2 bioluminescence levels in the majority of the mice measured. Chapter 3 introduces Cold Inducible RNA Binding Protein (CIRBP) and its functions. This is to provide extra background information for Chapter 4, where I have investigated if this protein conveys the sleep deprivation induced changes in clock gene expression. CIRBPs presence was not required to convey all sleep-wake driven changes in clock gene expression, but it's absence modulated three out of the five clock genes quantified. In line with the role of clock genes in sleep homeostasis, *Cirbp* KO mice had impaired REM sleep homeostasis. An unexpected finding was that *Cirbp* KO mice were more active, which was accompanied by changes in neuronal oscillations. In Chapter 5, the results and implications of both projects are discussed in a larger context on sleep, circadian rhythms and science in general.

Acknowledgements

One page is too short. Having wasted space on that, I will take this opportunity to acknowledge the people that contributed to this document, either by actively contributing to the/a step(s) that shaped this document, or simply by being around.

I acknowledge Paul. Paul, bedankt voor alle tijd en energie die je in mijn opleiding tot wetenschapper hebt gestoken. Je hebt me onverwurbbaar geleerd om het belang van de details in te zien. Als ik even de weg kwijt was, was jij er om me een zetje te geven in de goede richting. Ik knijp in mijn handen dat ik niet alleen van een integere en intelligente wetenschapper heb geleerd, maar ook met een goedhartig en geestig mens heb mogen samenwerken.

Thank you for accepting my invitation for the private thesis defense: Simon Archer, Jean-Pierre Hornung and Markus Schmidt. I am looking forward to discussing my thesis with you!

Yann Emmenegger, merci beaucoup pour ton aide, ce n'était pas possible sans toi!

Precious lab members: Kostas and Jeff::thank you for the fun, bla-bla-beer-bla-beer, allowing and occasionally correcting my Dutch PFC; you turned this PhD-ride into a magical unicorn tour. And Jeff, thanks for the translation of the abstract to French!; Charlotte, for all your feedback, input and conversations on more or less science; Maxime, for your scientific input and your non-scientific company. Sonia, for not letting me discard the flow through and your apéro's. Thank you, previous lab members for making me part of the Franken lab family: Geraldine, Francesco and Shanaz. Also, I'd like to thank all people mentioned above for their help with the sleep deprivations, plus Violeta Castelo Székely, Simone Mumbauer and Lisa Härrri. Iris, thank you for all the administrative support, you're a superb secretary. Annick, thank you as well, especially for finding a place for me when I arrived in Lausanne.

I would like to thank André Liane & Pascal Gos from the University of Geneva for their availability for any questions I had regarding the RT Biolumicorder; Thomas Curie, thank you for providing me with as many details possible on your previous study, which forms the backbone of this thesis.

Ulrike Toepel thank you for providing all the necessary infrastructure around the LNDS.

I would like to acknowledge the mouse caretakers, specifically: José Luis Huaman Larios, Fabienne Junod Fontollet, Mathieu Piguët and Alain Guéniot. Also, thanks to Armelle Bauduret, Fabienne Lammers and Katharina Hausherr who performed the genotyping of the mice.

People from the CIG, thank you for providing the infra structure: Laurian Walpen: IT, Carlos Reyna, Maryle Berger and Noura Egger from the magazine and Gilles Boss for all the bricolage.

Ioannis Xenarios, sometimes knowing that there is a mentor, is enough- thank you!

My friends from Lausanne, Nederland and around: thank you for being there, theses are important but other things as well -thank you for helping me remember! Bedankt voor jullie aanwezigheid, ook al lijken dissertaties het summum, er zijn belangrijker dingen. Gelukkig helpen jullie me om dat niet te vergeten.

Mam, bedankt voor je steun en tegelijkertijd kritische blik. Pap, je bent er altijd als het nodig is, bedankt. Kwark, ik zou geen ander broertje willen (op twee dingen na, guess what :-)).

Jasper, draak maar raak voor een knaak :: mr krab? Cliché maar jij haalt het beste in me naar boven. Whatever will be next, met jou erbij wordt het partij. Bedankt voor alles, maar in deze specifieke context vooral voor je ongelooflijke relativeringsvermogen. Ik kan er nog veel van leren.

Finally, I would like to acknowledge Alexandra Elbakyan, the founder of Sci-Hub, for making scientific papers accessible to everyone. It is surprising, and simultaneously disappointing, that even at the University of Lausanne, located in a rich country like Switzerland, many papers are still behind pay walls. We, as scientific community, should put more effort in changing this – or are we only publishing for the rich?

Abstract

The sleep-wake distribution (*i.e.* the duration and timing of sleep across the 24-h day) is orchestrated by the interaction of two processes: the sleep homeostat, which keeps track of time spent awake and asleep, and the circadian clock, which gates the timing of sleep. The mechanisms underlying the clock are well understood: overt rhythmic behavior in mammals is coordinated by the suprachiasmatic nucleus and at the molecular level by intertwining transcriptional-translational feedback loops of so-called clock genes, ensuring a period of ca. 24 hours. The substrate underlying the sleep homeostat is unknown, but clock genes appear implicated because: i) mutations and deletions of clock genes affect the sleep homeostat; ii) sleep deprivation (SD) impairs the binding of clock gene proteins to their target clock genes; iii) SD changes clock gene expression. In this thesis, a descriptive and a mechanistic study are presented to inspect more closely the sleep-wake distributions' contribution to clock gene expression. The descriptive study made use of a mouse model where bioluminescence is measured as a proxy for period-2 (PER2) protein levels, combined with electroencephalogram (EEG) recordings to determine sleep-wake state. Under undisturbed conditions, PER2 bioluminescence changed as a function of sleep and wake. Twelve 2Hr SDs scheduled across two days reduced the amplitude of PER2 bioluminescence in 3 out of 4 mice. Thus, sleep-wake state contributes to PER2 bioluminescence. However, the reliability of PER2 bioluminescence as a proxy for PER2 protein levels remains to be verified. In the second study, the contribution of Cold Inducible RNA Binding Protein (CIRBP) to SD-incurred changes in clock gene expression was investigated, based on the observations that i) daily changes in cortical *Cirbp* appear mainly sleep-wake driven, possibly through cortical temperature; ii) CIRBP is necessary for high amplitude clock gene expression *in vitro*. First, we established that the sleep-wake distribution drives the changes in cortical temperature of the mouse. Second, we found that the SD induced changes in cortical *Rev-erb α* was attenuated in the absence of CIRBP, whereas the expression of *Clock* and *Per2* was amplified. Third, and based on the premise that clock genes contribute to sleep regulation, we observed that *Cirbp* KO mice loose REM sleep after SD compared to their WT littermates. Altogether, this thesis i) supports the importance of considering the sleep-wake distribution when using clock gene expression as a state variable of the clock; ii) demonstrates that CIRBP modulates the SD incurred changes in cortical clock gene expression and contributes to REM sleep recovery.

Résumé

La distribution sommeil-réveil (la durée et le rythme du sommeil) est orchestrée par l'interaction de deux processus : l'homéostat du sommeil, qui garde le temps passé dans l'éveil et sommeil, et l'horloge circadienne qui détermine le moment chaque 24 heures à s'endormir. L'horloge biologique est bien étudiée et chez les mammifères elle est sous le contrôle des noyaux suprachiasmatiques. Au niveau moléculaire, des boucles de rétroaction transcriptionnelles-traductionnelles des gènes d'horloge donnent une période d'environ 24 heures. Le substrat sous-jacent à l'homéostat du sommeil reste inconnu, mais les gènes de l'horloge semblent impliqués, notamment par i) les modèles knock-out (KO) pour les gènes d'horloge affectent l'homéostat du sommeil; ii) la privation de sommeil (SD) peut dégrader la fixation protéique des gènes d'horloge par rapport les gènes eux-mêmes; iii) la privation du sommeil peut modifier l'expression des gènes de l'horloge. Cette thèse est composée de deux parties, une étude descriptive et une étude mécaniste qui sont mise en place pour examiner la relation entre la distribution sommeil-éveil et l'expression des gènes de l'horloge. La première étude a utilisé un modèle chez la souris où la bioluminescence était utilisé comme une mesure pour le niveau protéique d'un gène d'horloge, période-2 (PER2), en conjonction avec les enregistrements électrophysiologiques du cerveau (EEG) pour déterminer les états de la vigilance (sommeil, éveil). Dans les conditions non perturbées, la bioluminescence du PER2 a changé en fonction de la présence du sommeil ou l'éveil. Les privations du sommeil de 2-heures ont diminué l'amplitude de la bioluminescence dans 75% des souris, qui implique que PER2 est affecté par l'état de la vigilance. Par contre, la fiabilité de la bioluminescence comme un mesure pour l'expression du PER2, reste à vérifier. Dans la deuxième étude, la contribution du « Cold Inducible RNA binding protein » (CIRBP) aux changements dans l'expression des gènes d'horloge induits par la privation du sommeil été investigué, basée sur les observations suivantes: i) une privation du sommeil a fortement réduit l'amplitude circadienne du *Cirbp*; ii) CIRBP est nécessaire pour l'haute amplitude de l'expression des gènes d'horloge dans les cellules entrainées par la température. Principalement, nous avons établi que la distribution sommeil-éveil entraîne les changements de la température corticale chez la souris. A l'exception du Rev-erba, les changements dans l'expression des gènes d'horloge après une privation du sommeil n'était pas dépendue du CIRBP. Ensuite, nous avons observé que les souris *Cirbp*-KO sont plus actives pendant la phase de l'obscurité qui était en accord avec les changements observé dans la composition spectrale de l'EEG pendant l'éveil actif. Par exemple, les souris KO perdent leur sommeil paradoxal (REM) après une privation du sommeil, par rapport leurs contrôles (WT). En somme, cette thèse i) soutient l'importance de la distribution sommeil-éveil lors de l'utilisation de l'expression du gène d'horloge comme variable pour l'état d'horloge même ; ii) démontre que CIRBP ne transmet pas les changements généralisés de privation de sommeil dans l'expression des gènes de l'horloge, mais contribue à la qualité de l'éveil actif pendant la phase de l'obscurité.

To Sleep

O soft embalmer of the still midnight,
Shutting, with careful fingers and benign,
Our gloom-pleas'd eyes, embower'd from the light,
Enshaded in forgetfulness divine:
O soothest Sleep! if so it please thee, close
In midst of this thine hymn my willing eyes,
Or wait the "Amen," ere thy poppy throws
Around my bed its lulling charities.
Then save me, or the passed day will shine
Upon my pillow, breeding many woes,—
Save me from curious Conscience, that still lords
Its strength for darkness, burrowing like a mole;
Turn the key deftly in the oiled wards,
And seal the hushed Casket of my Soul.

John Keats

Chapter 1 Circadian and sleep homeostatic processes orchestrate the nycthemeral sleep-wake distribution

One of the biggest mysteries in biology concerns the regulation and function of sleep. With the development of the two-process model more than thirty years ago, a theoretical framework became available to study the mechanisms underlying sleep and waking. In the following chapter, I will introduce core concepts of the biology of sleep, circadian rhythms and the interaction between these two processes.

On the study, function and regulation of sleep

Little is known about the exact functions and the underlying mechanisms regulating sleep. In this section, an overview is provided explaining how sleep is characterized, its postulated functions and quantification of sleep homeostasis.

WHAT IS SLEEP?

To study sleep, agreement must be made on what this behavioral state entails. Sleep-wake states have been observed throughout the animal kingdom, although it greatly varies between species in duration and composition (Campbell & Tobler, 1984) which might be due to different evolutionary forces (Joiner, 2016). Because this thesis is based on work in the mouse, this chapter is dedicated to knowledge obtained of sleep in mammals.

Five behavioral hallmarks are dominant throughout the literature to characterize sleep, which are: 1) stereotypic or species-specific posture, 2) inactivity, 3) increased arousal threshold and 4) state reversibility (awakening) by stimulation. The fifth key hallmark of sleep is that it is homeostatically defended (Borbely & Neuhaus, 1979), which is assumed to be one of the key characteristics of sleep.

Despite these well-defined behavioral characteristics, the current widespread methodology to determine sleep-wake state is merely based on measures of neuronal activity. In mammals, sleep-wake states correlate with differences in neuronal activity, as measured by electroencephalogram (EEG) recordings (Campbell & Tobler, 1984). In mice, three distinct behavioral states are identified based on changes in the amplitude and frequency of the EEG and EMG: waking, rapid eye movement sleep (REM), and non-REM (NREM) sleep (see Figure 1-1, including a description of the

differences between states in the legend). NREM and REM sleep cycle in an ultradian (<24 hour) rhythm, where under normal conditions NREM is followed by REM and subsequently by waking. These NREM-REM-waking cycles of mice are much shorter in length than in humans but occur more frequently and both during the light and dark phase. Therefore, mice (and many other rodent species) are referred to as polyphasic sleepers, whereas humans who have one consolidated bout of sleep of ~8hrs during their rest phase in the dark are called monophasic sleepers. Because of the latter characteristic, humans are considered diurnal whereas mice, that are polyphasic but spend overall more time asleep during the light phase, are nocturnal under laboratory conditions.

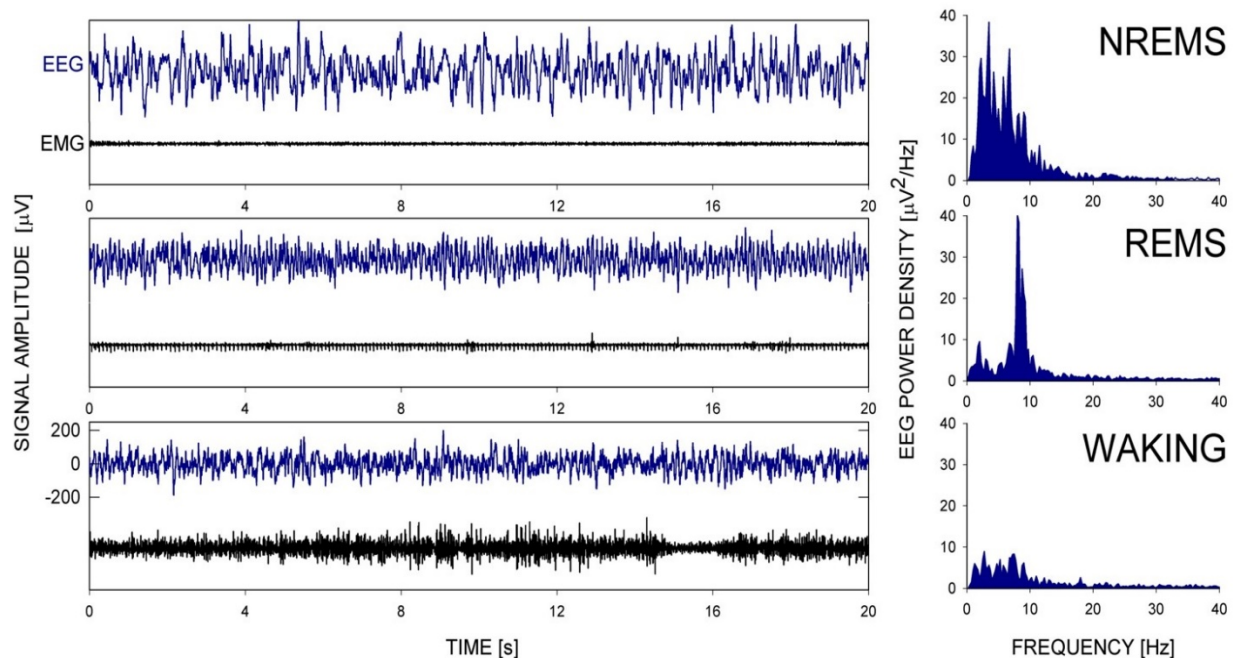


Figure 1-1 Three representative EEG and EMG traces during NREM, REM sleep and waking in a mouse (left), and spectral decomposition of the EEG signal (right). NREM sleep is defined by synchronous activity in the delta frequency (~0.5–4 Hz) and low and stable muscle tone, whereas REM sleep is characterized by regular theta oscillations (6–9 Hz) and muscle atonia with occasional twitches. Wakefulness is indicated by EEG activity of mixed frequency and low amplitude and with muscle tone that is present, but variable. Taken from (X. Xie et al., 2005).

FUNCTIONS OF SLEEP

Sleep must have an important function to make us spend 1/3 of our life in a state during which we cannot mate or forage and are very vulnerable to predators or other enemies. Therefore, perhaps one of the most interesting questions in biology attempts to answer the question “why we sleep”. A short summary of the most dominant theories is discussed.

Brain clearing

The central nervous system of mice has a glymphatic system that facilitates removal of metabolic waste products of the brain (Jessen, Munk, Lundgaard, & Nedergaard, 2015). The activity of the glymphatic system depends on sleep-wake state, with increased and decreased clearing during sleep and wake, respectively. During sleep, the interstitial fluid expands up to 60% due to shrinking of neurons, thereby draining the brain from metabolic waste products (L. Xie et al., 2013). During wakefulness, norepinephrine suppresses the activity of the glymphatic system (O'Donnell, Zeppenfeld, McConnell, Pena, & Nedergaard, 2012). Questions currently under investigation aim to address the presence of a glymphatic system in humans and the causal involvement of the glymphatic system in neurodegenerative diseases (Jessen et al., 2015) – see also Figure 1-2. This is exciting because it could provide a mechanistic link connecting the association between neurodegenerative diseases and impaired sleep.

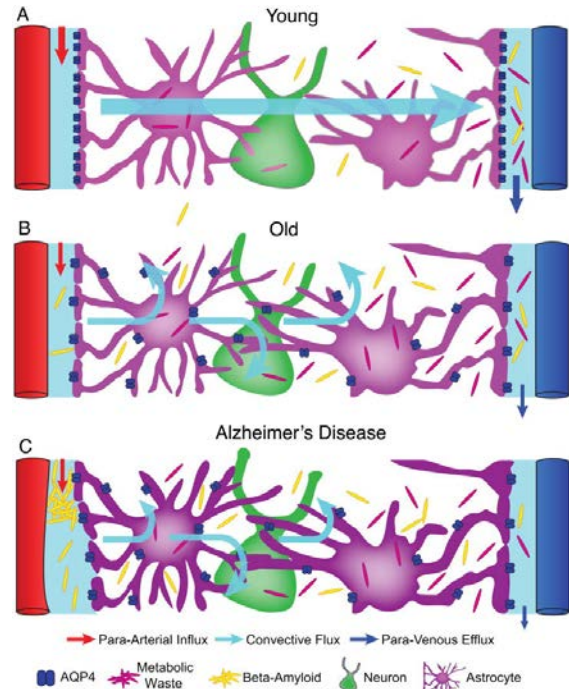


Figure 1-2 **Model for young, old and Alzheimer's disease glymphatic function.** In the young, glymphatic flux flows freely from arteries to the veins, whereas this is impaired in the elderly. In Alzheimer's disease, the reactivated astrocytes combined with protein aggregates (beta-amyloid), impair the flux further, thus reducing the metabolic waste flow. From Jessen et al., 2015.

Thermoregulatory function of sleep

Changes in brain temperature across the sleep-wake cycle have been observed in many different species [the rat: (Alfoldi, Rubicsek, Cserni, & Obal, 1990; Franken, Tobler, & Borbely, 1992b), the djungarian hamster (Deboer, Franken, & Tobler, 1994), and sheep (M. A. Baker & Hayward, 1968)] and occur independently of the supra-chiasmatic nucleus (F. C. Baker, Angara, Szymusiak, & McGinty, 2005; Edgar, Dement, & Fuller, 1993). Modelling cortical temperature based on the sleep-wake distribution demonstrated that more than 80% of the variance in cortical temperature is explained by the sleep-wake distribution (Franken et al., 1992b). The pre-optic area of the hypothalamus (POAH) controls temperature (reviewed in (Zhao et al., 2017)). Warming this area, thereby mimicking the sustained elevated temperature during prolonged wakefulness, increases

NREM sleep prevalence (Sakaguchi, Glotzbach, & Heller, 1979) and intensity (McGinty, Szymusiak, & Thomson, 1994). These observations contributed to the formation of the thermoregulatory function of sleep (McGinty & Szymusiak, 1990), which postulates that sleep functions to cool the brain. However, this interpretation has been disputed because upon sleep onset, brain temperature decreases much faster than the correlate of NREM sleep pressure, delta power between 0.75-4Hz (Franken, Tobler, & Borbely, 1992a). This makes absolute changes in temperature a poor predictor of sleep pressure and therefore temperature is unlikely to reflect directly a sleep-homeostatic process.

Energy conservation

A prominent hypothesis on the function of sleep postulates that sleep occurs to save energy (Berger & Phillips, 1995) and/or to replenish brain energy (Benington & Heller, 1995). These hypotheses are supported by numerous observations, indicating that energy utilization of the brain is lower during NREM sleep in comparison to wakefulness, both by indirect measures in humans (Madsen & Vorstrup, 1991) (Braun et al., 1997) and animals (reviewed in (DiNuzzo & Nedergaard, 2017)). Moreover, adenosine, which correlates with neural activity, contributes to sleep homeostasis (Porkka-Heiskanen & Kalinchuk, 2011).

In contrast to these previous hypotheses, where sleep functions to save energy through metabolic rate reduction, the energy allocation model postulates that different essential biological processes are fulfilled most efficiently during either sleep or wakefulness. Therefore, energy must be partitioned between behavioral states to fulfill all the demands (Schmidt, 2014).

Memory and synaptic plasticity

There is little doubt about the importance of sleep in memory consolidation (Rasch & Born, 2013). Brain plasticity is promoted during sleep and plays an important role in memory formation via consolidation (reviewed in (Abel, Havekes, Saletin, & Walker, 2013; Ackermann & Rasch, 2014; Groch, Zinke, Wilhelm, & Born, 2015)). What are the underlying mechanisms? Hebbian plasticity states that ‘neurons that wire together, fire together’, (Shatz, 1992) meaning that connections between synapses strengthen over the course of stimulation (also known as long term potentiation). Synaptic scaling occurs to prevent over-excitation (Turrigiano, 2008) (see figure 1.3). The function of synaptic scaling is incorporated in the synaptic homeostasis theory (SHY), which postulates that

during waking global synaptic strength is increasing and during sleep decreasing (reviewed in (Cirelli, 2017)).

The decrease in synaptic strength occurring over sleep would be directly reflected, or maybe even driven by delta power during NREM sleep (Tononi & Cirelli, 2012), although this is not a widely accepted hypothesis (Frank & Cantera, 2014). Besides NREM sleep, REM sleep is also implicated in memory formation (Boyce, Williams, & Adamantidis, 2017) also by mediating changes in structural plasticity (W. Li, Ma, Yang, & Gan, 2017). Thus, sleep supports memory formation, but the exact underlying mechanisms and the respective contribution of the two sleep-states remains unclear.

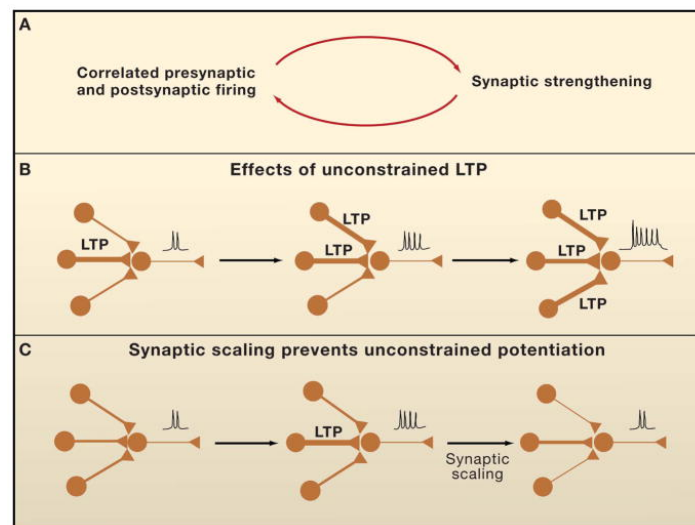


Figure 1-3 **Models of synaptic plasticity.** (A): run-away scenario where more excitation leads to stronger connections (LTP); however this is not sustainable on the long run because (B) synapse-specificity will be lost. (C) Adaptation of long term potentiation model by synaptic scaling, reverting run-away potentiation. From Turrigiano, 2008.

SLEEP HOMEOSTASIS AND ITS QUANTIFICATION

The sleep homeostat correlates with the time spent awake and asleep, during which sleep pressure is increasing and decreasing, respectively. The underlying physiological mechanisms regulating sleep homeostasis are unknown. Sleep homeostasis can be studied by applying a sleep

deprivation, after which or during different measures can quantify the sleep homeostatic rebound. A few of those measures will be discussed here.

Behavioral measures of sleep pressure are for example: subjective rating of sleepiness (Akerstedt, Anund, Axelsson, & Kecklund, 2014), sleep latency onset (Borbely, Achermann, Trachsel, & Tobler, 1989) and behavioral performance (Doran, Van Dongen, & Dinges, 2001). However, these are influenced by circadian time (*e.g.* sleep latency onset: (Dijk & Czeisler, 1995)), making them less reliable markers of sleep pressure.

Thus, a true sleep homeostatic marker reflects sleep pressure and is not compromised by other factors. In the EEG, delta power during NREM sleep (~ 0.5-4.0 Hz), also known as slow wave activity, reflects an intensity component of NREM sleep homeostasis (Borbely & Neuhaus, 1979). Sleep depriving mice from different strains reveals that the sleep homeostatic response greatly varies between mouse strains, suggesting that sleep homeostasis is controlled by genetic make-up (Franken, Chollet, & Tafti, 2001). Besides delta power in NREM sleep, increased theta power during quiet waking reflects increased time-spent-awake (Vyazovskiy & Tobler, 2005). However, this increase in theta power during an enforced wakefulness protocol shows a circadian modulation in humans (Finelli, Baumann, Borbely, & Achermann, 2000), and does thus not only reflect a sleep homeostatic process. The amount of NREM sleep that is recovered after a sleep deprivation is also thought to reflect a homeostatic process. However, this amount of NREM sleep is under greater circadian control than delta power (Dijk & Czeisler, 1995), and its dynamics are much slower than delta power. REM sleep, like NREM sleep, is also homeostatically regulated but primarily through time spent in this state (Franken, 2002).

Besides behavioral and electrophysiological markers, molecular correlates of sleep need have been proposed too. One example of a molecule reflecting sleep need is the cortical expression of the transcript *Homer1a*, which increases with time-spent-awake and can reliably be predicted based on the sleep-wake distribution (Maret et al., 2007). However, a knock-out study did not demonstrate a functional role for *Homer1a* in the response to sleep deprivation in terms of NREM delta power (Naidoo et al., 2012), although it was found to contribute to sleep-induced synaptic plasticity (Diering et al., 2017). Several studies demonstrated that a specific group of genes, called clock genes, reflect and are involved in the sleep homeostatic process. The following section presents first an introduction to clock genes and circadian rhythms, after which their role in the sleep homeostat will be discussed in the last section of this chapter.

Circadian rhythms: from molecular to overt behavior

HISTORY OF CIRCADIAN RHYTHMS

Since the discovery of circadian rhythms, a vast and growing number of studies helped to understand the proximate and ultimate mechanisms underlying this behavior. A cherry on the science-pie was the awarding of the Noble Prize 2017 in Physiology/Medicine to the circadian biologist Michael Young, Jeffrey Hall and Michael Rosbash *'for their discoveries of molecular mechanisms controlling the circadian rhythm'* (NobelPrize.org, 2017). Although circadian rhythms appear to be present in most life on earth, this chapter focuses on the mammalian biology of circadian rhythms.

The daily changes in environment are prominent and predictable and therefore being able to anticipate to those changes is beneficial. Therefore, circadian rhythms have evolved and are present in most life on earth (Bhadra, Thakkar, Das, & Pal Bhadra, 2017). For a rhythm to be circadian, it should be an endogenous, self-sustainable and entrainable oscillator that is temperature compensated (Pittendrigh, 1960). What are the underlying mechanisms that explain such a precise clock? In the 19-seventies, major advances were made to generate our current understanding of the substrates underlying the clock. Lesioning of the suprachiasmatic nuclei (SCN-x) was associated with a loss of behavioral circadian rhythms (Moore & Eichler, 1972; Stephan & Zucker, 1972). The discovery of this 'central' mammalian clock coincided with the finding of a genetic determinant on eclosion rhythms in *Drosophila* by a mutagenesis screen (Konopka & Benzer, 1971), pointing to a genetic regulation of circadian rhythms. The next break-through was in murine research, by the discovery of the *Clock* gene in the mouse by a genetic screen (Vitaterna et al., 1994). Over the last decennia, the neuro-endocrine and the genetic pathways of circadian rhythms have been elucidated further. An overview of our current knowledge is presented here.

REGULATION OF OVERT CIRCADIAN RHYTHMS

How to measure a circadian rhythm in vivo

Several outputs of the murine clock can be measured to determine its period, phase and amplitude. Examples are: locomotor activity (LMA), food and water intake, body temperature and the expression of clock genes. A consideration when using running wheels is that this behavior can modulate outputs of the clock such as body temperature and gene expression of clock components (Yasumoto, Nakao, & Oishi, 2015). Therefore, assessment of activity without running wheel, for

example by passive infrared sensors, is preferable when interested in circadian rhythms and using behavioral activity as an output of the clock.

Organization of circadian rhythms in mammals

To keep the internal timing system in pace and phase with the external world, ambient cues like light, [reviewed in (LeGates, Fernandez, & Hattar, 2014)] as well as non-phototic cues such as arousing events [in hamsters (M. H. Hastings et al., 1997) and food (Marchant & Mistlberger, 1997) can entrain behavioral rhythms. Light is directly integrated in the SCN which subsequently sends information to the periphery to inform about time-of-day and to keep phase coherence between organs. How this information is exactly conveyed is not clear, but it appears to rely on both molecular signals that are rhythmically expressed within the SCN and by neuronal activity and humoral signals [reviewed in (J. D. Li, Hu, & Zhou, 2012)]. Beyond its phase and period, the circadian amplitude of core body temperature is controlled by the SCN, partly via the timing of sleep and wake (Dijk, Duffy, & Czeisler, 2000). These temperature rhythms are also suggested to inform the periphery about time-of-day (Morf & Schibler, 2013).

The output of the clock can be ‘masked’ or repressed by external variables, without affecting the actual period or phase (see Figure 1-4). In this example, LMA is repressed during light exposure in nocturnal animals (Jud, Schmutz, Hampp, Oster, & Albrecht, 2005), while its circadian rhythm, as

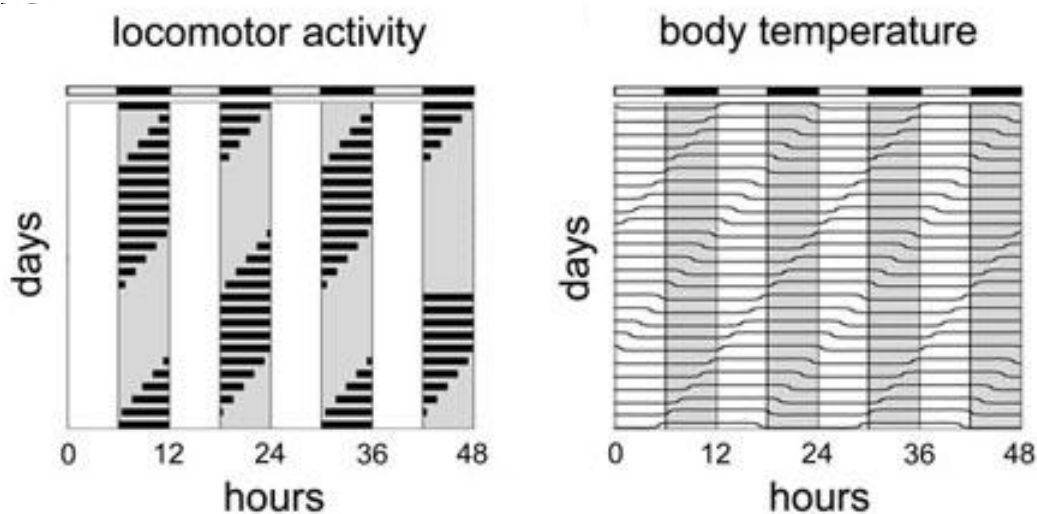


Figure 1-4 **Clock outputs, such as LMA, can be masked by external factors.** In these simplified actograms, a nocturnal organism is exposed to a light:dark cycle of 6hrs:6hrs. Activity is repressed during the periods with light, but circadian rhythms remain intact as there is an evident circadian rhythm in locomotor activity, as well in the other clock-output, body temperature. Adapted from Jud et al., 2005.

measured by body temperature and phase of the daily activity onset, still follows a circadian rhythm (Figure 1-4, right panel).

MOLECULAR ORGANIZATION OF CIRCADIAN CLOCKS

Genes underlying circadian rhythmicity at the cellular level

Almost each mammalian cell has an autonomous transcriptional auto-regulatory feedback-loop of which the basics are discussed here. A substantial amount of mRNA transcripts are cycling with estimations ranging from 3 to 16% in different tissue of mice (Zhang, Lahens, Ballance, Hughes, & Hogenesch, 2014), up to 81.7% of protein coding transcript across all tissues of the baboon (Mure et al., 2018). This rhythmicity is regulated by intertwining transcriptional-translational feedback loops.

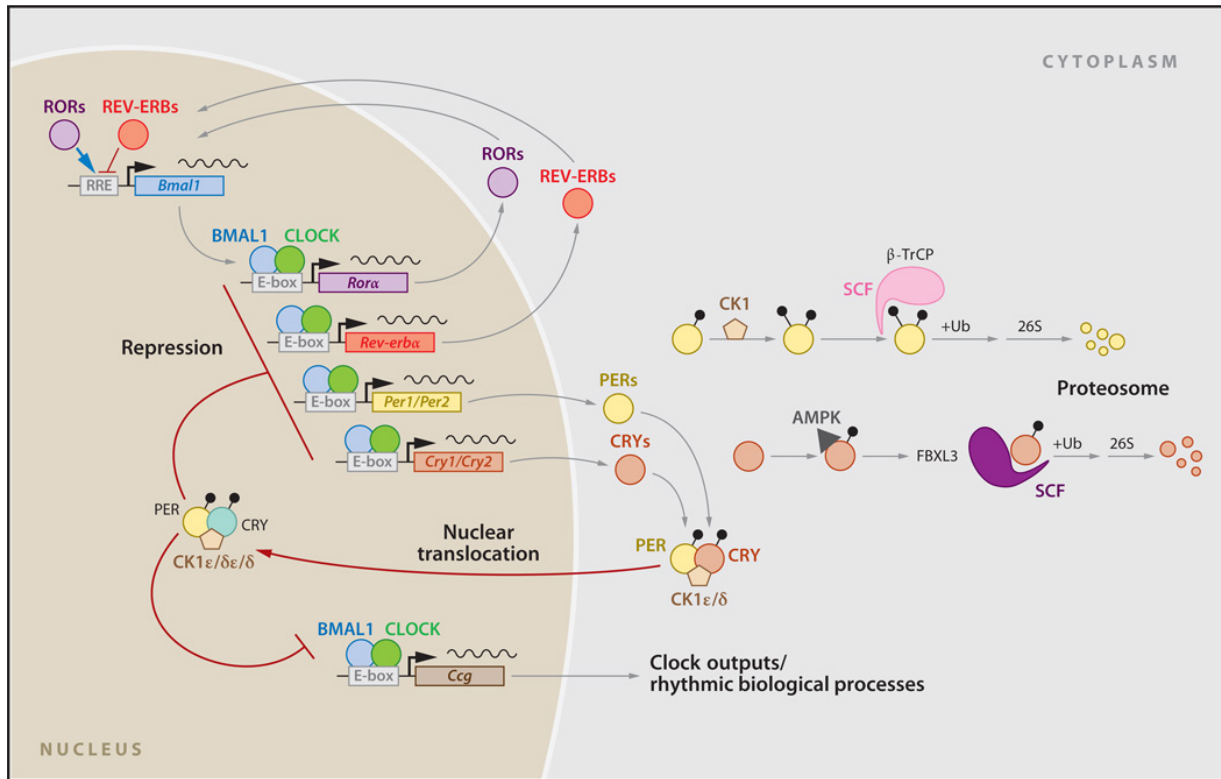


Figure 1-5 . **Each cell has an autonomous transcriptional-translational autoregulatory feedback loop.** The transcription of Per and Cry mRNAs is driven by the binding of the heterodimerized proteins BMAL1 and CLOCK, who bind to the E-boxes. Per and Cry transcripts are translated into proteins and subsequently inhibit BMAL1 and CLOCK from initiating their own transcription. BMAL1 and CLOCK drive as well the expression of REV-ERB α and ROR by binding to their E boxes as well, after which REV-ERB α as a protein inhibits and ROR promotes respectively. the transcription of BMAL1. Schematic taken from: (Mohawk, Green, & Takahashi, 2012). The most relevant abbreviations for this thesis are mentioned in this chapter. The third loop, concerning the transcription factors of the PAR-bZip family, is not depicted here.

The core components of this clock gene network are the activators CLOCK (and its homologue in the forebrain, NPAS2) and BMAL1, and the repressors PER1, PER2, PER3 and CRY1, CRY2. CLOCK-BMAL1/NPAS2 heterodimerize and bind to E-box elements of their target genes, the repressors *Per1-3* and *Cry1-2* (Gekakis et al., 1998; Reick, Garcia, Dudley, & McKnight, 2001). Subsequently, PERs and CRYs form large protein complexes (Aryal et al., 2017; Duong, Robles, Knutti, & Weitz, 2011), preventing BMAL1/CLOCK from initiating their own transcription (Sangoram et al., 1998). PER1-3 and CRY1,2 are both degraded by ubiquitin kinases pathways, and their degradation is controlled by casein kinases (CKIs) and FXBL3, resp. (see Figure 1-5).

There is a second canonical positive feedback loop where transcription of REV-ERB α and retinoic acid related orphan receptor α (ROR α) is initiated by BMAL1/CLOCK, after which REV-ERB α protein inhibits and ROR promotes the transcription of BMAL1 by competing for ROR-binding elements (Preitner et al., 2002; Sato et al., 2004).

CLOCK/BMAL1 drive a third loop by initiating transcription of the PAR-bZIP transcription factor family members (*i.e.* DBP, TEF, HLF), which function themselves as transcription factors. Once translated, these transcription factors compete with the repressor NFIL3 for the transcription of RORs (Mitsui, Yamaguchi, Matsuo, Ishida, & Okamura, 2001) [not incorporated in Figure 1-5].

With the development of the Chromatin Immunoprecipitation-sequencing (ChIP-seq) tool, the circadian clock components that function as transcription factors have been further identified [reviewed in (Takahashi, 2017)]. After transcription, a poor overlap of only 30% was found between rhythmic introns and their corresponding exons (Koike et al., 2012; Menet, Rodriguez, Abruzzi, & Rosbash, 2012), supporting the hypothesis that beyond transcription initiation, other post-transcriptional processes partake in steady-state circadian rhythms of mature transcripts and proteins. Several of these post-transcriptional mechanisms have been described, such as mRNA stability, translation and alternative splicing [reviewed in (Preussner & Heyd, 2016)]. An intriguing example concerns the gene *Cirbp* (Cold Inducible RNA Binding Protein). Temperature is considered a major output of the clock by circadian biologist. The temperature-driven transcript *Cirbp*, which is constitutively expressed under constant temperature, is more efficiently spliced at lower temperatures, thereby giving rise to circadian oscillations in mature *Cirbp* and CIRBP (Gotic et al., 2016). Interestingly, the same protein is essential for high amplitude clock gene expression under temperature entrainment conditions by controlling the cellular localization of Clock (Morf et al.,

2012) and/or by affecting transcript stability via regulating alternative polyadenylation (Liu et al., 2013). CIRBP will be further discussed in Chapter 3.

Besides post-transcriptional mechanisms, post-translational mechanisms add an additional layer of regulation to the clock by controlling phosphorylation, ubiquitination, acetylation and SUMOylation [reviewed in (Hirano, Fu, & Ptacek, 2016)], for example by regulating the degradation of PER and CRY proteins.

Studies have investigated the effect of mutations in clock genes to overt circadian behavior. From these experiments, we learned that most mutations in one clock gene refine the amplitude and period length. However, *Bmal1* alone is necessary to keep the overt behavioral and molecular clock ticking. However, functional impairment of genes that are closely related, for example *Cry1-2* knock-out, also induced arrhythmicity [summarized in (Lowrey & Takahashi, 2011), table 6.1].

TEMPERATURE COMPENSATION AND ENTRAINMENT

Temperature compensation prevents a change in the period of the clock at different physiological relevant constant temperatures, whereas temperature entrainment enables the clock to entrain to external temperature cycles of ca. 24 hours. Hints of mechanisms underlying these two processes start to emerge. I will review here briefly the most important experimental findings.

The ability to temperature compensate was first shown in the eclosion rhythm of *Drosophila* at an ambient temperature range from 16 to 26°C (Pittendrigh, 1954). From there on, a convincing body of evidence appeared, showing that at the molecular level, the period of mammalian cells are temperature compensated both in peripheral tissues [*e.g.* (Izumo, Johnson, & Yamazaki, 2003; Reyes, Pendergast, & Yamazaki, 2008)] and in the SCN (Buhr, Yoo, & Takahashi, 2010).

What biological mechanisms are responsible for temperature compensation? A first effort to explain this phenomenon proposed two temperature-dependent but opposing reactions, that together prevent the clock from ticking faster when temperature increases (J. W. Hastings & Sweeney, 1957). A mechanism underlying this hypothesis was proposed to rely on Period-genes (Kurosawa & Iwasa, 2005). This is supported by the finding that in *Drosophila*, *Per* transcript is temperature-sensitive spliced (Majercak, Sidote, Hardin, & Edery, 1999). Furthermore, mammalian PER₂ has two temperature-sensitive phosphorylation sites. The phosphorylation of these sites determines if PER₂ will have a slow or fast degradation rate, thereby slowing the degradation rate at higher temperatures (Zhou, Kim, Eng, Forger, & Virshup, 2015). It remains to be determined if the above-mentioned mechanisms also contribute to temperature entrainment.

A recent model proposed an ‘adaptive temperature sensor’ which explains both temperature compensation and entrainment. This model, which was experimentally confirmed in *Drosophila*, assumes that sensors feed temperature information to the circadian clock and that the sensors’ components scale with the changes in temperature, while keeping the phase relationship between different clock components intact. This mechanism was found to operate independent of heat shock factors was found (HSF) (Kidd, Young, & Siggia, 2015). This is contrary to mammalian cells, where HSF-1 is important in peripheral cells for temperature compensation and entrainment (Buhr et al., 2010) and entrainment (Saini, Morf, Stratmann, Gos, & Schibler, 2012). Importantly, the adult intact SCN is at most times of the day resistant to rhythmic external temperature cycles in terms of entrainment (Buhr et al., 2010).

CIRCADIAN CLOCK PATHOLOGIES

Aberrant behavior of the clock machinery can give rise to circadian pathologies. The most studied example is the Familial Advanced Sleep Phase Syndrome (FASPS). Carriers of this autosomal dominant point mutation in *Per2* are 4-hours phase advanced; *i.e.* they go to bed at 7:30 pm and wake up at 4:30am. The mutation induces hypo-phosphorylation at the CKI ϵ -site of PER2, thereby making PER2 more prone to degradation and shortening the molecular period (Toh et al., 2001). This human phenotype, and its underlying mechanism, is somewhat comparable to the tau-mutant hamster, which is remarkable for its short period of only ~20hrs and has a defect in PER2 phosphorylation due to a mutation in CKI ϵ (Lowrey et al., 2000). Opposite to FASPS is the delayed sleep phase syndrome (DSPS) which is, amongst others, associated with a mutation in the *Per3* gene (Archer et al., 2003).

CIRCADIAN OR SLEEP-WAKE DRIVEN?

The aforementioned studies investigating cyclic transcripts assumed rhythmicity to be of circadian origin. However, considering sleep-wake state reveals that most rhythmic transcripts are in fact sleep-wake driven. In the cortex of the mouse, more than 80% of the transcripts is driven by sleep-wake state and not by circadian time (Maret et al., 2007). By applying a forced desynchrony protocol in humans, a similar sleep-wake driven contribution to daily rhythmic transcription in the blood transcriptome was found (Archer et al., 2014). Transcripts that were merely driven by sleep-wake state included those who are part of the clock gene machinery, such as *Per2*. In the following section, the link between the sleep homeostat and circadian rhythms will be further discussed.

Process S and Process C: interacting processes

Our sleep-wake distribution, *i.e.* the duration and timing of sleep, is the result of two interacting processes: the circadian clock and the sleep homeostat. How these two processes give rise to the sleep-wake distribution is conceptually approached by the ‘two process model of sleep regulation’ (S. Daan, Beersma, & Borbely, 1984). Sleep timing is gated by high sleep pressure and a simultaneous decrease in the circadian drive to stay awake (see Figure 1-6). The molecular mechanisms underlying the circadian clock are relatively well known, as opposed to our understanding of the biology regulating the sleep homeostat. However, it has become evident that these two processes interact with each other. For example, enforced wakefulness affects the neuronal activity of the master-clock, the SCN (Deboer, Detari, & Meijer, 2007), whereas characteristics of NREM sleep slow waves, which correlate with power in the delta band, are modulated by the circadian clock depending on the brain region (Lazar, Lazar, & Dijk, 2015). Similar

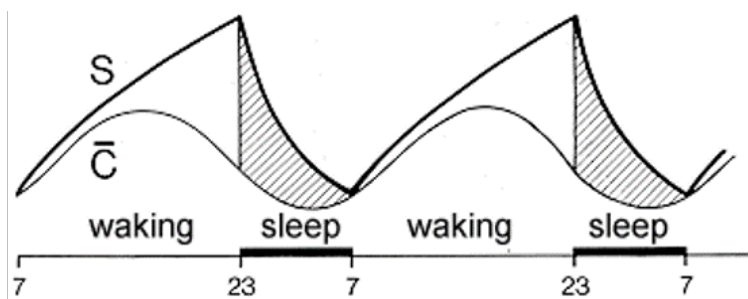


Figure 1-6 **The two-process model predicts the sleep-wake distribution.** Sleep pressure, as visualized by S, accumulates during time-spent-awake and dissipates during NREM sleep. C estimates the circadian timing of sleep. These two components together determine our sleep-wake distribution. Taken from <http://www.pharma.uzh.ch/static/sleepcd/demo/regulat/chap3/tpm000.htm>

interactions between the circadian and sleep homeostatic processes, have been reported in a fMRI study (Muto et al., 2016). Also the prevalence of REM sleep depends on circadian time and time slept (Dijk & Czeisler, 1995). The mechanism facilitating this cross talk is unknown. Here, a possible link through clock

genes, will be discussed.

CLOCK GENES ARE INVOLVED IN SLEEP HOMEOSTASIS

Besides their role in circadian rhythms, clock genes are also contributing to sleep homeostasis. An extensive review of the arguments demonstrating this hypothesis can be found in (Franken, 2013). The three main arguments advocating for a role of clock genes in sleep homeostasis will be provided here.

Gene mutation / knock-out	Homeostatic phenotype (WT versus mutant)		Reference
	NREM delta power after sleep deprivation	amount of recovered sleep relative to BL	
Bmal1 (KO)	Decreased (but did not appropriately analyze the data)	Less NREM sleep	(Laposky et al., 2005)
Clock(Δ_{19} -mutation)	No (but summed amount of delta power differs like in BL)	Less REM sleep	(Naylor et al., 2000)
Cry1 /Cry2 (dKO)	Increased	Less REM and NREM sleep	(Wisor et al., 2002)
Dbp (KO)	Similar as WT	18hrs after SD no significant differences	(Franken, Lopez-Molina, Marcacci, Schibler, & Tafti, 2000)
Dec2 (human mutation introduced in mouse genome)	Decreased	Less NREM sleep	(He et al., 2009)
Npas2 (KO)	Shift to faster frequencies, slower build-up process S	Less NREM sleep (males only)	(Franken et al., 2006)
Per2 (Brdm1)	Decreased	More REM sleep	(Kopp, Albrecht, Zheng, & Tobler, 2002)
Per3 (KO)	Increased	Less REM sleep	(Hasan, van der Veen, Winsky-Sommerer, Dijk, & Archer, 2011)
Per3 (hPer3 4/4 and 5/5)	Increased only Per3 ^{5/5}	No differences	(Hasan et al., 2014)
Rev-erb α (KO)	Decreased	No differences	(Mang et al., 2016)

Table 1-1 Clock gene mutations can modulate the sleep homeostatic response to sleep deprivation in mice.

First, animals with mutations in clock genes exhibit an altered response to sleep deprivation in terms of delta power during NREM recovery sleep and/ or in the amount of sleep recovered (see Table 1-1 for an overview that includes significant findings in murine studies).

Secondly, sleep deprivation affects the binding of clock proteins to their circadian target genes. Specifically, the binding of the transcription factors BMAL1 and NPAS2 to their circadian target genes *Dbp* and *Per2* was decreased after sleep deprivation, suggesting that sleep pressure affects the dynamics of the circadian clock loop (Mongrain, La Spada, Curie, & Franken, 2011).

Third, sleep deprivation affects the expression of clock genes. Controlling for sleep-wake state shows that supposedly circadian expressed genes and proteins, such as *Per2*, are affected by time-spent awake [(Archer et al., 2014; Curie, Maret, Emmenegger, & Franken, 2015; Curie et al., 2013; Maret et al., 2007) , reviewed in (Archer & Oster, 2015)], indicating that their expression is not solely circadian driven, but also the resultant of sleep-wake state. Importantly, PER2 levels in the SCN are insensitive to sleep deprivation (Curie et al., 2015).

MECHANISMS CONVEYING SLEEP-WAKE STATE TO CLOCK GENE EXPRESSION

What mechanism is responsible for rendering sleep-wake state information to clock gene expression? As discussed above, sleep deprivation reduces the binding of BMAL1, CLOCK and

NPAS2 to *Per2* and *Dbp*, independent of the sleep-deprivation induced changes in transcript levels [increases (*i.e.* *Per2*) or decreases (*i.e.* *Dbp*)], suggesting that factors other than reduced binding also contribute to sleep deprivation induced changes in clock gene expression. One such mechanism that has been experimentally established is through corticosterone, because adrenalectomy attenuates the sleep deprivation-induced increase in cortical *Per2*, and even abolishes the increase in *Per1* and *Per3* (Mongrain et al., 2010). Besides glucocorticoids, many other elements change with sleep-wake state, such as light exposure, redox state, temperature and cytokine levels, which in turn can all affect clock gene expression (Franken, 2013) although this still needs to be experimentally proven. Also, oxygen consumption changes with sleep-wake state (Jung et al., 2011) and oxygen levels can modulate the expression of clock genes (Adamovich, Ladeux, Golik, Koeners, & Asher, 2017).

In the second experimental chapter, another sleep-wake driven mechanism will be discussed, namely that sleep-wake state information is rendered through changes in cortical temperature, which subsequently drives the expression of *Cirbp*. Because CIRBP is necessary for high amplitude clock gene expression *in vitro* (Liu et al., 2013; Morf et al., 2012), we hypothesized that it also partakes in the sleep deprivation-induced changes in clock gene expression. Based on the results of this experiments and previous studies, I concluded that the clock in its response to sleep deprivation is sensitive to the presence of CIRB. Because the sleep deprivation induced changes in clock gene expression were not all modulated by CIRBPs presence, this suggests that other sleep-wake driven pathways as well contribute to the sleep deprivation driven changes in clock gene expression.

MEASURING CLOCK GENE EXPRESSION *IN VIVO*

With the progress of technology, tools have become available to measure clock gene expression *in vivo*. Markers were engineered, such as bioluminescent or fluorescent reporters, that are under the same transcriptional control as the gene of interest. In particular, the PER2::LUCIFERASE construct, developed by the Takahashi-lab, has become a widespread tool to monitor PER2 levels. With this technique, bioluminescence is measured, that is emitted by the interaction of the reporter enzyme luciferase and with its provided substrate, luciferin (Yoo et al., 2004). Initially, this construct was applied to study PER2 levels in *in vitro* studies but later also *in vivo* by anaesthetizing mice and quantifying bioluminescence emission of specific organs (Curie et al., 2015; Tahara et al., 2012). The big advantages of these *in vivo* studies are that the number of animals used are dramatically reduced compared to conventional experiments, and each animal serves as its own

control, thereby improving the experimental design by controlling for interindividual variation. However, this method still has the drawback of having to handle and anaesthetize the animals before the measurements; factors that are known to affect clock gene expression (Antle & Mistlberger, 2000; Cheeseman et al., 2012).

Recently, devices have been developed to overcome these possible confounding factors by measuring bioluminescence *in vivo*. One of these devices was developed by the Schibler laboratory (University of Geneva, Switzerland) and dubbed 'RT Biolumicorder' (Saini et al., 2013). A photon multiplier tube (PMT) counts the numbers of photons emitted by the mouse as a proxy for gene expression (Saini et al., 2013). Mice can be housed in this apparatus for up to two weeks, and food intake and light exposure can be controlled remotely. For one of the chapters in this thesis, I developed a strategy to simultaneously record EEG and bioluminescence (see 'Monitoring PER2 bioluminescence under undisturbed and attenuated sleep-wake rhythms').

Besides the RT Biolumicorder, other tools have been developed to monitor (clock) gene expression in behaving mice. Several studies have reported on clock gene expression in the SCN by measuring bioluminescence through an optic fiber (Ono, Honma, & Honma, 2015; S. Yamaguchi et al., 2001; Y. Yamaguchi et al., 2016). Other tools have been developed as well.

The Honma laboratory used two Charge-Coupled Device cameras to track the position of a mouse and its tissues by scintillators. The coordinates and intensity of the bioluminescence signal are subsequently handled by an algorithm that outputs the intensity of individual tissues (Hamada et al., 2016). To overcome the shortcomings of a design that relies on bioluminescence, the Zhang laboratory designed a fluorescent marker that is expressed under the control of the *Cry1* promoter. They recorded successfully fluorescence from the SCN and several other brain areas. An advantage of working with this technique is that it can be used while mice are exposed to an LD cycle (Mei et al., 2018), which is not possible when using luciferase-reporters because of the low intensity of the bioluminescence signal.

WHAT IS SLEEP, WHAT IS CIRCADIAN

The techniques discussed above have so far only investigated the expression of clock genes within a circadian context. However, the signals measured might be the resultant of the interaction between the sleep-wake distribution and circadian time, like discussed before for clock gene expression. The impact of sleep-wake state on clock gene expression in freely moving mice is addressed in the upcoming experimental chapter.

'Never waste any time you can spend sleeping'

Frank H Knight

Chapter 2 The contribution of sleep-wake state to PER2 bioluminescence in un-anaesthetized mice

Marieke MB Hoekstra, Yann Emmenegger, Paul Franken

Center for Integrative Genomics, University of Lausanne, Lausanne, VD Switzerland

Summary and contributions

SUMMARY

In this project, we investigated i) how the sleep-wake distribution contributes to changes in PER2 in a freely behaving mouse and ii) if a reduction in the daily amplitude of NREM sleep by repeated short sleep deprivations affects the circadian amplitude of PER2. Prior to the biological experiments, we determined that luciferin administration via an osmotic mini-pump was the most preferable for our experiment, and that the majority of the bioluminescence was emitted by the kidneys. Next, we measured simultaneously sleep-wake state and PER2 bioluminescence under undisturbed conditions, and found that PER2 bioluminescence varied as a function of sleep-wake state. A simple model, assuming a linear increase and decrease during waking and sleep respectively, mimicked well the phase but not the amplitude of PER2 bioluminescence. Improvements of the model can provide clues on the underlying mechanisms. In the second experiment, mice were sleep deprived for two hours every four hours during two days. This protocol successfully reduced the NREM sleep amplitude by ca. 50%. In a separate cohort of mice, these sleep deprivations reduced the amplitude of PER2 bioluminescence in three out of four mice. Altogether, we are the first to show that also in freely behaving conditions, the sleep-wake distribution importantly contributes to changes in PER2 bioluminescence, confirming previously obtained data from sleep deprivation experiments. Further experiments need to address if bioluminescence reflects PER2 protein levels.

CONTRIBUTIONS

Note that this manuscript is work in progress and therefore some of the results need further analysis or experiments to draw reliable conclusions (indicated in the manuscript). The design of the experiments, analyses, statistics, visualization of the results and writing of the manuscript was performed by myself under supervision of Paul Franken. Yann Emmenegger, the lab technician, was available in case of questions and problems in the mouse facility. He also taught me how to perform the surgical interventions.

First, the favorable route of luciferin was determined. We took advantage of a mouse model that expresses constantly luciferase under control of a synthetic promotor (Y. A. Cao et al., 2004). I performed the experiments.

Next, Yann Emmenegger and I determined the peripheral source of bioluminescence in SKH1 x PER2:LUC mice with an IVIS Xenogen apparatus. Florence Morgenthaler-Grand assisted us while performing these experiments, and Francis Derouet took care of the administration that came with bringing mice from our animal facility to their facility, where the imaging systems were.

To quantify how PER2 bioluminescence varies with sleep-wake state, we used a knock-in mouse model where PER2 is fused with the reporter luciferase (Yoo et al., 2004). I implanted the mice with EEG, EMG and an osmotic mini-pump, and initiated the recordings, organized the sleep deprivations and collected the data afterwards. For central recordings, Yann Emmenegger and myself implanted mice with EEG, EMG, cannula connected to an osmotic mini-pump. All the sleep deprivations were performed with the help of fellow lab members. The EEG data was afterwards annotated for sleep-wake state by Yann Emmenegger and myself.

Our last experiment concerned a model where a behaviorally rhythmic mouse was exposed to an 'arrhythmic' sleep-wake schedule. To determine in retrospect the efficiency of our sleep deprivation, I implanted SKH1 and B16 mice with EEG, EMG and thermistors with the help of Yann Emmenegger. The SKH1xPER2::LUC mice were implanted with an osmotic mini-pump to follow PER2 bioluminescence. Mice were sleep deprived for 2hrs every 4hrs during two days under constant dim red light. I scheduled the experiments and am very thankful for the help I got with this this, notably: Lisa Härrä, Yann Emmenegger, Charlotte Hor and Jeff Hubbard; and special thanks to those who supported me during the graveyard shifts: Maxime Jan, Kostas Kompotis, Violeta Castelo-Szekely and Sonia Jimenez. The EEG data of this experiment was annotated by Sonia Jimenez and Yann Emmenegger.

Abstract

The expression of the circadian clock gene, period-2 (Per2), is increased after sleep deprivation (SD). However, how the association between the sleep-wake distribution and PER2 levels holds under baseline conditions, has never been studied. To address this question, we measured Per2 expression in a freely behaving mouse by measuring bioluminescence as a proxy for PER2 protein levels along with EEG recordings. Our results show that PER2 bioluminescence is increasing during spontaneous waking and decreasing during spontaneous sleeping. Furthermore, attenuating the daily amplitude of the sleep-wake distribution by SDs around the clock, reduced in three out of four mice the PER2 bioluminescence amplitude. Further experiments need to address whether the sleep-wake evoked changes in bioluminescence mirror changes in PER2 protein levels.

Introduction

The sleep-wake distribution is coordinated by the interaction of a circadian and a homeostatic process (S. Daan et al., 1984). Understanding how these two components give rise to sleep and waking remains challenging because manipulation of sleep affects both processes. For example, the expression of the gene Period-2, which is also an essential part of the molecular circadian clock loop, is increased after sleep deprivation (SD) from ZT0 to ZT6 in cortex and liver (Curie et al., 2013; Franken, Thomason, Heller, & O'Hara, 2007; Maret et al., 2007), and also increases PER2 protein in the cortex, as well affects the circadian PER2 dynamics in liver and kidney (Curie et al., 2015). Furthermore, removal of the circadian amplitude of the sleep-wake distribution by lesions of the suprachiasmatic nucleus leads to an attenuation of the circadian amplitude of clock gene transcripts and proteins (Akhtar et al., 2002; Curie et al., 2015; Tahara et al., 2012). This underscores the sleep-wake dependent expression of clock genes.

Over the last decennia, technical progress allowed for monitoring of clock gene expression *in vitro* and *ex vivo* by the development of bioluminescence reporters expressed concomitantly with clock gene transcripts or protein (such as (Yoo et al., 2004)). Subsequently, these constructs were used to follow clock gene expression *in vivo* (Curie et al., 2015; Tahara et al., 2012), allowing for a within-subject design and reducing tremendously the number of animals used. However, this method still required handling and anaesthetizing the animals before measurements; factors capable of affecting clock gene expression (Antle & Mistlberger, 2000; Cheeseman et al., 2012). Recently, novel devices have been developed, overcoming these possible confounding factors by measuring bioluminescence in unanaesthetized, freely moving mice (Hamada et al., 2016; Mei et

al., 2018; Saini et al., 2013). In theory, these techniques allow for monitoring of clock gene expression in parallel with spontaneous sleep-wake behavior across several days. This is particularly relevant because sleep deprivation induces an, albeit mild, increase in corticosterone, which subsequently affects the expression of clock genes such as *Per1-3* (Mongrain et al., 2010).

Therefore, we inspected how PER2 bioluminescence is affected by changes in sleep-wake state in mice. We indeed found that under undisturbed conditions, sleep-wake state transitions are followed by changes in PER2 bioluminescence. By experimentally reducing the circadian amplitude of the sleep-wake distribution, the circadian amplitude of PER2 bioluminescence was also attenuated in three out of four mice. Altogether, our data points to an important contribution of sleep-wake state to PER2 bioluminescence.

Results

MEASURING PER2 BIOLUMINESCENCE IN PARALLEL WITH SLEEP-WAKE STATE

To follow PER2 levels, we measured bioluminescence from a mouse knock-in model where luciferase is fused, and thus expressed simultaneously, with PER2 (Yoo et al., 2004). Delivery of luciferin is discussed in the next section. To monitor PER2 bioluminescence emitted from the cortex (referred to as central PER2 bioluminescence) C57BL/6J (B6) x PER2::LUC mice were used because their pelage prevents detection of peripheral photons, thus increasing the signal-to-noise ratio. To

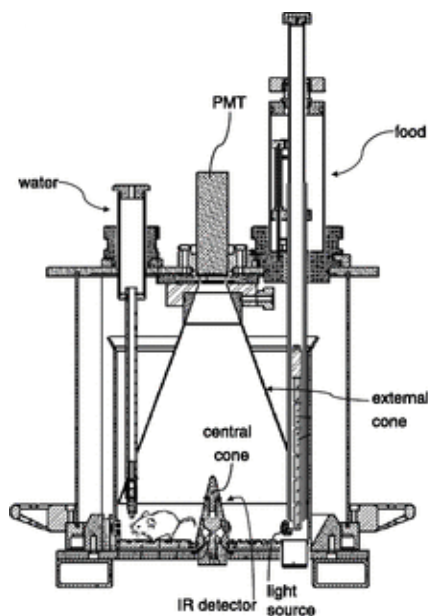


Figure 2-1 The RT biolumicorder. Taken from (Saini et al., 2013).

monitor peripheral PER2 bioluminescence, hairless immunocompetent SKH1 mice, heterozygous for the PER2::LUC construct, were used. During the experiments, mice were housed in constant darkness in a light-enclosed cage that contained a photon multiplier tube (PMT), a food hopper, a water dispenser, an activity sensor and a light source (see Figure 2-1). For an in-depth description of this apparatus, consult (Saini et al., 2013). For the SD, mice were moved from the RT Biolumicorder to a cage outside of the RT Biolumicorder in dim red light. We

monitored sleep-wake state in parallel with PER2 bioluminescence. To achieve this, mice were implanted with electroencephalogram (EEG) and electromyogram (EMG) electrodes to record brain- and muscle activity, respectively, using the wireless Neurologger system (Neurologger, TSE Systems GmbH, Germany). Offline, wakefulness, NREM and REM sleep was annotated per 4-seconds based on the EEG and EMG traces. A detailed description of the protocols and experimental designs can be found in the Material and Methods section at the end of this paper.

DETERMINING THE ROUTE OF LUCIFERIN ADMINISTRATION

First, the optimal route of luciferin administration was determined. Previous studies made use of osmotic mini-pumps implanted subcutaneously or intraperitoneally to deliver luciferin (Curie et al., 2015; Saini et al., 2013; Tahara et al., 2012). Providing luciferin via the drinking water was suggested as an alternative route (Schibler, 2014) and is preferred because it decreases stress for the mouse, caused by the implantation of the pump, and is economically favorable. However, drinking behavior has a strong circadian component (Bainier, Mateo, Felder-Schmittbuhl, & Mendoza, 2017) and could therefore periodically limit luciferin availability. An experiment performed in the Schibler lab addressed this concern by exposing *Bmal1-luc* and PER2::LUC mice to luciferin dissolved in drinking water. Opposite phases of bioluminescence were observed in these two strain of mice, thus advocating against a rate-limiting effect imposed by administering luciferin via drinking water (Schibler, 2014).

We confirmed that providing luciferin in the drinking water of PER2::LUC mice led to rhythmic bioluminescence detection (data not shown). However, activity onset was rapidly followed by increased bioluminescence, providing ground to doubt the dissociation between PER2 bioluminescence and drinking behavior. To address these concerns, bioluminescence was

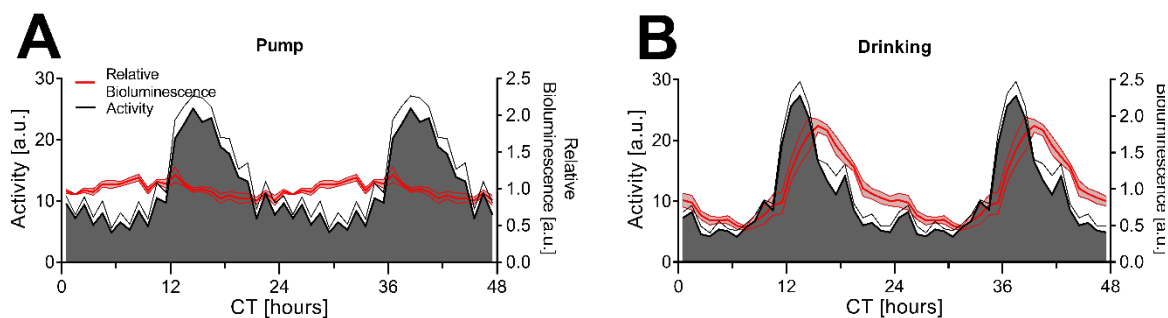


Figure 2-2 Overall bioluminescence during different routes of luciferin administration: via an osmotic mini-pump (A) or in the drinking water (B) in CAG mice (n=4) double plotted, mice kept in constant darkness.

measured in a mouse that constitutively expresses luciferase under the control of the synthetic CAG promoter (Y. A. Cao et al., 2004). Mice received luciferin via the drinking water or via an osmotic mini-pump in two separate experiments. Despite an assumed constant delivery of luciferin and/or constant production of luciferase, changes in bioluminescence of mice implanted with the pump appeared nevertheless rhythmic (Figure 2.2A), with levels increasing during the subjective light phase and decreasing during the subjective dark phase. When luciferin was delivered in the drinking water, the bioluminescence amplitude was increased compared to luciferin administration in the pump. Furthermore, its peak indeed coincided approximately with the expected peak of drinking behavior, which is around CT16 (Bainier et al., 2017) (Figure 2.2B). Therefore, we decided to adhere to the osmotic mini-pump for the subsequent experiments.

DETERMINING THE SOURCE OF BIOLUMINESCENCE

Previously, bioluminescence has been quantified separately in cortex, liver and kidney by imaging and 3D reconstruction with the IVIS 3D Xenogen apparatus (Curie et al., 2015). In our set-up, the RT Biolumicorder collects photons emitted from all tissues and can thus not differentiate between bioluminescence emitted from different tissues. Therefore, we quantified which peripheral organ(s) in mice carrying the PER2::LUC construct was/were the major source of bioluminescence. To this end, two male heterozygous PER2::LUC SKH1 mice were implanted with an osmotic mini-pump (model 1002; 35mg/mL luciferin) and five days later lightly anaesthetized

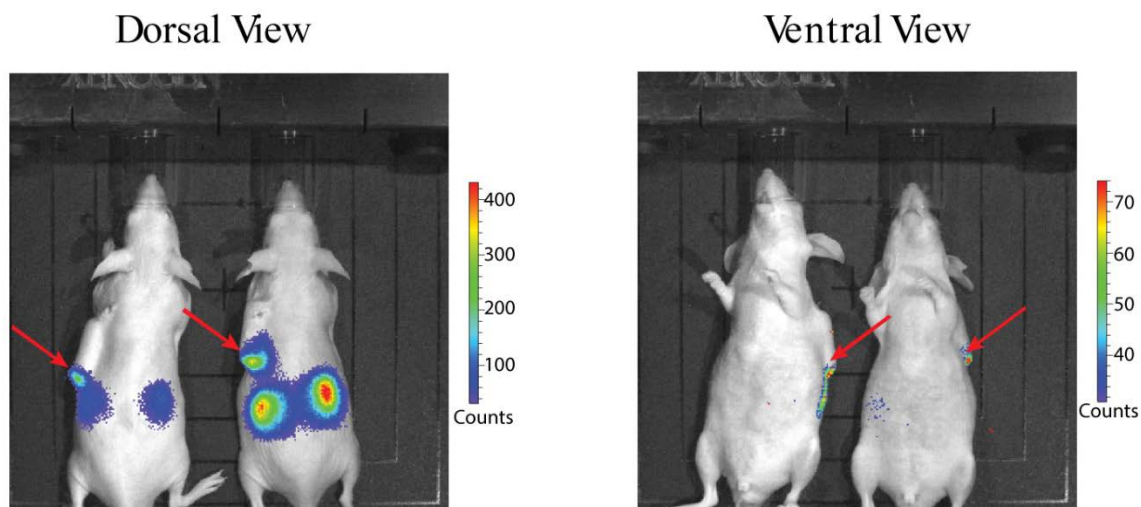


Figure 2-3 **The main source of bioluminescence is emitted by tissue located dorsally in the mouse.** Note that the scale bar of the dorsal view has higher values than the scale bar of the ventral view. The red arrows indicate the location of the flow moderator of the osmotic mini-pump.

with 2.5% isoflurane and imaged for 60 seconds (Xenogen IVIS Lumina II) around ZT6. The main source of dorsal bioluminescence overlapped with the expected location of the kidney (see Figure 2.3, Dorsal View), whereas ventrally almost no bioluminescence was detected (Figure 2.3, Ventral View). During the experiment in the RT Biolumicorder, most bioluminescence quantified is of dorsal origin due to the orientation of the mouse relative to the PMT. Altogether, this suggests that the kidneys are the main source of peripheral bioluminescence in PER2::LUCxSKH1 mice.

While determining the source of bioluminescence, we observed that the flow moderator of the osmotic mini-pump was emitting photons, reminiscent of phosphorescence (indicated by red arrows in Figure 2.3). This bioluminescence signal decreased by 85% over 15 minutes (see Figure 2-11, supplementary data) and is therefore unlikely to interfere with our experiments that take place in constant darkness for several days. Nevertheless, a blue flow moderator cap with less phosphorescence activity was used for subsequent experiments.

SPONTANEOUS SLEEP-WAKE STATE RELATES TO PERIPHERAL PER2 BIOLUMINESCENCE

SD affects *Per2* gene transcripts and protein levels (Curie et al., 2015; Curie et al., 2013), but there is no knowledge on the contribution of sleep-wake state under baseline conditions to PER2 levels. Does the sleep-wake distribution also contribute to changes in PER2 under freely behaving

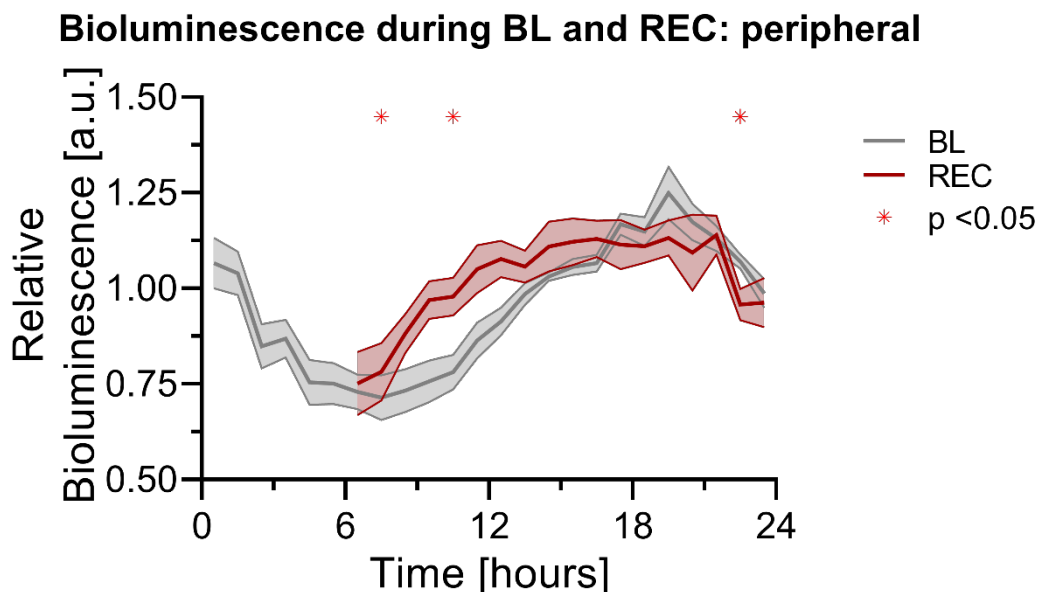


Figure 2-4 Hourly normalized bioluminescence levels emitted by the periphery during the second baseline day and after the sleep deprivation throughout the recovery. Sleep deprivation significantly affects the time course of bioluminescence ($F(17,68)=2.9$, $P=0.0011$). Significant results ($p < 0.05$) of post-hoc paired t-tests are indicated by a red asterisk (*). $n=5$.

conditions? We first addressed this question in the periphery, and obtained sleep-wake state and peripheral PER2 bioluminescence recordings during 2.5 days of baseline in constant darkness, a 6h SD and two recovery days from five SKH1 heterozygous PER2::LUC male mice (see Figure 2-12 in the Supplementary Data for raw data of the 2.5 days of baseline of each individual mouse). No correction for circadian time has been made, thus the hourly values plotted refer to the time under LD conditions. First, we assessed if we replicated previously published results concerning the effect of SD on renal PER2 bioluminescence. Indeed, SD significantly increased PER2 bioluminescence during the recovery, (see Figure 2-4) like the changes observed previously in the kidneys (Curie et al., 2015).

Next, we determined whether sleep-wake state affects PER2 bioluminescence under undisturbed baseline conditions. Although the circadian modulation of the bioluminescence trace is clearly visible over the 2.5 day of baseline recordings, there are additional changes on the bioluminescence trace that occur simultaneously with changes in sleep-wake state (see Figure 2-5).

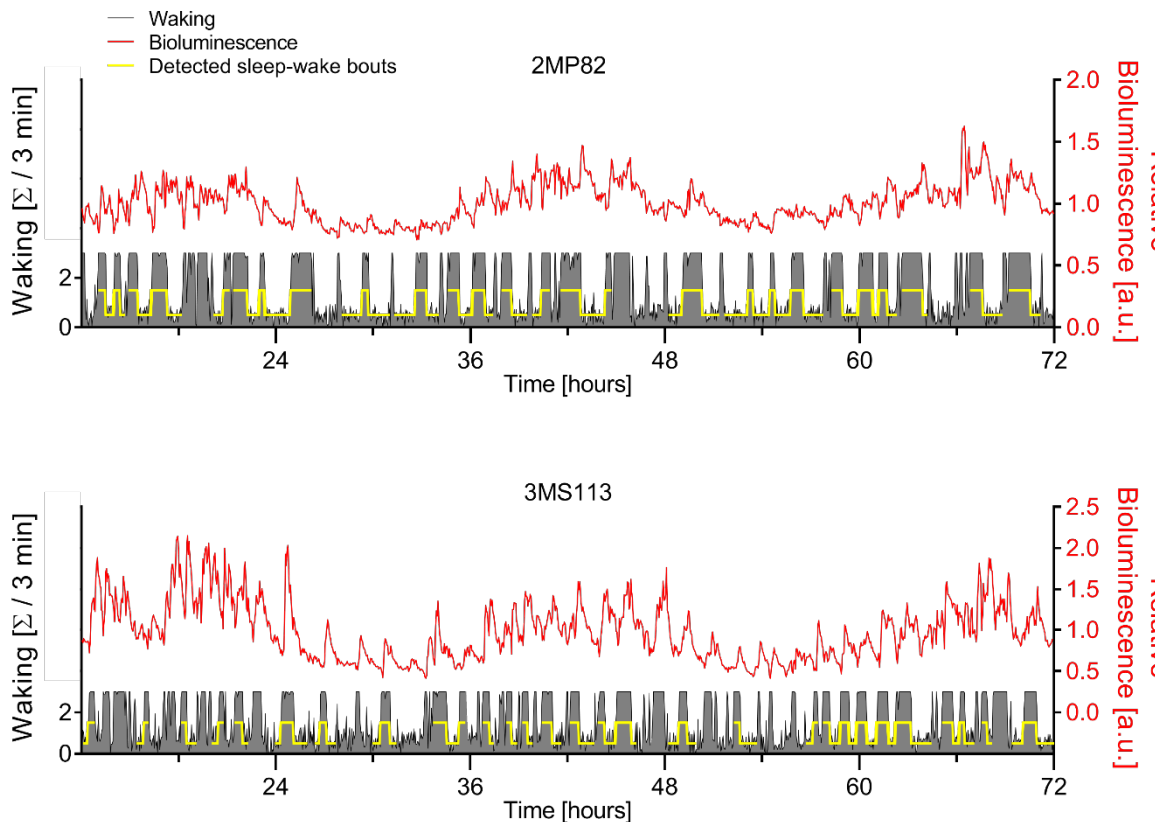


Figure 2-5 **Changes in sleep-wake state are accompanied by changes in bioluminescence.** Note the circadian oscillation in the bioluminescence trace with additional changes that seem to align with the changes in sleep-wake state.

PER2 bioluminescence appears to increase during waking dominated bouts and to decrease during sleep dominated bouts. To quantify this observation, transitions from sleep to wake and wake to sleep were selected. The sleep-wake and bioluminescence data was averaged over 3-min intervals. Selected transition events had to last for at least 15 minutes before and after the transition where time spent in sleep or wake dominated bouts should be at least 50% in that designated state. With these criteria, we detected on average (mean \pm SEM, n=5) 14.8 \pm 2.3 transitions from sleep to wake and 19.4 \pm 2.3 transitions from wake to sleep during the 2.5 baseline days. The timing of these transitions is indicated by the yellow traces in the representative two examples in Figure 2-5.

Indeed, a transition from wake to sleep was accompanied with a 22% reduction (relative to t=0 at transition) in bioluminescence after 40 minutes of sleep dominated bouts [77.8%, SEM: 4.1] whereas a transition from sleep to wake correlated with an 34% increase in bioluminescence within 40 minutes [% , 134.1, SEM:5.3]. The changes in bioluminescence relative to sleep-wake state transitions were delayed (mean \pm SEM [minutes], wake to sleep transition: 2.1 \pm 0.6; sleep to wake transition: 3.6 \pm 0.9, based on the dynamics of the average transition per mouse of data averaged per 3 minutes).

The cortical response of *Per2* to SD depends on time of day (Curie et al., 2013). Are the sleep-wake evoked responses in peripheral PER2 bioluminescence also dependent on time of day? A sinewave was fit to each individuals' bioluminescence trace and subsequently divided into rising and falling limbs (see Figure 2-6A). We compared the bioluminescence dynamics of transitions occurring at the rising limb with those occurring at the falling limb. The number of transitions was not different between rising and falling limb (paired t-test, sleep to wake rising: 6.6 \pm 1.12; falling:8.2 \pm 1.5, t(4)=-1.17, p=0.31; wake to sleep: rising:11 \pm 1.4, falling: 8.4 \pm 1.9, t(4)=1.03, p=0.36). The

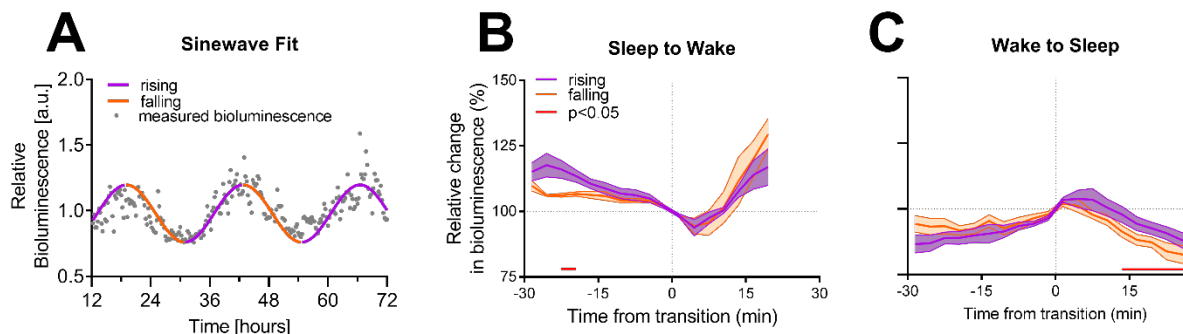


Figure 2-6 **Time-of-day affects sleep-wake evoked PER2 dynamics.** Categorizing of PER2 bioluminescence trace in rising and falling limb of the sinewave (A). Changes in bioluminescence when transitioning from sleep to wake and vice versa (B-C). The timing of the transition significantly affects the shape of the curve (factor Time from Trans* Rising/Falling, sleep to wake: F(16,64)=3.5, p=0.0002; wake to sleep: F(19,76)=2.46, p=0.0030; post-hoc paired t-test, n=5).

dynamics in bioluminescence were indeed affected by their timing relative to the circadian sinewave. Bioluminescence initially decreased faster during sleep at the transition from sleep to wake on the rising limb (Figure 2-6B), whereas sleep occurring on the falling limb after the transition from wake to sleep decreased faster (Figure 2-6C). Further analyses, for example inspecting subtle changes in sleep-wake structure between the rising and falling limb and dependency on the bioluminescence offset value at the transition can provide further clues about the origin of these circadian differences in bioluminescence dynamics.

As a first attempt to understand the contribution of the sleep-wake driven changes in PER2 bioluminescence, we applied a simple linear model based on the sleep-wake annotation that was averaged per 3-min intervals. If an interval had > 50% waking, it was annotated as waking, otherwise it was deemed sleep. The change in bioluminescence was estimated based on the average individual slope of the bioluminescence changes occurring in the first 40 minutes after the transition. This simple approach captured relatively well the phase of the circadian changes in bioluminescence (Figure 2-7), but further efforts will be made in improving the model. For example, next steps will focus on optimizing the model by using an exponential instead of a linear function to account for upper and low levels.

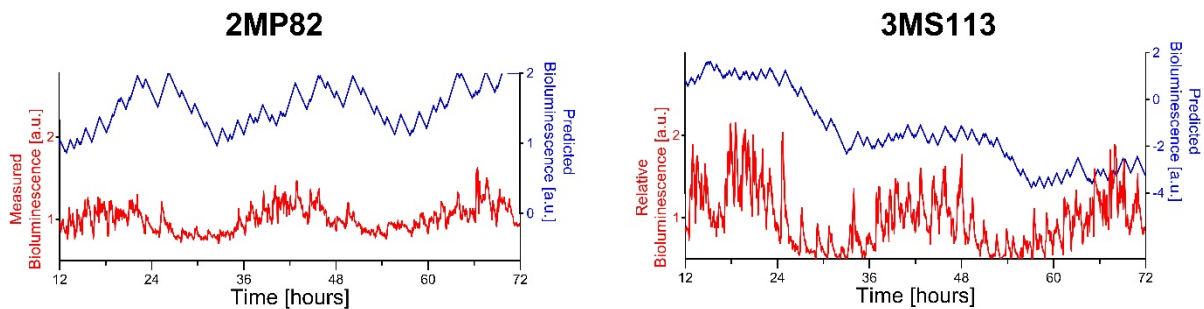


Figure 2-7 **Modelling PER2 bioluminescence based on the sleep-wake distribution** predicts the daily changes in bioluminescence in terms of phase. Mouse 3MS113 had excess sleeping, which caused the predicted PER2 bioluminescence to be below 0, due to the assumption of a linear relationship between the sleep-wake distribution and PER2 bioluminescence.

QUANTIFYING CENTRAL PER₂ BIOLUMINESCENCE AND SLEEP-WAKE STATE

Next, we aimed to record bioluminescence emitted from the brain in parallel to sleep-wake state. For these experiments, homozygous male B6 PER₂::LUC mice were implanted with EEG and EMG, a cannula to infuse luciferin in the right lateral ventricle and a glass cone that was placed on a depression made in the skull bone, allowing photons to pass from the left cortex. The use of the glasscone combined with central infusion of luciferin was previously used to measure bioluminescence emitted from the cortex with the Xenogen device (Curie et al., 2015). Luciferin had to be infused centrally because central PER₂ bioluminescence was not detected when administering luciferin peripheral (data not shown).

We successfully recorded uninterrupted sleep-wake state in six mice during the 2.5 days of baseline recording, a six-hour SD and two days of recovery. However, we were concerned about the quality of the bioluminescence data because of the following reasons.

First, the amplitude of the circadian dynamics of the bioluminescence recording appeared weak. In all but one mouse, the low values of bioluminescence occurring during the rest phase reached a floor effect, where the signal-to-noise ratio appeared to be too low to detect biological relevant

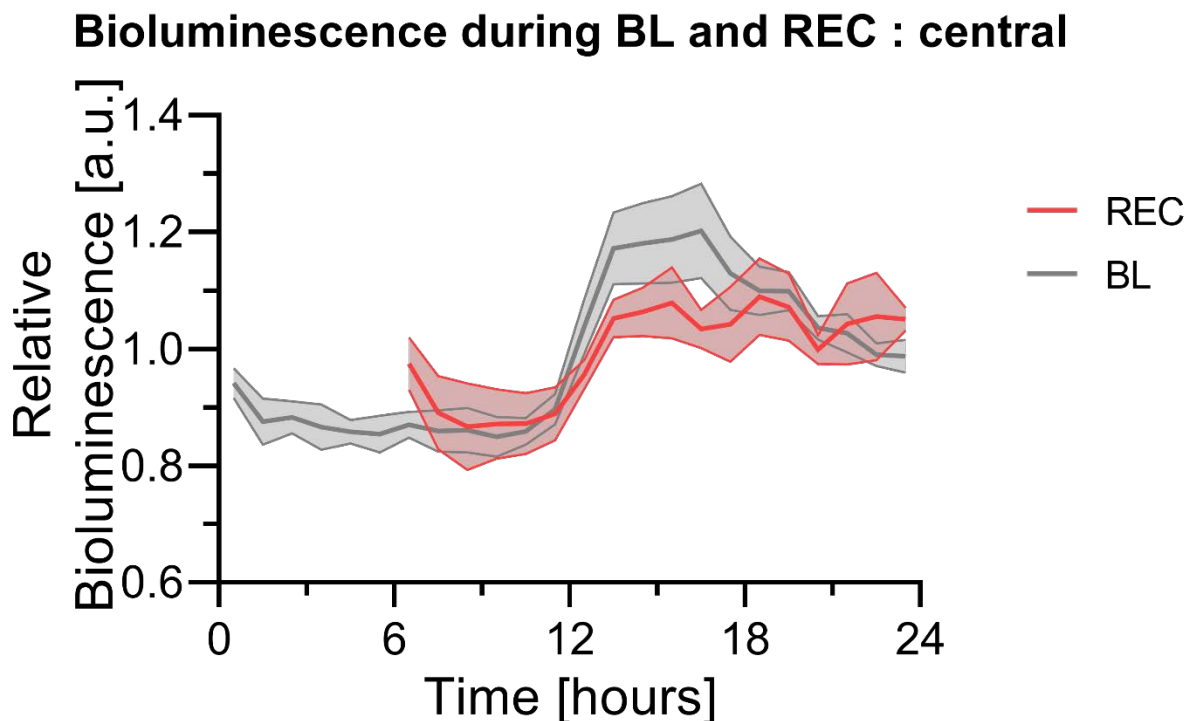


Figure 2-8 **Hourly relative normalized bioluminescence levels emitted by the cortex during the second baseline day and during the recovery.** No significant effect of sleep deprivation or sleep deprivation interacting with time was observed (RM ANOVA, factor Time and SD: resp.: $F(1,5)=1.3$, $p=0.31$; $F(17,85)=1.5$, $p=0.11$).

levels of bioluminescence. See Figure 2-13 in the Supplementary Data for the six recordings during the two-and-a-half baseline days, and note the high amplitude only in the first

mouse (A9522). Indeed, recordings from mice that are implanted with a 'sham' osmotic mini-pump (infusing a salt solution) still led to a detection of appr. 70 photons / 4sec as background bioluminescence. This value is close to the lowest levels detected in the mice implanted for central recordings of bioluminescence, as indicated by the stippled line in Figure 2-13, Supplementary Data.

Secondly, the previously reported increase in PER2 after SD was not significantly increased in our study as reported before (Curie et al., 2015) although it was close to reaching the preset significance threshold (paired t-test, $t(5)=2.2$, $p=0.078$). Altogether, it was decided to perform further experiments with peripheral PER2 bioluminescence only.

PER₂ BIOLUMINESCENCE UNDER REDUCED CIRCADIAN AMPLITUDE OF SLEEP

Under undisturbed conditions, it remains challenging to dissect the circadian and sleep-homeostatic driven contribution to Per2 expression, because sleep is gated by the circadian time. Previous studies lesioned the SCN (SCNx) of mice, thereby eliminating this circadian gating of sleep and thus the circadian amplitude of sleep. This method attenuated the amplitude of PER2 bioluminescence (Curie et al., 2015; Tahara et al., 2012), indicating that contribution of the circadian process to the sleep-wake distribution exerts an effect on PER2 bioluminescence.

In rats, a SD method is established where NREM sleep pressure as measured by EEG NREM delta power [1-4Hz] is kept relatively constant across the circadian day by applying enforced wakefulness for two hours every four hours over two days (Yasnikov & Deboer, 2010), here referred to as the 2hOn/Off protocol. This procedure is expected to mimic the sleep-wake distribution of a SCNx rodent while keeping the SCN intact. We investigated 1) if also in the mouse this protocol attenuated the daily amplitude in NREM sleep distribution and NREM sleep pressure and; 2) if the flattened sleep-wake distribution affects the circadian PER2 amplitude.

The effect of 2h on/off protocol on sleep-wake characteristics

Five EEG and EMG implanted and tethered SKH1 and BL6 male mice were kept for 48 hours to establish a baseline. At t=48h, mice were sleep deprived by gentle handling every four hours for two hours during two consecutive days. Both baseline days and sleep deprivation days were under dim red light conditions. One SKH1 mouse was excluded due to excessive sleeping during the SD. SKH1 mice are an outbred strain that have not been phenotyped for sleep. When we compared the sleep-wake parameters of B6 with SKH1 mice, it is interesting to point out that the prominent increase in waking during the subjective dark phase of B6 mice is unexpectedly attenuated in SKH1 mice (Supplementary Data, Figure 2-14). Nevertheless, the focus of the rest of this experiment is on the results of the SKH1 mice, because this strain of mice is also used in the peripheral PER2 bioluminescence experiment.

The two baseline days in constant darkness were significantly different from each other in terms of hourly NREM sleep-wake distribution (1-W RM ANOVA, factor DayxError: $F(3,9)=16.3$, $p=0.0005$). Because after-effects of entrainment wane over the course of constant darkness (Serge Daan & Pittendrigh, 1976), we decided to consider only the results of the second baseline day (BL) for further analysis. In comparison to BL, mice spent more time awake during the two sleep deprivation days (SD₁ and SD₂) and thus less time in NREM and REM sleep [% per average day, paired t-tests, mean±SEM, awake: BL: 53.2 ± 1.3 , SD: 65.3 ± 1.9 , $t(3)=-7.4$, $p=0.005$; NREM BL: 39.5 ± 1.1 , SD: 30.2 ± 2.1 , $t(3)=6.1$, $p=0.009$; REM: BL: 7.3 ± 0.3 , SD: 4.5 ± 0.4 , $t(3)=5.1$, $p=0.01$].

First, we inspected the distribution of NREM sleep by accumulating this behavioral state per 4hrs during BL and SD₁ and SD₂ (Figure 2-9, lower graph). A 4hr time-interval was chosen to ensure that also the sleep that was occasionally caught during the the sleep deprivations, was accounted for. Indeed, the amplitude of the NREM sleep distribution was reduced across the sleep deprivation days in comparison to the baseline day (amplitude of sine fit, fixed period at 24hr, mean±SEM, BL: 12.75 ± 0.44 ; SD₁: 6.05 ± 1.24 ; SD₂: 5.74 ± 0.87 , paired t-test, BLvsSD₁: $t(3)=5.3$, $p=0.0135$; BLvsSD₂ $t(3)=6.1$, $p=0.009$). This reduction in amplitude was not different between the two sleep deprivation days ($t(3)=0.24$, $p=0.82$) (Supplementary Data, Figure 2-15). However, the amplitude of NREM sleep is still significantly greater than 0 during the 2hOn/Off protocol (one sample t-test, SD₁: $t(3)=4.9$, $p=0.02$, SD₂: $t(3)=6.6$, $p=0.007$), indicating that the sleep-wake distribution under this SD protocol is still modulated by a circadian process.

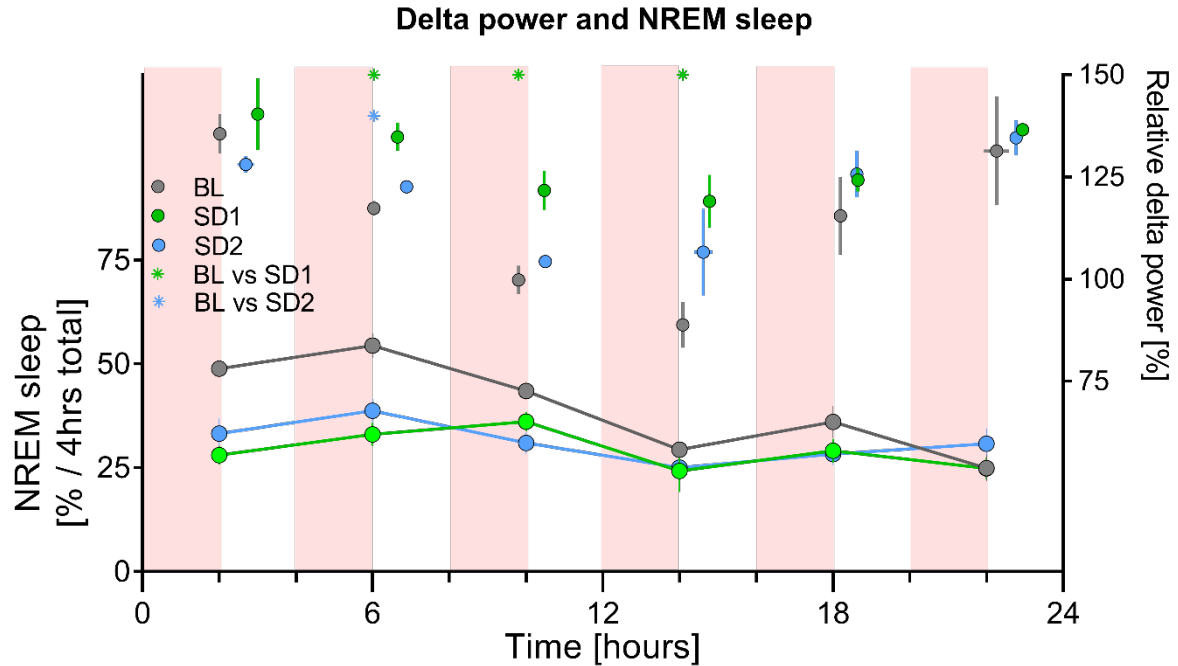


Figure 2-9 **Distribution of NREM sleep and delta power dynamics across the baseline and sleep deprivation days.** Data averaged per 4hrs, $n=4$, pink areas indicate timing of sleep deprivation during SD1 and SD2. For delta power, significant differences from BL to SD1-2 baseline are indicated by * (paired t-test).

Next, we assessed the effect of our protocol on NREM sleep pressure. To this end, NREM delta power was averaged across NREM sleep epochs per four hours (Figure 2-9, upper graph). The reduction in NREM delta during baseline conditions from ZTo to ZT12 (under the former LD conditions) was attenuated during the sleep deprivation days (2-way RM ANOVA; Cond: $F(2,54)=8.9$, $p=0.0005$), likely due to the reduction in NREM sleep.

These observations, reduced circadian amplitude of NREM distribution and of NREM EEG delta power compare, are partly alike the results obtained in the study from Yasenkov and DeBoer 2010. They concluded that most, if not all, of their circadian NREM sleep rhythmicity was abolished by their 2h sleep deprivation protocol, because it could not fit significantly to a 24-h cosine function (Yasenkov & Deboer, 2010). We also find a strong reduction in circadian amplitude of NREM sleep, but the amplitude is still >0 (see Figure 2-15) and therefore we concluded that the NREM sleep distribution is still circadian, albeit attenuated. Following on this, a significant effect of the sleep deprivation on NREM EEG delta power was observed (Figure 2-9), but there still appears to be a circadian rhythm (this has not been formally addressed yet).

We also collected locomotor activity (LMA) data from the EEG implanted mice by monitoring movements with passive infrared sensors (PIR). Because the experimenters' movements during the SDs are also captured by the PIR sensors, LMA data obtained during the SD and its corresponding

baseline values were omitted from analyses. As expected, time-of-day significantly affects hourly values of activity (2-W RM ANOVA, Factor Time: $F(11,99)=3.4$, $p=0.0005$). Surprisingly, we did not detect a significant effect of the 2hOn/Off protocol on LMA (Time x Cond, $F(22,99)=1.4$, $p=0.11$) (Figure 2-16, Supplementary data), underscoring the importance of using EEG-based measures to determine sleep-wake state. These data are in congruence with the observation that food intake across the 2hOn/Off protocol in the mice housed in the biolumicorder also shows a strong circadian component (Supplementary data, Figure 2-17).

Thus, sleep depriving SKH1 mice for two hours every 4 hours during two consecutive days attenuates the amplitude of the circadian sleep-wake distribution. The NREM delta power' dynamics are flattened accordingly by the intervention. However, a circadian modulation of the sleep-wake distribution is nevertheless still present.

The effect of 2hOn/Off protocol on PER2 bioluminescence

Next, we set out to determine PER2 bioluminescence dynamics under the same 2hOn/Off protocol in a separate cohort of mice, that were implanted with an osmotic mini-pump to deliver luciferin. After two habituation days in the RT Biolumicorder under LD, mice were kept in constant dark for two baseline days after which the 2hOn/Off protocol was initiated at, under previous LD conditions, ZTo. During the sleep deprivations, mice were taken from the RT Biolumicorder and sleep deprived in a different cage under constant dim red-light conditions. Therefore, bioluminescence was only measured during the 2-hours rest opportunities in between the SDs when the mice were in the RT Biolumicorder.

Like in the EEG study, only baseline day 2 (BL) and SD1 and SD2 were further analyzed. The bioluminescence dynamics are significantly different across these three days (3-way RM ANOVA, $F(46,138)=1.7$, $p=0.0107$) (Figure 2-10, upper panel). Is this due to a reduction in amplitude of bioluminescence? A sinewave was fit to the 30-min values of bioluminescence during SD1 and SD2 of the rest periods and the corresponding baseline values (GraphPad Prism, non-linear regression, sine wave with non-zero baseline, period>20Hr). A comparison of the amplitudes between BL, SD1 and SD2 is non-significant (paired t-test: BL versus SD1: $t(3)=1.95$, $p=0.15$; BL versus SD2: $t(3)=0.93$, $p=0.42$; see Figure 2-10) although three out of the four mice had a reduction in amplitude incurred by the 2hOn/Off protocol.

Thus, by imposing every four hours a two-hour sleep deprivation, we significantly attenuated the amplitude of the circadian distribution of NREM sleep. Based on our EEG experiment, we concluded that the 2hOn/Off protocol did not suffice in removing completely the circadian components of sleep-wake distribution. Although there are indications that the amplitude of bioluminescence was affected, this was not significant in our study, which could be due to an underpowered design.

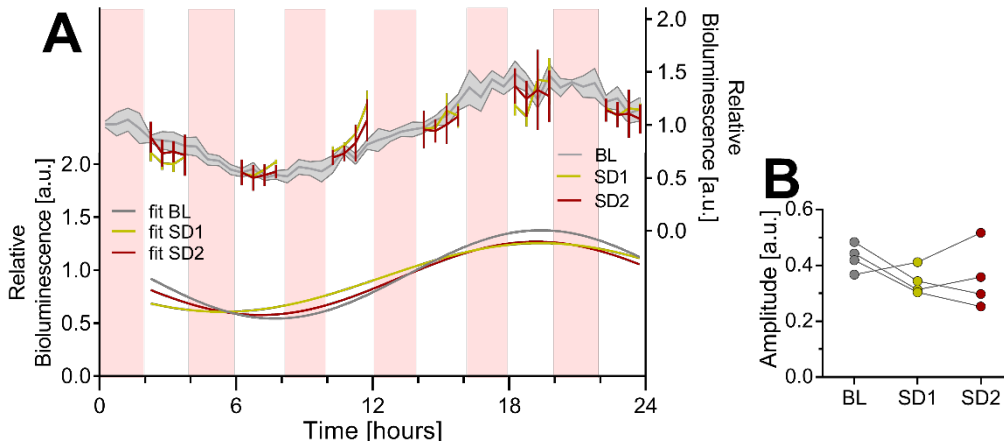


Figure 2-10 **Bioluminescence during the baseline recording and across the two sleep deprivation days.** Normalized bioluminescence from four SKH1 mice. Amplitude shows a decrease in 3 out of 4 mice from BL to SD1-2.

Discussion

In this study, we demonstrated that peripheral PER2 bioluminescence, mostly emitted by the kidneys, is changing as a function of spontaneous sleep-wake state. Reducing the circadian amplitude of the sleep-wake distribution by performing multiple short sleep deprivations across two days led to a reduction of the nycthemeral amplitude of NREM sleep and reduced the amplitude of PER2 bioluminescence in three out of the four mice studied. Altogether, these results support the importance of considering both circadian time and sleep-wake state when gauging PER2 levels.

Here, I will discuss further some biological and technical considerations of this study. Because our central recordings of PER2 bioluminescence are deemed not trustworthy, the focus in this discussion section will be on the peripheral results.

DIRECT VERSUS INDIRECT EFFECTS OF SLEEP-WAKE STATE ON PER₂ BIOLUMINESCENCE

The three different experiments indicated that sleep-wake state importantly contributes to PER₂ bioluminescence, but that the dynamics of these sleep-wake modulated changes in PER₂ bioluminescence appear to be different from experiment to experiment. First, sleep deprivation led to an increase in PER₂ bioluminescence during the first hours of the recovery phase, when mice spend more time asleep. This potentially contrasts with the results of the second experiment, where under undisturbed conditions, waking evoked increases and sleep decreases in PER₂ bioluminescence within half an hour, pointing a more direct regulation of sleep-wake states to PER₂ bioluminescence. Last, the 2hOn/Off sleep deprivation experiment, incurred a reduction in the amplitude of the circadian sleep-wake distribution and subsequently led to a reduction in the amplitude of the PER₂ bioluminescence signal in three out of the four mice measured. What can we conclude from these results? At the mechanistic level, we could differentiate between direct and indirect sleep-wake driven changes in PER₂ bioluminescence (experiment 2, and experiment 1 and 3, respectively).

There are several sleep-wake driven mechanisms that contribute directly to the expression of clock genes such as *Per2* (reviewed in (Franken, 2013)). An example of such a clock-independent mechanism is the glucocorticoid increase during sleep deprivation, which partly drives the sleep deprivation incurred increase in *Per2* (Mongrain et al., 2010). Furthermore, in a molecular arrhythmic liver of a rhythmic-behaving mouse, *Per2* is the only transcript that remains rhythmic, indicating that its expression can also be driven by rhythmic systemic cues (Kornmann, Schaad, Bujard, Takahashi, & Schibler, 2007). The next experimental chapter (Chapter 4), will explore further one of these mechanisms. Importantly, the effect of SD on clock gene expression is mostly reversed after 4 hours of recovery sleep (Wisor et al., 2002), implying that no clock shifting is incurred by the SD.

However, SD does not only affect PER₂ protein levels and *Per2* transcripts, but also the expression of other clock genes (*e.g.* *Dbp*, *Per1*, *Per3*, *Rev-erba*) (Mang et al., 2016; Maret et al., 2007; Mongrain et al., 2010; Wisor et al., 2002; Wisor et al., 2008). Impairment of the clock machinery by mutations modulates the SD incurred changes in *Per2* expression (Wisor et al., 2008). Furthermore, SD decreases the binding of CLOCK and BMAL₁ to some of their target genes (Mongrain et al., 2011). Together, this suggests that sleep-wake rhythms directly impinge on the clock machinery, thereby affecting its output in terms of clock gene expression.

Thus, the effect of wakefulness can: i) act on the expression of clock genes directly, as in the example of *Per2*; ii) impinge on the whole molecular clock which subsequently affects expression of clock genes, like the DNA-binding experiment showed; iii) act first on clock gene expression after which these changes affect the circadian clock machinery (an increase in PER2 will reduce the DNA binding of BMAL1 and CLOCK). An important experiment to be able to differentiate between these options, could make use of a mouse model where the molecular clock is arrested (Kornmann et al., 2007), thus leaving the effect of sleep deprivation on *Per2* to be completely attributed to mechanisms independent of the clock machinery.

IMPROVING CENTRAL RECORDINGS

We expected that the signal-to-noise ratio was too low in our central bioluminescence experiments. In the previous study, a region of interest was imaged and thus signals other than the one of interest were excluded (Curie et al., 2015). Other groups have improved the signal-to-noise ratio by implanting mice with optical fibers to quantify central bioluminescence in a specific area of the brain (see for example (Ono et al., 2015; Y. Yamaguchi et al., 2016)), which is a technique that could be considered when monitoring central PER2 and sleep-wake state.

Another improvement worth considering is amplification of the bioluminescence signal. A synthetic luciferin has been developed (Cyc-luc) that can travel across the blood-brain-barrier, has high intra-cellular uptake and a relatively slow half-life (Evans et al., 2014), which are all improvements over our current design. Moreover, the space saved from the cannula by administering the Cyc-luciferin peripherally can be used to monitor two cortices simultaneously instead of only one, thus further increasing the signal-to-noise ratio.

IS BIOLUMINESCENCE OR PER₂ SLEEP-WAKE DRIVEN?

We assume that bioluminescence levels directly reflect PER2 levels, because luciferase is expressed in parallel with PER2. In this assumption, luciferase should be the rate limiting step in the conversion of luciferin to oxy-luciferin (Yoo et al., 2004). That this expectation holds under *in vivo* conditions is supported by previous work from our lab, where the SD induced changes in bioluminescence levels in cortex and liver were paralleled with changes in PER2 protein levels in these organs, as quantified by western blot (Curie et al., 2015). However, there are some concerns about the quality of the data presented here, especially with respect to the changes in

bioluminescence that are associated with spontaneous changes in sleep-wake state. These concerns will be discussed here, and if possible, solutions will be proposed.

First, there are reasons to doubt that luciferin is in excess, ensuring thereby that luciferase is the rate limiting factor. A study thoroughly addressing these concerns found that -for their experimental design- luciferin needed to be above a concentration $0.2 \mu\text{g}/\mu\text{l}$ in blood plasma to be at sufficient concentrations (Hamada et al., 2016). We probably have ca. 20 times lower levels of luciferin in blood plasma (extrapolated from Hamada et al., 2016), thus the luciferin concentration in our experiment might not be in excess and thereby be a rate-limiting step.

Another consideration is that the supply of luciferin by the osmotic mini-pump is unlikely to be completely constant. Temperature changes with sleep-wake state, thereby affecting the release rate of the osmotic mini-pump; *i.e.* an increase of 2°C , which is within the mouse's range of body temperature shifts (Refinetti, 2010), leads to a 10% increased release rate (Alzet, http://www.alzet.com/products/guide_to_use/pump_selection.html). Therefore, one may wonder if these possible (sleep-wake driven) changes in substrate availability contribute to bioluminescence dynamics. A study addressed this concern by quantifying PER2::LUC and *Bmal1-eluc* bioluminescence in the SCN. Because *Bmal1*'s expression occurs in opposite phase of PER2's and the same was noted for their bioluminescence (Ono et al., 2015), this is interpreted as an argument against an activity-driven release of luciferin. Also, our data showed that subcutaneous temperature and bioluminescence are ca. 4 hrs out of phase (data not shown), supporting that at least the large circadian changes in bioluminescence are not driven by changes in luciferin availability due to sleep-wake driven changes in temperature. Moreover, the bioluminescence measured from the CAG mice increased and decreased when body temperature is expected to be at its lowest and highest values, respectively, also arguing against sleep-wake driven luciferin availability.

Still, concentrations luciferin could be at the level where it acts as a rate limiting factor. Experiments can be performed with increasing concentrations of luciferin to test if the spontaneous sleep-wake evoked changes in bioluminescence are of similar magnitude at different luciferin concentrations. Another consideration for further experiments is the use of a different luciferin, as discussed above (Cyc-luciferin, (Evans et al., 2014)).

Besides substrate availability, changes in body posture could potentially affect the detection of bioluminescence signals [see (Saini et al., 2013), supplementary figure 3]. However, our transition analysis reveals that there is a lag between the change in sleep-wake state and the change in bioluminescence; thus, once mice enter sleep, bioluminescence continues to increase during the

first minutes after the transition before the signal starts to decrease. This makes it unlikely that sleep-wake evoked changes in PER2 bioluminescence are due to body posture.

Hence, a definitive answer to these concerns can only be provided by quantifying PER2 protein levels. Can changes occur in period-proteins over such a short time-scale as we observed during spontaneous sleep-wake behavior? Transcription of Period-1 can be induced within 10 minutes in the SCN after a light pulse (Shigeyoshi et al., 1997). For Period protein changes, studies have shown that these are detectable from 30-minutes *in vitro* (R. Cao et al., 2015) and within 1-hour *in vivo* (Al-Safadi et al., 2014) after exposure to a serum shock and forced swim test, respectively, while making use of conservative protein quantification techniques. Thus, the changes in PER2 bioluminescence that occur in parallel to changes in sleep-wake state might truly reflect changes in PER2 protein, but a sensitive quantification technique needs to be deployed to ensure this.

NEXT STEPS

In this study, we established a relationship between PER2 bioluminescence and sleep-wake state. Despite common believe, this points to an important contribution of sleep-wake state to clock gene expression. Modelling studies aim to address further the mechanisms underlying this relationship to understand the effect of sleep deprivation and spontaneous wakefulness on the expression of PER2. However, the methodological concerns raised should not be ignored. Results and conclusions drawn can thus be interpreted at the level of PER2 bioluminescence, until further studies have shown that PER2 protein levels are also changing as a function of spontaneous sleep-wake state.

Acknowledgements

We are greatly in depth to those who sacrificed their time and their sleep for the mouse' sleep deprivations: Lisa Härri, Yann Emmenegger, Charlotte Hor and Jeffrey Hubbard, and special thanks for those who were available during the graveyard shifts: Maxime Jan, Kostas Kompotis, Violeta Castelo-Szekely and Sonia Jimenez.

Material and Methods

The specifics of the following experiments are discussed: i) the preferable route of luciferin administration; ii) changes in spontaneous sleep-wake state in parallel to PER2 bioluminescence and iii) the zhOn/Off experiment. Please note that the technical details differ between experiments; they are specifically addressed.

MICE AND HOUSING CONDITIONS

Unless otherwise mentioned in the results section, mice were kept under a 12 h-light/12 h-dark cycle and were after surgery singly housed with food and water available *ad libitum*. Experiments that aimed to focus on cortical readings of bioluminescence were performed on C57BL/6J (B6) mice homozygous for the Per2::luciferase construct (Yoo et al., 2004). To obtain measurements from the periphery, B6 PER2::LUC mice were back-crossed with hairless SKH1 mice for several generations until these mice were hairless but still carried the PER2::LUC construct.

SURGICAL PROCEDURES AND EXPERIMENTAL DESIGN

Route of luciferin administration

Four male CAG mice were housed for two subsequent experiments in constant darkness in the RT Biolumicorder. Each experiment lasted at least six days. During the first experiment, 0.5 mg/mL luciferin was dissolved in the drinking water. At the end of this experiment, mice received subcutaneously an osmotic mini-pump (Alzet, model 1002) under light anesthesia (isoflurane; 2-4% mixed with O₂) containing 70 mg/mL of luciferin and were allowed to recover for two days before bioluminescence and activity was monitored during the second experiment in the RT Biolumicorder. The flow moderator on the osmotic mini-pump was conventional.

Spontaneous changes in sleep-wake state

To quantify sleep-wake state in parallel to PER2 bioluminescence, mice were implanted with electroencephalogram (EEG) and electromyogram (EMG) electrodes under deep ketamine/xylazine anaesthesia. Three gold-plated screws (frontal, parietal and cerebellar) were screwed into the skull over the right cerebral hemisphere, where the cerebellar screw served as a reference. Two additional screws were used as anchor screws. For the EMG, a gold wire was inserted into the neck musculature along the back of the skull. The EMG and three EEGs were subsequently soldered to a connector and cemented to the skull.

Peripheral PER2 bioluminescence

For the peripheral recordings, heterozygous male SKH1xPER2::LUC mice were implanted with an osmotic mini-pump (model 1002, Alzet; luciferin 35mg/mL) under light anaesthesia, two days before habituation to the RT Biolumicorder cage. Two of the five mice received the special flow moderator that lacks the phosphorescent properties that were observed with the conventional flow moderator (Alzet, color flow moderator, Blue, product number 0002609).

Central PER2 bioluminescence

For central recordings, homozygous B6 PER2::LUC male mice were implanted with EEG/EMG as described above and with a cannula delivering luciferin solution in the lateral ventricle. The cannula was implanted with a stereotax (1 mm lateral, ± 0.3 mm posterior to bregma and 2.2 mm deep) and connected to an osmotic mini-pump (model 1004, Alzet, luciferin: 70mg/mL) that was implanted subcutaneously. To detect bioluminescence emitted from the cortex, a depression was made in the skull opposite to the area where the cannula was implanted. A glass cylinder was placed on top of this depression and fixed with dental cement.

After the first recovery day, mice were habituated to the weight of the wireless EEG by attaching a dummy to their connector. 8-10 days post-surgery, mice were placed in the RT Biolumicorder (Lesa Technology SA, Geneva, Switzerland) at the end of the light phase (~ZT10-ZT12) for two days in LD to habituate to the novel environment. At the end of the second habituation day, the dummy was replaced with a wireless EEG (Neurologger, TSE Systems GmbH). After two-and-a-half days of baseline recording in constant darkness, mice were sleep deprived for six hours at a time they were expected to rest (ZT0 under LD conditions) by gentle handling. After SD, mice were placed back into the RT Biolumicorder for the subsequent two recovery days.

*2HR ON/OFF experiment*Mice to determine sleep-wake state

Five male B6 and SKH1 mice were implanted with EEG, EMG and thermistors to record brain and muscle activity, and brain temperature, respectively, to determine post-hoc sleep-wake state. The surgery took place under deep xylazine/ ketamine anesthesia; for details see (Mang & Franken, 2012). Briefly, six gold-plated screws (diameter 1.1 mm) were screwed bilaterally into the skull over the frontal and parietal cortices. Two screws served as EEG electrodes and the remaining four screws anchored the electrode connector assembly. As EMG electrodes, two gold wires were inserted into the neck musculature. A thermistor (General Electrics, P20AAA102M) was placed on top of the left cortex (2.5 mm lateral to the midline, 2.5 mm posterior to bregma). The EEG and

EMG electrodes and thermistor were soldered to a connector and cemented to the skull. Mice recovered from surgery during several days before they were connected to the recording cables in their home cage for habituation to the cable and their environment, which was at least 6 days prior to the experiment. The recovery and habituation was under LD 12:12 conditions.

During the baseline recording and sleep deprivation days, red light at very low intensity was present to allow the experimenters to visually observe the mice (spectral photometer (International Light Technologies), white light [PAR#21777]: 0.50 nE/m²/sec; blue light [+BLU#21853]: 0.0 nE/m²/sec; red light [TRED#22237]: 0.35 nE/m²/sec). Mice were sleep deprived for two hours with the 'gentle handling' method as described here (Mang & Franken, 2012). Deviations from the protocol were that paper tissue was provided at any times the mice appeared to be difficult to keep awake.

Mice for bioluminescence data collection

Mice were implanted with an osmotic mini-pump (Alzet, 1002, luciferin concentration: 35 mg/mL; blue flow moderator) two days before the habituation. At the end of the light phase (~ZT10-ZT12), mice were moved from their cage to the RT Biolumicorder for 2-3 days of habituation in LD. They were housed for 2.5 days in DD, after which the sleep deprivation was initiated at, under LD conditions, lights on (ZTo). At the start of each SD, mice were moved from the RT Biolumicorder and placed into a novel cage that was in the same room as the EEG-implanted mice. Fifteen minutes before the end of each SD, mice were brought back to their RT Biolumicorder cage.

DATA COLLECTION OF SLEEP-WAKE STATE

Spontaneous changes in sleep-wake state

During the first experiments, we used a version of the Neurologger where the batteries were placed outside of the logger (n=3 out of total of 5 mice of the peripheral recordings) and where the Neurologger also needed to be replaced after 2.5 days of recording. For technical and user-friendly reasons this version of the NeuroLogger was replaced by an updated version where the batteries are stored inside a tray, making the recording less prone to disruptions. Moreover, we could record for the full 5.5. days of recording with the same Neurologger.

Batteries (Hearing Aid; Ansmann, 312 PR41, 1.45 V 180 mAh) were inserted into the Neurologger. This insertion was timed with the clock of the computer that controlled the RT Biolumicorder to *post hoc* align the EEG/EMG signals with the bioluminescence. Time stamps provided by the SyncBox (NeuroLogger, TSE) were used to verify the start and end time of the EEG/EMG recording.

The cerebellar electrode was used as a reference for both EMG and EEG. Data was sampled at 256 Hz. After the recording, data was loaded in Somnologica (Somnologica 3, MedCare) to determine offline the mice's behavior as 'wakefulness', REM sleep' or NREM sleep' per 4-second epochs based on the EEG and EMG signals. To visually aid the scoring, the parietal signal was subtracted from the frontal signal to enhance the identification of slow waves and theta waves within the same trace. Wakefulness was characterized by EEG activity of mixed frequency and low amplitude, and present but variable muscle tone. NREM sleep (NREM) was defined by synchronous activity in the delta frequency (1–4 Hz) and low and stable muscle tone. REM sleep (REM) was characterized by regular theta oscillations (6–9 Hz) and EMG muscle atonia.

2HR ON/OFF experiment

EEG and EMG signals, T_{cx} and locomotor activity were recorded continuously for 96 h. The recording started at the beginning of the subjective rest phase, ZT0. The analog EEG and EMG signals were amplified (2,000 \times) and digitized at 2 kHz and subsequently down sampled to 200 Hz and stored. Like the EEG and EMG traces obtained with the Neurologger, the data was loaded in SomnoLogica and sleep-wake state was determined per 4-second epochs, as previously. The EEG was subjected to a discrete Fourier transformation yielding power spectra (range: 0–100 Hz; frequency resolution: 0.25 Hz; time resolution: consecutive 4-sec epochs; window function: Hamming). Hardware (EMBLA) and software (Somnologica-3) were purchased from Medcare Flaga (EMBLA, Thornton, USA). LMA was monitored with passive infrared activity (ActiMetrics, US, Wilmette) and recorded with ClockLab (ActiMetrics, US, Wilmette).

DATA ANALYSIS

Route of administration

Data was collected from mice housed for at least four subsequent days in DD in the RT Biolumicorder. Circadian time was determined to inspect the circadian changes in bioluminescence relative to locomotor activity. To this end, the period length per mouse was determined based on activity measurements (1-min resolution) by chi-square analysis in ClockLab. Subsequently, the activity and bioluminescence data were folded according to the period. The activity data was averaged per 10 minutes and activity onset was visually determined for each mouse and set at CT₁₂. The aligned activity and bioluminescence data were subsequently averaged per circadian hour. Data is visualized as mean \pm SEM. The bioluminescence data is expressed relative to the values half a day before and half a day later (moving average, window of 1440).

Spontaneous sleep wake state and bioluminescence

Bioluminescence and activity were sampled at a resolution of 4-seconds, which is the same resolution of the epochs for sleep-wake state determination. Data processing was subsequently performed in MatLab 2017b (The MathWorks, Inc., Natick, Massachusetts, United States). Linear trends were removed from the signal by the built in function 'detrend'. Subsequently, the bioluminescence signal was expressed relative to the overall mean per mouse to account for interindividual differences. Changes in PER2 would be expected to occur at a slower rate than 4-seconds. Therefore, sleep-wake and bioluminescence data are averaged per blocks of 3 minutes.

Transitions were detected on sleep-wake state data that was averaged per 3 minutes. With this resolution, we found blocks of wakefulness that visually accompany increases in bioluminescence. By setting the threshold at 50% (at least half of the time had to be spent in the designated state), and including transitions that lasted at least 15 minutes on both sides, we reliably detected wake- and sleep dominated bouts. A sinewave was fit through the bioluminescence data (averaged per 15 min) to determine occurrence of transitions on either the rising or falling limb (MatLab, $fit = Y_0 + a * \sin(\frac{2*pi}{b} * t + c)$).

2HR ON/OFF experiment

Sleep-wake state determination: Per four hours during BL, SD1 and SD2, an average of NREM EEG delta power [1-4Hz] is calculated per mouse and was normalized between individuals by expressing it relative to the mean delta power reached between ZT8 and ZT12 during the first two baseline days.

Bioluminescence data

Data obtained five minutes before and ten minutes after the sleep deprivations was excluded from analysis. Subsequent data normalization of the bioluminescence data was as above.

No correction for circadian time was made in either the 2HR ON/OFF experiment, nor in the experiment where spontaneous sleep-wake distribution was correlated with PER2 bioluminescence, implying that each individual mouse was measured at a slightly different circadian time.

STATISTICS

Statistics were performed in R (version 3.3.2) and Prism (version 7.0). The threshold of significance was set at $p=0.05$. Deviations from the mean are representing standard error of the mean. The specific use of statistical tests is addressed in the results section.

Supplementary data

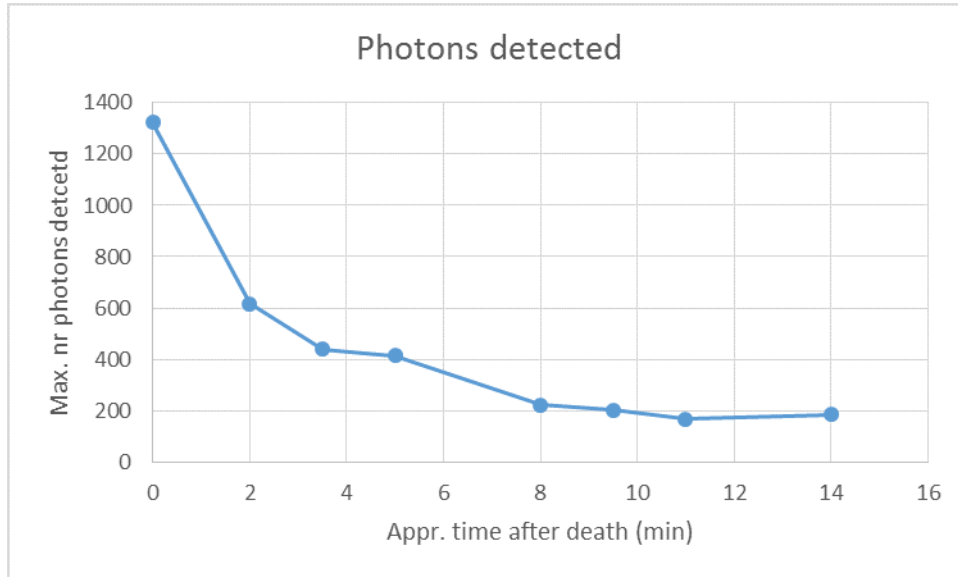
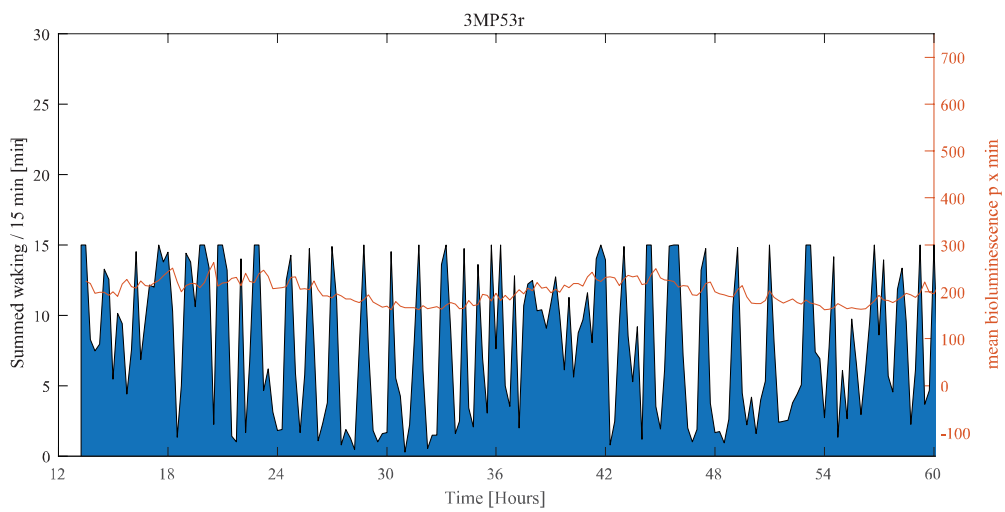
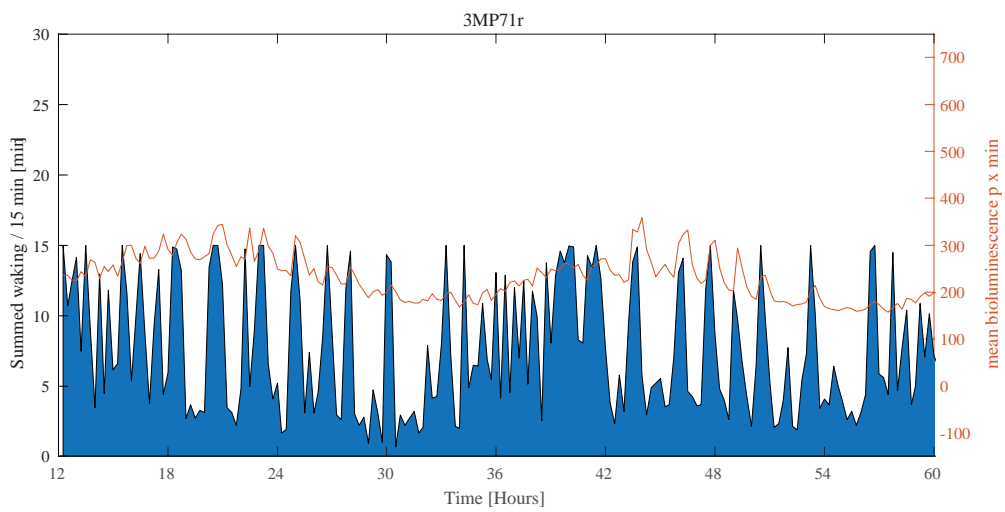
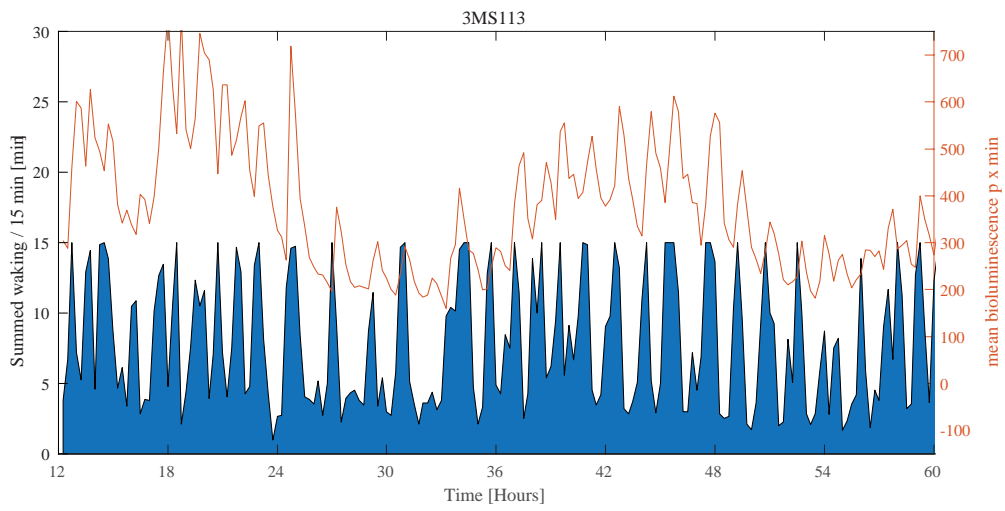


Figure 2-11 **The cap of the osmotic mini-pump emits photons.** After the mouse was sacrificed, bioluminescence was still detected around the area of the flow moderator cap. The number of photons rapidly decreased over time.

Bioluminescence recordings from the periphery combined with sleep-wake state



(1/2)

Bioluminescence recordings from the periphery combined with sleep-wake state
2/2

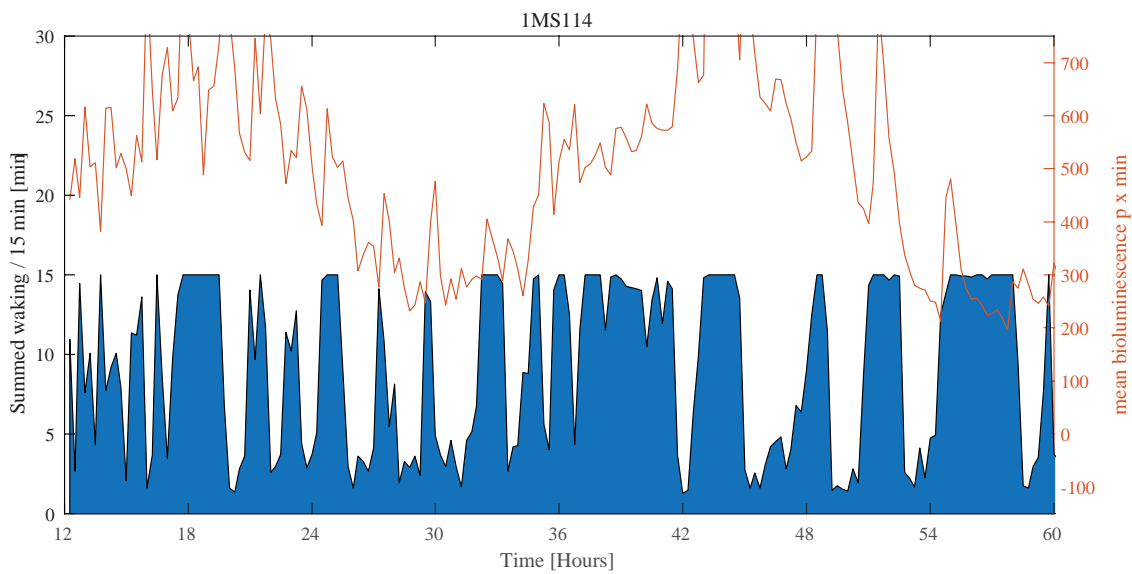
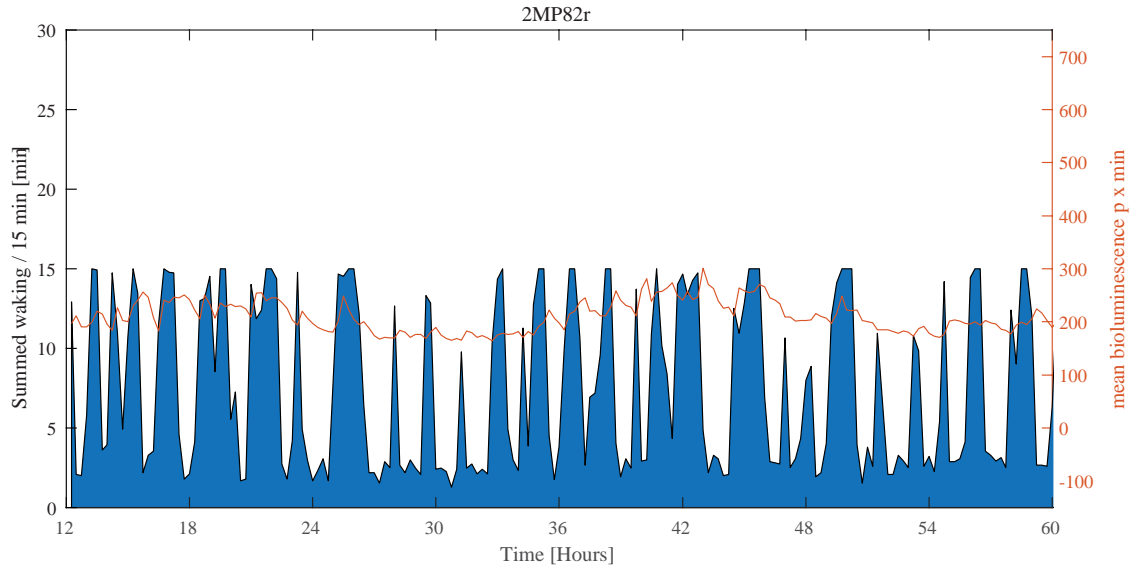
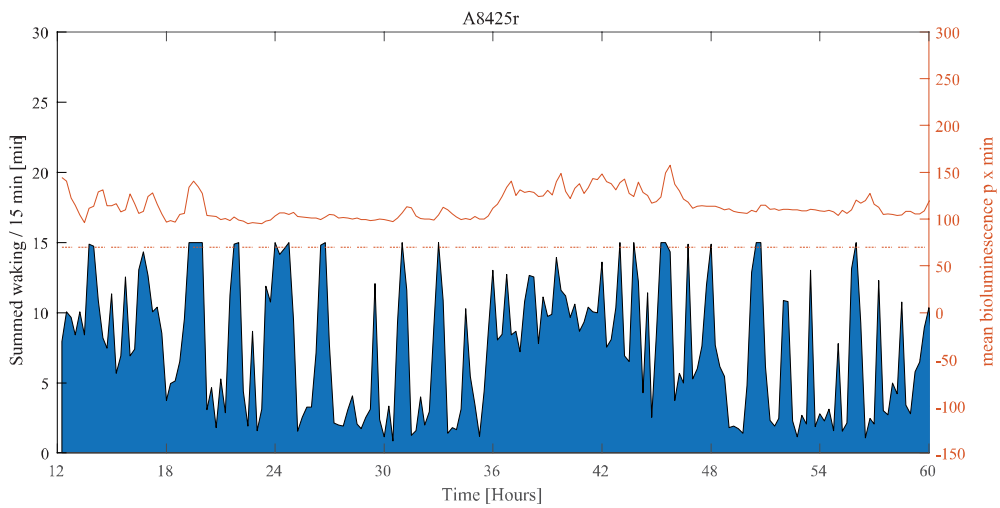
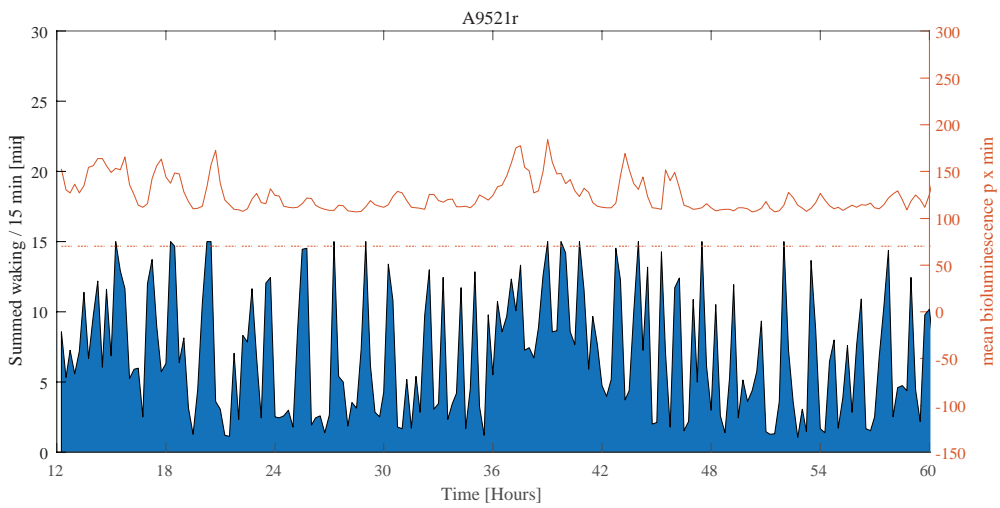
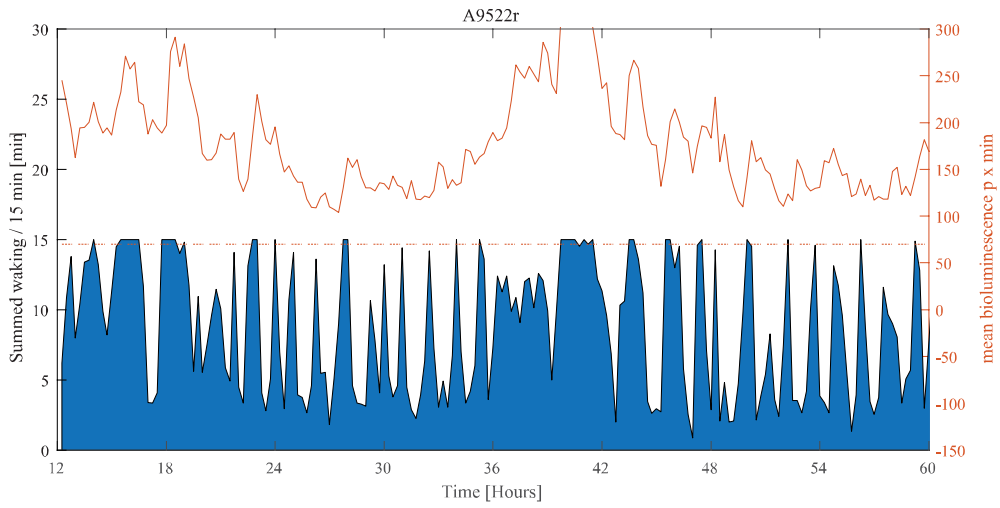


Figure 2-12 Raw data of sleep-wake state and bioluminescence from each individual mouse during the 2.5 days of baseline recording.

Central Bioluminescence recordings combined with sleep-wake state (1/2)



Central Bioluminescence recordings combined with sleep-wake state (2/2)

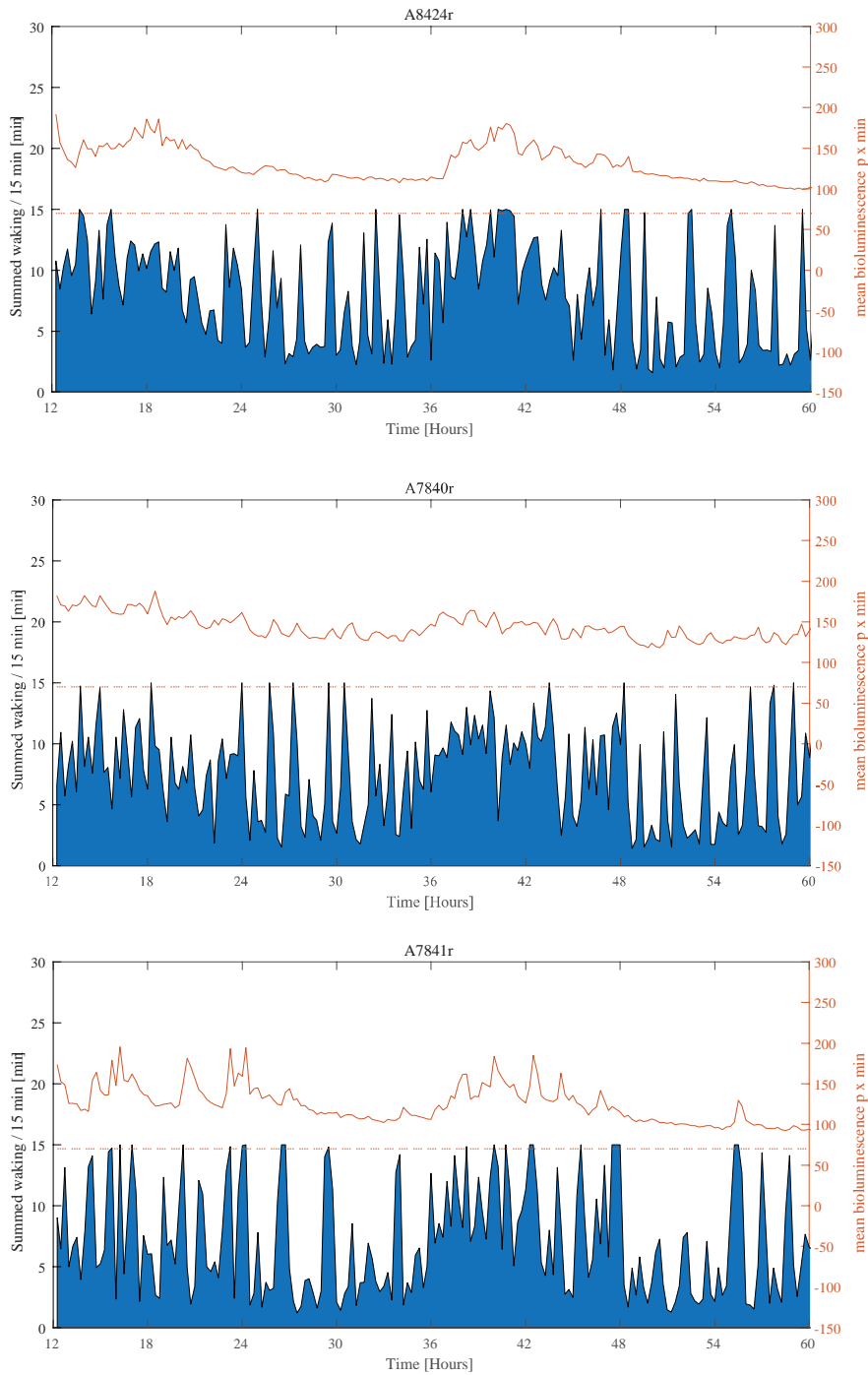


Figure 2-13 Recordings of central bioluminescence combined with sleep-wake state

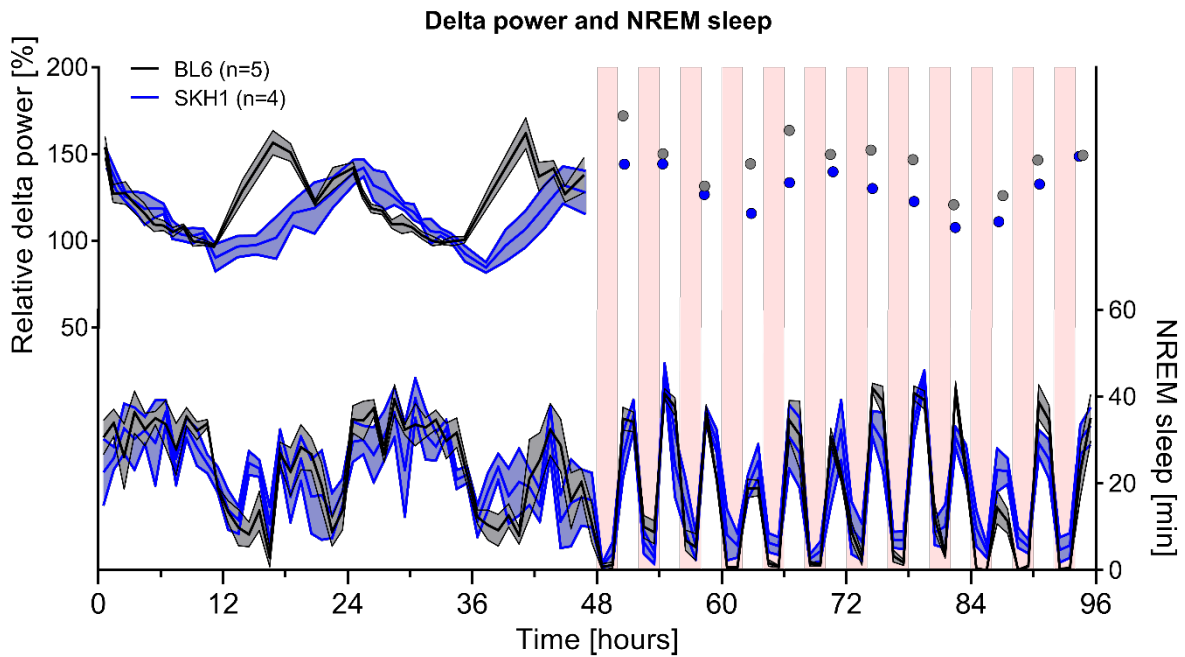


Figure 2-14 SKH1 & BL6 mice, NREM sleep and delta power. NREM delta power (upper panel) and NREM sleep (lower panel) in five B6 male mice and four SKH1 male mice across two baseline days and the two sleep deprivation days in constant darkness. The sleep deprivations are indicated by the pink areas. Note the attenuated reduction in NREM sleep in SKH1 mice during beginning of the subjective dark phase (T12-24, T36-48), correlating with the attenuated increase in NREM delta power (upper panel) in SKH1 mice. To understand if these changes in NREM EEG delta power are indeed induced by the changes in NREM sleep distribution, the sleep-wake distribution will be used to model the changes in sleep pressure (this is scheduled but not presented in this thesis). For subsequent analysis mentioned in the text, only the SKH1 mice are used

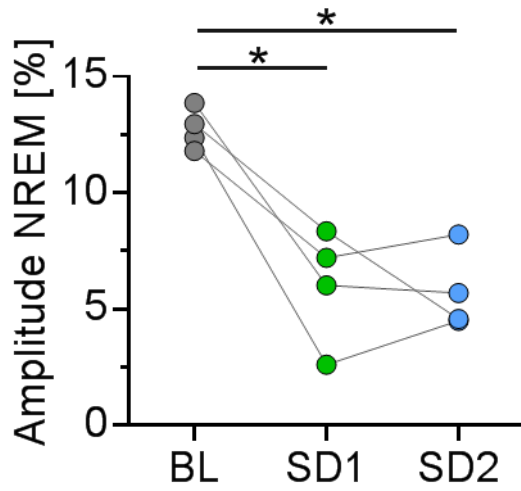


Figure 2-15 . The amplitude of NREM sleep is attenuated across the sleep deprivations days.

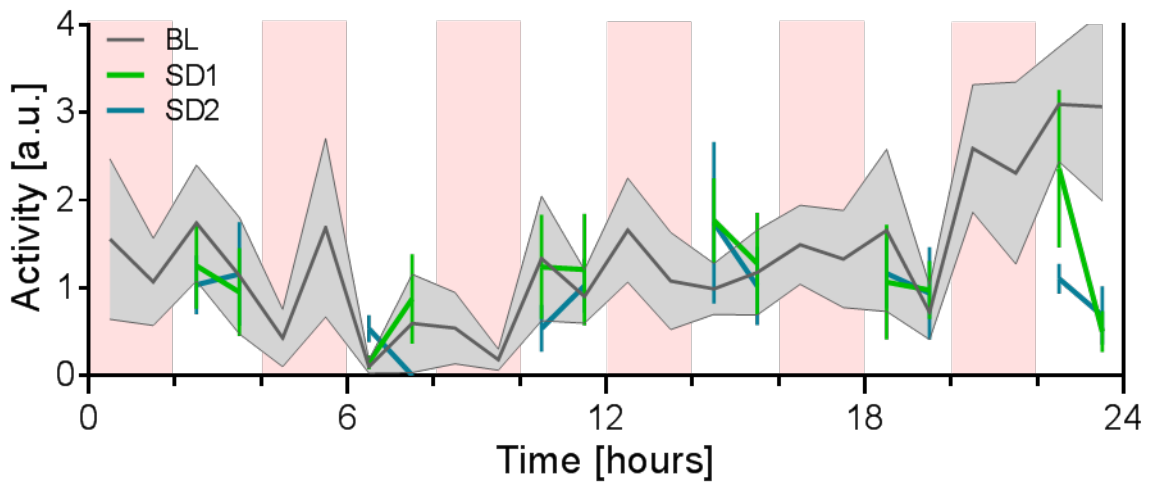


Figure 2-16 Activity measured in EEG implanted SKH1 mice. The averaged number of movements per hour (movements / minute) are not significantly affected by the sleep deprivation protocol compared to baseline movements at the subjective same Zeitgeber time.

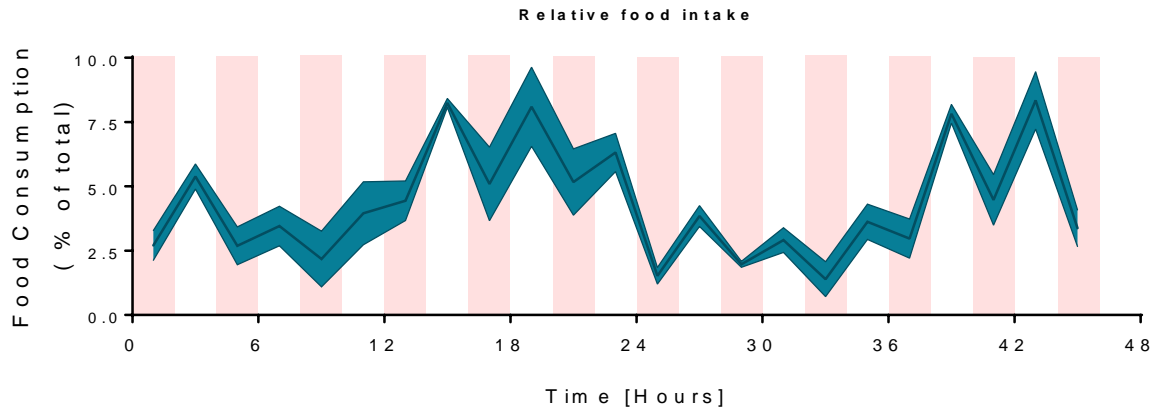


Figure 2-17 **Food intake during the two days of sleep deprivation shows a circadian oscillation.** Food intake was quantified every two-hours in the mice (n=4) housed in the biolumicorder during the 2hOnOff experiment. Be aware that baseline food intake was not measured and is therefore lacking.

Life ... is a relationship between molecules.

Linus Pauling

Chapter 3 Cold Inducible RNA Binding proteins: regulations and functions

RNA BINDING PROTEINS

RNA binding proteins (RBPs) are post-transcriptional regulators that shape the abundance of mRNA in time and space by binding and transporting mRNAs in the cell (Glisovic, Bachorik, Yong, & Dreyfuss, 2008). Furthermore, RBPs can induce alternative splicing (Fu & Ares, 2014), alternative polyadenylation (Erson-Bensan, 2016) and RNA editing. A well-known example of the latter is a nucleotide conversion in the transcript of the gene *Apob* by RBP RBM47, leading to two different protein isoforms that are separately expressed in the liver and small intestine (Fossat et al., 2014).

Malfunctioning of RBPs is associated with different diseases, among which the well-known Fragile X syndrome. This disease is caused by multiple CGG repeats in the 5'UTR region of the FMRP1-gene, leading to silencing of the gene and a subsequent decrease in levels of FMRP-protein. This leads to deregulation of mRNAs and protein synthesis in neurons, thereby giving rise to behavioral problems of people carrying the tandem repeat mutation (Bagni & Oostra, 2013). RBPs are associated with other neurological disorders, as well as with muscular atrophies, metabolic disorders and cancer (Cooper, Wan, & Dreyfuss, 2009; Darnell, 2013; Lukong, Chang, Khandjian, & Richard, 2008).

CIRBP AND RBM3

The Cold Inducible RNA Binding Protein CIRBP was simultaneously discovered in mouse testis upon cold shock (Nishiyama et al., 1997) and in human cancer cell lines after UV radiation (Sheikh et al., 1997). Soon thereafter, the RNA Binding Motif 3 protein RBM3 was also identified as being cold inducible in human cell lines (Danno et al., 1997). Because of their molecular and functional similarities, both RBM3 and CIRBP will be discussed in this chapter. CIRBP and RBM3 combined will be referred to under the abbreviation CRP, for Cirbp Rbm3 Proteins (CRP)s.

Gene, transcript, protein and localization

On the human genome, CIRBP is localized on chromosome 19, p13.3 and RBM3 is found on the X chromosome, 11.23 (UCSC Genome Browser). CIRBP and RBM3 proteins possess two RNA recognition sites at the N-terminal side to which mRNA can bind. An arginine-glycine rich domain is found in the C-terminal. Therefore, CRPs are part of the glycine-rich subfamily class IV of

proteins, which are highly conserved with respect to their amino acid sequences and function (Zhu, Buhner, & Wellmann, 2016). Homologs of human Cirbp are conserved in vertebrates, with a high similarity in mammals.

Isoforms of CRPs are described both at the mRNA and protein level. *Rbm3* has at least two different alternative splicing events that lead to different mRNA isoforms (summarized in Figure 3-1). An alternative splicing event between exon 5 and 6 adds an extra arginine residue (Arg+) and this correlates with the cellular localization of RBM3 in neuronal rat cultures (Smart et al., 2007). These two isoforms exist as well in mice. Data obtained from sleep deprivation studies revealed that the second alternative splicing event leads to a long and short 3'UTR of *Rbm3*. The short isoform decreases whereas the long isoform increases after sleep deprivation (see Figure 1 in Wang et al., 2010) (H. Wang, Liu, Briesemann, & Yan, 2010). The function of this opposite response is not clear, neither is the effect of sleep deprivation on the presence of the Arg(+) isoform.

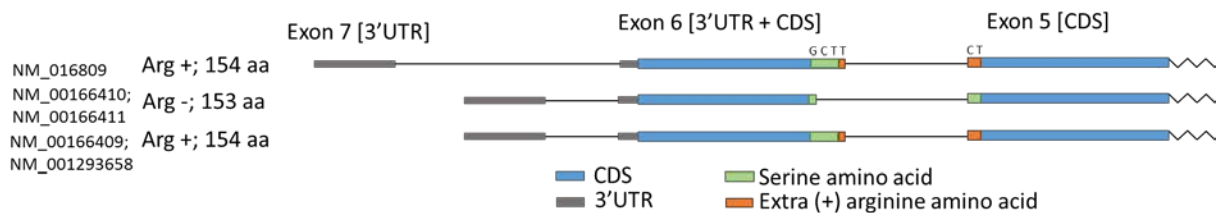


Figure 3-1 **The mouse *Rbm3* isoforms.** The long isoform only exists with an extra arginine residue, while the short isoform exists both and with and without the arginine.

REGULATION OF CRPs BY TEMPERATURE

What mechanism mediates the effect of temperature on CRPs transcript and protein levels? Several studies aimed to answer this question, of which the majority focused on Cirbp. Temperature can affect the transcription start site of *Cirbp* (Al-Fageeh & Smales, 2009), but not via the use of different promoters (Al-Fageeh & Smales, 2013). So-called Mild Cold Responsive Elements have been detected in the 5'UTR of *Cirbp*, mediating the effect of low temperature (32°C) on *Cirbp* levels via the transcription factor Sp1. The binding of this transcription factor is temperature dependent (Sumitomo et al., 2012). However, these two mechanisms, different transcription start sites and temperature-dependent activity of transcription factors, were not reproduced in a recent study. Instead, temperature was demonstrated to directly affect the splicing efficiency of pre-CIRBP-mRNA, thereby determining the amount of mature transcript, with lower temperatures [33°C] accompanied by higher splicing efficiency (Gotic et al., 2016). It was suggested that a similar

mechanism occurs for *Rbm3* transcripts (see table S6 of Gotic et al., 2016). Pharmacological blocking of the temperature-sensitive TRPV-4 channel protein attenuates the effect of hypothermia on CRPs protein levels (Fujita et al., 2017), but this can be compensated for by TRPV₃ and TRPV₈ channels (Fujita et al., 2018). RBM₃'s translational temperature dependency is linked to the internal ribosome entry site, which exhibits increased translation efficiency at lower (32°C) temperatures (Chappell, Owens, & Mauro, 2001). A recent study suggested another mechanism: the increase in RBM₃ after exposure to 32°C was due to reprogramming of the translome, thereby favoring the translation of cold-inducible proteins (Bastide et al., 2017).

Further studies need to assess the exact contributions of these temperature sensitive mechanisms, and if they differ between for example cell types and organisms.

ASSOCIATIONS AND FUNCTION OF CRPs

Development

RBM₃ levels change throughout development of the brain. The highest expression of RBM₃ in the rat is found during early development, after which overall RBM₃ levels decrease (Chip et al., 2011). RBM₃ levels remain relatively elevated in zones of high translation rates such as the subparaventricular zone and the dentate gyrus in the rat (Pilotte, Cunningham, Edelman, & Vanderklish, 2009). Interestingly, these changes in RBM₃ levels during the first days (until ca. P10) are paralleled by changes in sleep-wake state and EEG spectral composition (Cirelli & Tononi, 2015), posing the exciting possibility that RBM₃ is also functionally involved in neuronal development.

Hibernation

Another phenomenon which is characterized by changes in CRPs, sleep-wake state and EEG spectral composition, is hibernation. During hibernation, core body temperature decreases dramatically. RBM₃ transcript increases upon hibernation in liver, heart, brain [golden mantled ground squirrel] (Williams et al., 2005), as well as in skeletal muscle, liver, heart, brown adipose tissue and hypothalamus [arctic squirrels] (Yan, Barnes, Kohl, & Marr, 2008). In hibernating black bears, *Rbm3* increases in liver and heart (Fedorov et al., 2011), but this finding has not been confirmed at the protein level (Epperson, Dahl, & Martin, 2004; Shao et al., 2010).

Several times during the hibernation season, hibernators undergo synaptic remodeling which is characterized by a massive loss of neuronal connectivity that is rewired upon euthermia (reviewed in (Arendt & Bullmann, 2013)). During these euthermia bouts, animals enter NREM sleep which is accompanied by a spectacular increase in NREM EEG delta power (S. Daan, Barnes, & Strijkstra, 1991; Trachsel, Edgar, & Heller, 1991) (Figure 3-2). This observation is contradicting the SHY hypothesis (see Chapter 1), because instead of downscaling during sleep, the increased NREM EEG delta power correlates here with rewiring of the synaptosome.

What mechanisms underlie these massive changes in the brain? A study that artificially induced hypothermia in mice as a model for hibernation found that the synaptic re-formation depends on RBM3 (Peretti et al., 2015), which is downstream regulated by the cold-induced protein RTN3 (Bastide et al., 2017). As opposed to RBM3, CIRBP is less likely to play a prominent role in hibernation, as its expression is not affected by hibernation in the cited studies. However, one study found that alternative splicing of *Cirbp* occurs in the heart of hibernating hamsters, possibly facilitating faster CIRBP protein synthesis upon entering hibernation (Sano, Shiina, Naitou, Nakamori, & Shimizu, 2015), although no data corroborating this suggestion has been published so far.

Role of CRPs in the central nervous system

Given RBM3s' exciting function in hypothermia, it would be interesting to know if CRPs are in other ways contributing to neural functioning. RBM3 enhances local protein synthesis in dendrites upon cold exposure (Smart et al., 2007), which is conveyed through

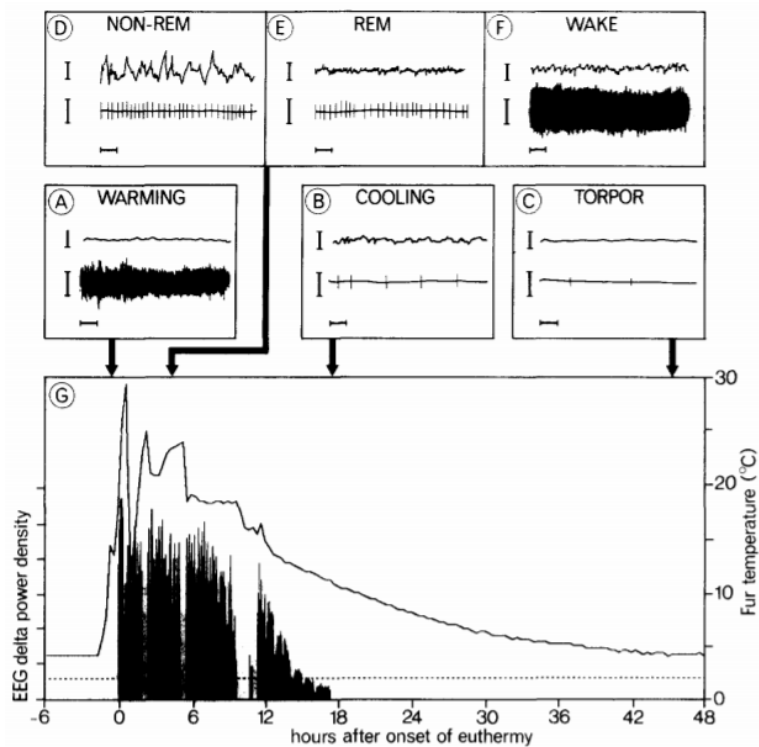


Figure 3-2 **Brain activity, muscle tone and fur temperature during hibernation.** EEG and EMG traces of three different sleep-wake states (upper panel; D-F), during three different 'thermic' states (middle panel; A-C) and delta power during NREM sleep (lower graph) of a hibernating ground squirrel (Daan et al., 1991).

downregulation of miRNAs (Dresios et al., 2005; Pilotte, Dupont-Versteegden, & Vanderklish, 2011), although another study was unable to confirm this mechanism (Bastide et al., 2017). In contrast, they found that the transcription machinery is reprogrammed upon cold exposure thereby favoring a relative increase in the translation of CRPs, thereby enabling cold-induced proteins to escape global protein synthesis downscaling during hypothermia (Bastide et al., 2017).

Hypothermia is the most robust neuro-protecting treatment to limit brain damage (Dietrich, Atkins, & Bramlett, 2009). In the cascade of changes initiated by hypothermia, is there also a role for CRPs? *In vitro*, both CIRBP and RBM3 inhibit apoptosis during hypothermia (32°C) (Chip et al., 2011; Saito et al., 2010), CIRBP possibly via acting on the H₂O₂-induced apoptosis (S. Li, Zhang, Xue, Liu, & Zhang, 2012). Moreover, *in vivo* silencing of CIRBP attenuates the protective effect hypothermia has on traumatic brain injury induced apoptosis (G. Wang et al., 2016).

Sleep and circadian rhythms

To date, no specific study has specifically addressed the role of CRPs in the regulation or function of sleep and wake. However, some interesting observations regarding associations between sleep-

The effect of sleep deprivation on CRPs						
Species	Tissue	Sleep deprivation /waking leads to:	Technique used	SD-specs	Miscellaneous	Study
Mouse	Cortex	<i>Cirbp</i> and <i>Rbm3-short</i> decrease, <i>Rbm3-long</i> increase	Micro-array (Affymetric 430_2)	GH	Time course study	(Maret et al., 2007; H. Wang et al., 2010)
Mouse	Cortex	<i>Cirbp</i> and <i>Rbm3-short</i> decrease	Micro-array (Affymetric Mouse Gene 1.0 ST array)	GH, 6hrs (ZTo-ZT6)	Changes are observed despite adrenalectomy	(Mongrain et al., 2010)
Mouse	Liver	<i>Cirbp</i> and <i>Rbm3-short</i> decrease	Micro-array (Affymetric 430_2)	GH, 6hrs (ZTo-ZT6)	x	(Maret et al., 2007)
Mouse	Cortex - astrocytes	<i>Cirbp</i> decrease	Micro-array (Affymetric 430_2)	3 groups: sleep, spontaneous wakefulness and enforced wakefulness (4hrs)	x	(Bellesi, de Vivo, Tononi, & Cirelli, 2015)
Mouse	Hippo-campus	<i>Cirbp</i> and <i>Rbm3-short</i> decreased, <i>Rbm3_long</i> increased	Micro-array (Affymetric 430_2)	GH; 5hrs (timing differs across experiments)	x	(Vecsey et al., 2012)
White-crowned sparrow	Cortex	<i>Cirbp</i> decreases	Micro-array (Affymetric Chicken GeneChip)	Human presence for 6hrs	x	(Jones, Pfister-Genskow, Benca, & Cirelli, 2008)
Humans	Blood transcriptome (majority of RNA from leukocytes)	Decrease in <i>Cirbp</i> and <i>Rbm3</i>	Micro-array (G2514F, AMADID 026817; Agilent + customized probes)	Forced desynchrony protocol	x	(Archer et al., 2014)
Mice	Cortex	Decrease <i>Cirbp</i> & <i>Rbm3-short</i> , increase <i>Rbm3-long</i>	RT-qPCR	GH; 6hrs starting at ZTo	x	(H. Wang et al., 2010)

Table 3-1 The effect of sleep deprivation on CRP-transcripts in different studies and species. GH: gentle handling.

wake state, circadian time and CRPs have been made and will therefore be further discussed here, as well as its implications.

After the discovery of CIRBP in cold-shocked testes of mice, the same research group investigated if daily rhythms in *Cirbp* could be observed. Their study revealed a robust rhythm of *Cirbp* in cortex and SCN, but not in testis and, unexpectedly, neither in liver. Moreover, no rhythm in *Cirbp* was detected in brain tissue of mice that were housed in constant darkness (Nishiyama et al., 1998). These findings are not confirming recent reports on daily rhythms in *Cirbp* in different tissues, including the liver. One could speculate that the rhythmic expression was present in the first studies, but that the assays used were not sensitive enough yet to detect those changes.

It was only a decennium later that *Cirbp* re-appeared in the rhythmic literature, when the transcript was identified as one of the few transcripts remaining rhythmic in a molecular arrhythmic liver of a behavioral rhythmic mouse (Kornmann et al., 2007). Subsequent experiments showed that sleep deprivation decreases the expression of *Cirbp* and the short isoform of *Rbm3* whereas it increases the expression of the long isoform of *Rbm3*, in different tissues and species (see Table 3-1). Experiments that controlled for sleep-wake state across the nycthemeron showed that most of the cortical variance of *Cirbp* and *Rbm3* in the mouse is driven by the sleep-wake distribution (see Figure 3-3) (Maret et al., 2007; H. Wang et al., 2010). Because the sleep-wake distribution also accounts for >80% of the variance in cortical temperature (Franken et al., 1992b), these changes in CRPs are likely to be conveyed through temperature.

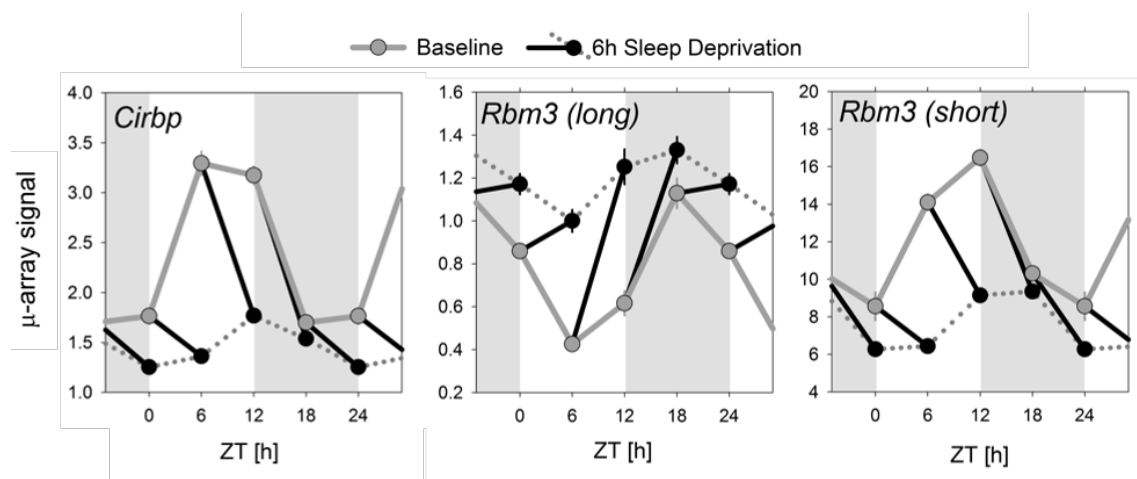


Figure 3-3 CRPs are mainly driven by the sleep-wake distribution. The nycthemeral amplitude of CRPs is significantly attenuated when controlling for sleep-wake state (mouse, cortex; Maret et al., 2007, based on GSE9442). Graphs by courtesy of Paul Franken.

This sleep-wake driven property of CRPs raises several exciting hypotheses. For instance, is RBM3 also functionally involved in the changes in synaptic connections that occur across waking and sleeping? Given that RBM3 (but not CIRBP) plays a crucial role in rewiring neurons after hypothermia, this poses the exciting possibility that RBM3 is also functionally involved in the sleep-wake driven modulations of synaptic connections. Another hypothesis is partly based on results from the circadian field, which showed that CIRBP and RBM3 are functionally implicated in the regulation of molecular circadian rhythms by mediating high amplitude clock gene expression in temperature synchronized cells *in vitro* (Liu et al., 2013; Morf et al., 2012); *i.e.* in the absence of CRPs, clock gene expression remains rhythmic albeit with lower amplitude. Two different, but not necessarily exclusive mechanisms, were held responsible for this observation. The first study found that reducing *Cirbp* by silencing its mRNA, affects the cellular localization of *Clock* (Morf et al., 2012), which in turn reduces the circadian amplitude of other clock genes. The second study discovered that both CIRBP and RBM3 are participating in alternative poly-adenylation, thereby affecting transcript stability (Liu et al., 2013). However, alternative poly-adenylation of core clock genes was not found to be compromised upon silencing of *Cirbp* and *Rbm3*, thus CRPs exert their effects on the clock via alternative poly-adenylation of other transcripts that in turn affect the amplitude of clock gene expression.

Could the changes in CIRBP during a sleep deprivation, possibly through changes in brain temperature, mediate the sleep deprivation-induced changes in clock gene expression? This question forms the base for the project discussed in the second experimental chapter.

An experiment is never a failure solely because it fails to achieve predicted results. An experiment is a failure only when it also fails adequately to test the hypothesis in question, when the data it produces don't prove anything one way or another.

Robert Pirsig

**Chapter 4 Cold-Inducible RNA-binding protein (CIRBP)
adjusts cortical clock gene expression and REM sleep
recovery following sleep deprivation in mice**

Marieke MB Hoekstra, Yann Emmenegger, Paul Franken

Center for Integrative Genomics, University of Lausanne, Lausanne, VD Switzerland

Summary and contributions

SUMMARY

The aim of this project was to investigate a possible mechanism through which the sleep-wake distribution contributes to changes in clock gene expression, namely via the cold-induced gene *Cirbp*. If CIRBP indeed conveys the sleep-wake driven changes in clock gene expression, *Cirbp* KO mice would exhibit an altered sleep homeostatic phenotype, based on the premise that clock genes function in sleep homeostasis. In this project, we determined i) the contribution of sleep-wake state and locomotor activity to cortical temperature in the mouse; ii) if the sleep deprivation induced changes in clock gene expression are dependent on CIRBP and iii) whether *Cirbp* KO mice have a different sleep homeostatic phenotype. We found that, like in other rodents, the sleep-wake distribution is the major determinant of changes in cortical temperature and that these differences are not affected by genotype. The sleep deprivation incurred changes of cortical *Rev-erba* were attenuated in the absence of CIRBP, whereas the expression of *Clock* and *Per2* was increased. *Cirbp* KO mice did not recover as much REM sleep lost after the sleep deprivation as compared to their WT littermates. CIRBP suppresses locomotor activity and modulates spectral composition of the EEG during active waking.

CONTRIBUTION TO THE PROJECT:

For this project, most of the experiments were initiated before I was involved. Therefore, my input for the design of the experiments was limited to the EEG recordings that included cortical temperature. The design of the other experiments was done by Paul Franken. Yann Emmenegger had started with the collection of the data. The analysis and visualization of the results, statistics and preparation of the manuscript was done by myself under the supervision of Paul Franken.

The implantation of mice with EEG and EMG was done by Yann Emmenegger. I contributed to the EEG/EMG implantation of mice with a thermistor. The sleep deprivations were performed with the help of all colleagues from the lab. Yann Emmenegger annotated the EEG data. The analyses of sleep-wake state, its spectral composition and cortical temperature were aided by algorithms in-house available (written by Paul Franken) and modified by myself wherever necessary.

Cortices and livers were collected and frozen by Yann Emmenegger. I homogenized the tissue, isolated RNA and transformed the latter into cDNA for RT-qPCR. Based on discussions with Paul Franken and Charlotte Hor (post-doc in our lab), I selected transcripts of interest. After Charlotte

Hor taught me how to design primers and probes, I designed the sequences and tested them for amplification efficiency before using them on the biological samples. Hannes Richter (Genomic Technologies Facility) provided support where necessary to perform the RT-qPCR and explained how to use the qBase software to analyze the results.

Abstract

Sleep depriving mice affects clock gene expression, suggesting that these genes partake in sleep homeostasis. The mechanisms linking wakefulness to clock gene expression are, however, not well understood. We propose CIRBP because its rhythmic expression is i) sleep-wake driven; ii) necessary for high-amplitude clock gene expression *in vitro*. We therefore expect *Cirbp* knock-out (KO) mice to exhibit attenuated sleep-deprivation (SD) induced changes in clock gene expression, and consequently to differ in their sleep homeostatic regulation. Lack of CIRBP indeed blunted the SD-incurred changes in cortical expression of the clock gene *RevErb α* , but amplified the changes in *Per2* and *Clock*. Concerning sleep homeostasis, KO mice accrued only half the extra REM sleep WT mice obtained during recovery. Unexpectedly, KO mice were more active during the dark phase and differed in neuronal oscillations during active waking. Thus, after SD, CIRBP adjusts cortical clock gene expression and expedites REM sleep recovery.

Keywords: mice, sleep, *Cirbp*, cortical temperature, clock genes, locomotor activity, REM sleep, circadian rhythms

Introduction

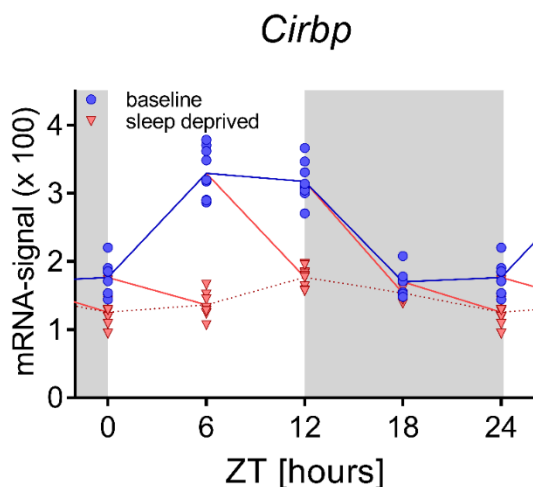
The sleep-wake distribution is coordinated by the interaction of a circadian and a sleep homeostatic process (S. Daan et al., 1984). The molecular basis of the circadian process consists of clock genes that interact through transcriptional/translational negative feedback loops. CLOCK/NPAS2:BMAL1 heterodimers drive the transcription of many target genes, among which *Period* (*Per1-3*), *Cryptochrome* (*Cry1, -2*), *Rev-Erbs* and *RORs*. Subsequently, PER:CRY complexes inhibit CLOCK:BMAL1 transcriptional activity and thus prevent their own transcription. In a secondary loop, REV-ERB α and ROR α regulate the transcription of BMAL1, and together with other transcriptional feedback loops, a stable period of ca. 24 hours is ensured (Lowrey & Takahashi, 2011).

The sleep homeostatic process keeps track of time spent awake and time spent asleep, during which sleep pressure is increasing and decreasing, respectively. The mechanisms underlying this process are to date unknown. However, accumulating evidence implicates clock genes in sleep homeostatic processes [reviewed in (Franken, 2013)]. This is supported by studies showing that mutations in circadian clock genes induce an altered sleep homeostatic response to sleep deprivation (SD) in several species [e.g. (Mang et al., 2016; Shaw, Tononi, Greenspan, & Robinson, 2002; Viola et al., 2007; Wisor et al., 2002)]. Furthermore, SD affects the expression of clock genes

such as *Rev-erba*, *Per2* and *Dbp* (Mongrain et al., 2010), but the mechanisms through which SD leads to changes in clock gene expression remain unclear.

In this study, we examined one such mechanism and hypothesized that the SD-induced changes in clock gene expression occur through Cold-Inducible RNA Binding Protein (CIRBP) (Mongrain et al., 2010). Decreasing temperature *in vitro* increases CIRBP levels (Nishiyama et al., 1997) and the daily changes in body temperature of the mouse are sufficient to drive robust cyclic levels of *Cirbp* and CIRBP *in vitro* (Morf et al., 2012). Although the daily changes in cortical temperature (T_{cx}) appear circadian, in the rat more than 80% of its variance is explained by the sleep-wake distribution (Franken et al., 1992b). Hence, the daily rhythms of cortical *Cirbp* become strongly attenuated when controlling for these sleep-wake driven changes in T_{cx} by SDs (see SFig1, based on Gene Expression Omnibus number GSE9442 from Maret et al., 2007). Furthermore, *Cirbp* is the top down-regulated gene after SD (Mongrain et al., 2010; H. Wang et al., 2010) underscoring again its sleep-wake dependent expression. But how does CIRBP relate to SD induced changes in clock gene expression?

We propose CIRBP as mechanism linking sleep-wake state information to clock gene expression because of its role in conveying temperature information to clock gene expression. More specifically, the temperature-driven changes in CIRBP are required for high amplitude clock gene expression in temperature synchronized cells (Morf et al., 2012) (Liu et al., 2013). Therefore, we (and others (Archer et al., 2014)) hypothesized that changes in clock gene expression during SD are a consequence of the sleep-wake driven changes in CIRBP. We used mice lacking CIRBP (*Cirbp* KO) (Masuda et al., 2012) to test this hypothesis. We first assessed whether also in the mouse the daily changes in T_{cx} are driven by the sleep-wake distribution and what the contribution of locomotor



Supplementary Figure-1 **The sleep-wake distribution drives daily changes of central *Cirbp* expression in the mouse.** At the onset of the baseline rest phase (ZT0), when mice spend more time asleep and thus T_{cx} decreases, *Cirbp* expression increases (blue symbols and lines), whereas at ZT12, when mice spent most of their time awake and T_{cx} increases, *Cirbp* decreases. When controlling for these diurnal changes in sleep-wake distribution by performing four 6h sleep deprivations starting at either ZT0, -6, -12, and -18, the diurnal amplitude of *Cirbp* is greatly reduced (red symbols represent levels of expression reached at the end of the sleep deprivations). Nine biological replicates per time point and condition from three different inbred strains of mice were used, and RNA was extracted from whole brain tissue (see Maret et al. 2007 for details). Data are accessible under GEO GSE9442.

activity (LMA) to these changes was. Because we expected that the SD led to changes in clock gene expression in KO mice, a sleep homeostatic phenotype was anticipated as well based on the premise that clock genes partake in sleep homeostasis (Franken, 2013).

Our experiments revealed that also in the mouse the sleep-wake distribution is the major determinant of changes in T_{cx} with a significant albeit small contribution of LMA. The data further demonstrated that lack of CIRBP did attenuate the sleep-deprivation (SD) induced changes in the cortical expression of *Rev-erb α* , whereas it unexpectedly augmented the sleep deprivation induced-response of *Per2* and *Clock*. In line with the role of clock genes in sleep homeostasis, *Cirbp* KO mice accrued only half the extra REM sleep WT mice obtained during recovery sleep, whereas no evidence of altered dynamics of NREM EEG delta power [0.75-4.0 Hz] was found. Unexpectedly, we noted that *Cirbp* KO mice were more active during the dark phase without increasing their time spent awake. This was accompanied by changes in neuronal activity during active waking. Altogether, our data suggests that *Cirbp* contributes to some of the SD induced changes in clock gene expression but also underscore that other sleep-wake driven pathways contribute as well.

Results

THE RELATION BETWEEN CORTICAL TEMPERATURE (T_{cx}), SLEEP-WAKE DISTRIBUTION, AND LOCOMOTOR ACTIVITY (LMA)

The dependence of T_{cx} on sleep-wake state has been demonstrated in a number of mammals (Alfoldi et al., 1990; M. A. Baker & Hayward, 1968; Deboer et al., 1994; Franken et al., 1992b; Hayward & Baker, 1968) but not in the mouse. Moreover, no study so far specifically controlled for LMA when quantifying the contribution of sleep-wake state to T_{cx} . We therefore measured T_{cx} , LMA (determined with passive infra-red sensors) and sleep-wake state (derived from electroencephalogram (EEG) and electromyogram (EMG) recordings) in wild-type (WT) and *Cirbp* KO mice during two baseline days, a 6hr SD and the subsequent two recovery days. Because the relationship between T_{cx} , LMA, and waking in WT and KO mice was alike, we illustrated the results in WT mice only.

Fast changes in T_{cx} occur at sleep-wake state transitions

A representative example of a 96h recording of LMA, sleep-wake state and T_{cx} is depicted in Figure 1. Consistent with mice being nocturnal animals, the mouse shows more waking and LMA

and overall higher T_{cx} levels during the dark phase. Sleep depriving mice by gentle handling on the third recording day from ZTo-6 led to an almost uninterrupted period of 6hr waking during which LMA and T_{cx} reached values comparable to bouts of spontaneous wakefulness under undisturbed baseline conditions (*i.e.*, ZT12-18). A closer inspection of the rapid changes in T_{cx} suggest that sleep-wake state transitions underlie these fluctuations. We further quantified these sleep-wake evoked changes in T_{cx} by selecting and aligning transitions between consolidated bouts of NREM and REM sleep and wakefulness during the two baseline days (Fig 1B). When entering NREM sleep, T_{cx} consistently decreased, whereas at a transition into wake and REM sleep, T_{cx} increased. The latter transition was characterized by a fast and consistent change in T_{cx} ; within 1.5 minutes, T_{cx} increased by 0.4°C. The subsequent transition from REM sleep into wake leads to an initial decrease in T_{cx} and contrasts with the waking-evoked increase in T_{cx} when transitioning from NREM sleep to wake. Altogether, these results provide evidence that sleep-wake state importantly contributes to changes in T_{cx} . The sleep-wake state evoked changes in T_{cx} at these transitions did not differ between genotypes (2-way RM ANOVA, factors GT and Time; GT: $p > 0.13$, GTxTime: $p > 0.09$).

Daily cycles in T_{cx} are determined by sleep-wake state

Can the rapid changes in T_{cx} , evoked by sleep-wake state transitions, explain the large daily amplitude (Fig.2A)? We investigated how waking and LMA relate to diurnal changes in T_{cx} by inspecting these variables per hour. The LMA data was \log_2 transformed to allow for parametric assessment. T_{cx} , waking and LMA oscillated over the course of the 24h averaged baseline day (BL) (2-way RM ANOVA, Factor Time: $F(23,207)=70.5; 27.2; 22.5$; $p < 0.0001$, respectively, Fig2A; Factor GT x Time (1,24); T_{cx} : $F(23,207)=0.9$, $p=0.63$; waking: 1.7, $p=0.03$, LMA: 1.21, $p=0.24$). The amplitude in T_{cx} during baseline (BL), calculated as the averaged differences between the highest and lowest hourly value of the two baseline days, did not differ between genotypes (WT: 2.34 ± 0.1 , KO: 2.33 ± 0.1 ; t-test: $t(9)=-0.02$, $p=0.98$). The time course of waking and LMA both resembled that of T_{cx} . This observation was supported by the strong correlation between T_{cx} and waking (waking: Fig 2B left; WT: $R^2=0.76$; KO: $R^2=0.81$, $p < 0.0001$) and between T_{cx} and LMA (Fig 2B right: WT: $R^2=0.60$; KO: $R^2=0.72$, $p < 0.0001$).

To assess the influence of waking on T_{cx} at a time of day when T_{cx} is normally low and mice spend most of their time asleep, mice were sleep deprived between ZTo and ZT6. The SD successfully increased waking by 97% compared to time spent awake during BL at the same time of day (ZTo-6, paired t-test: waking [min/hour] BL: 21.7 ± 0.9 , SD: 58.6 ± 0.3 ; $t(10)=-38.1$, $p < 0.0001$), as

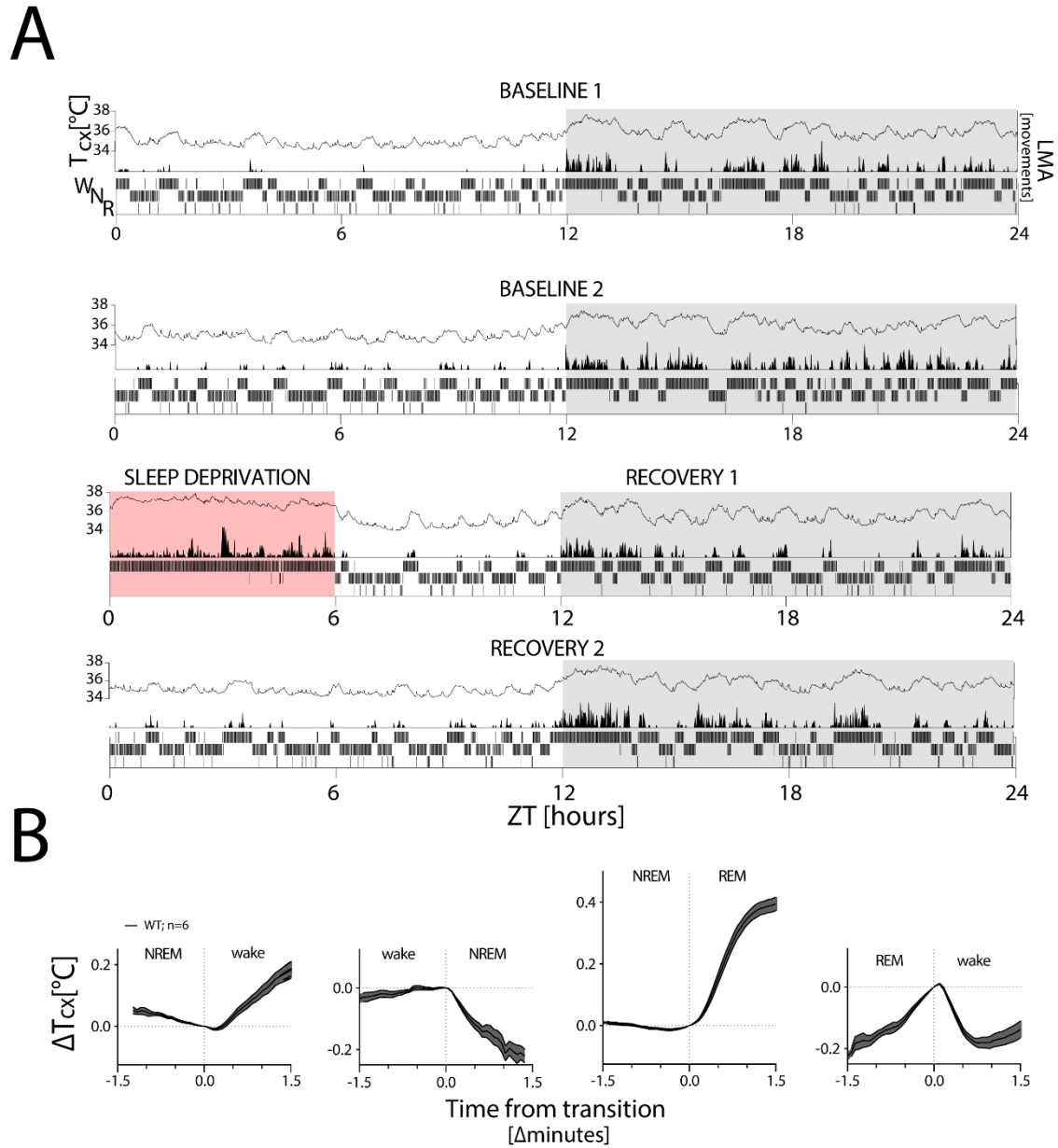


Figure 1 T_{cx} changes with sleep-wake state. (A) A representative four-day recording of one mouse in LD 12:12 (in white:grey) during two baseline days (top 2 panels), followed by a 6hr SD (in red; third panel) and two recovery days (bottom 2 panels), with within each panel T_{cx} (top; line graph), LMA (middle; area plot) and sleep-wake states (bottom; hypnogram). T_{cx} and sleep-wake states are averaged per minute to aid visualization; LMA is collected and plotted per minute (see Methods). (B) T_{cx} , depicted as mean \pm SEM, relative to T_{cx} at the sleep-wake transition (as determined by last value before and first value after transition). T_{cx} increases when transitioning from NREM sleep to wake and to REM sleep ($F(1,5)=22.6$; $p<0.005$ and $F(1,5)=229$; $p<0.0001$, respectively), decreases when transitioning from wake to NREM sleep ($F(1,5)=42.6$; $p=0.001$). The transition from REM sleep to wake did not significantly affect overall T_{cx} ($F(1,5)=1.8$, $p=0.24$). Transition data obtained from baseline recordings (see Methods for transition detection).

well increased LMA ($\log_2[\text{movements}]$, BL: 2.2 ± 0.3 , SD: 6.9 ± 0.1 ; $t(10) = -20.3$, $p < 0.0001$). These changes led to sustained elevated T_{cx} ($^{\circ}\text{C}$): BL: 34.7 ± 0.07 , SD: 36.6 ± 0.06 , $t(10) = -44.3$, $p < 0.0001$), suggesting that wakefulness and/or LMA drives changes in T_{cx} . Genotype did not contribute or interact with these changes (2-way ANOVA, GT*SD/BL: $p > 0.39$). However, factors accompanying the SD other than extended waking, such as stress, could have contributed to the SD-induced changes in T_{cx} . To address this issue, we selected within each mouse the longest uninterrupted spontaneous waking bout occurring during BL (average bout length: 100 ± 19 minutes). We then compared T_{cx} during the last 10 minutes of this spontaneous waking bout (to reduce any effects of differences in T_{cx} at bout-onset) with T_{cx} reached in the last 10 minutes of an equivalent time spent awake from the start of the SD on. T_{cx} reached during the SD and spontaneous wakefulness did not differ (Fig 2B; also not in KO mice: $t(5) = 0.84$, $p = 0.44$). Thus, factors other than extended wakefulness, such as light exposure and circadian time, which differed between the longest waking bout under BL from the SD conditions, do not importantly contribute to the changes in T_{cx} during the SD.

Considering the strong correlation between LMA and T_{cx} (WT: $R^2 = 0.72$; $p < 0.0001$; KO: $R^2 = 0.78$; $p < 0.0001$), it could be hypothesized that LMA explains partly the sleep-wake associated changes in T_{cx} . To investigate this further, the respective contribution of waking and LMA to changes in T_{cx} was quantified by a partial correlation analysis. Although LMA did significantly contribute, substantially more of the variance in T_{cx} was explained by waking in both genotypes (paired t-test on Fisher Z-transformed R^2 -values from each mouse's partial correlation of hourly waking and T_{cx} , and hourly LMA and T_{cx} : WT: $t(5) = 5.1$, $p = 0.004$; KO: $t(5) = 10.7$, $p = 0.0001$, and see also Fig 2D for R^2 -partial correlation coefficients, based on hourly data from all WT mice combined). We then determined the variance that could not be explained by the correlation between waking to T_{cx} (*i.e.* the residuals) by calculating the difference between the observed T_{cx} in a given hour and the predicted T_{cx} based on the time-spent-awake in that hour. The linear regression overestimated and underestimated T_{cx} during the light phase and dark phase, respectively (Fig 2E,F; BL1 and BL2). Fitting a sinewave through the residuals of the two baseline days revealed a circadian distribution, reminiscent of the circadian modulation of the residuals of this relationship in the rat (Franken et al., 1992b). However, considering also the residuals of the SD and recovery reveals a consistent parallel with the distribution of LMA expressed per unit of waking across the whole course of the experiment (Fig 2G).

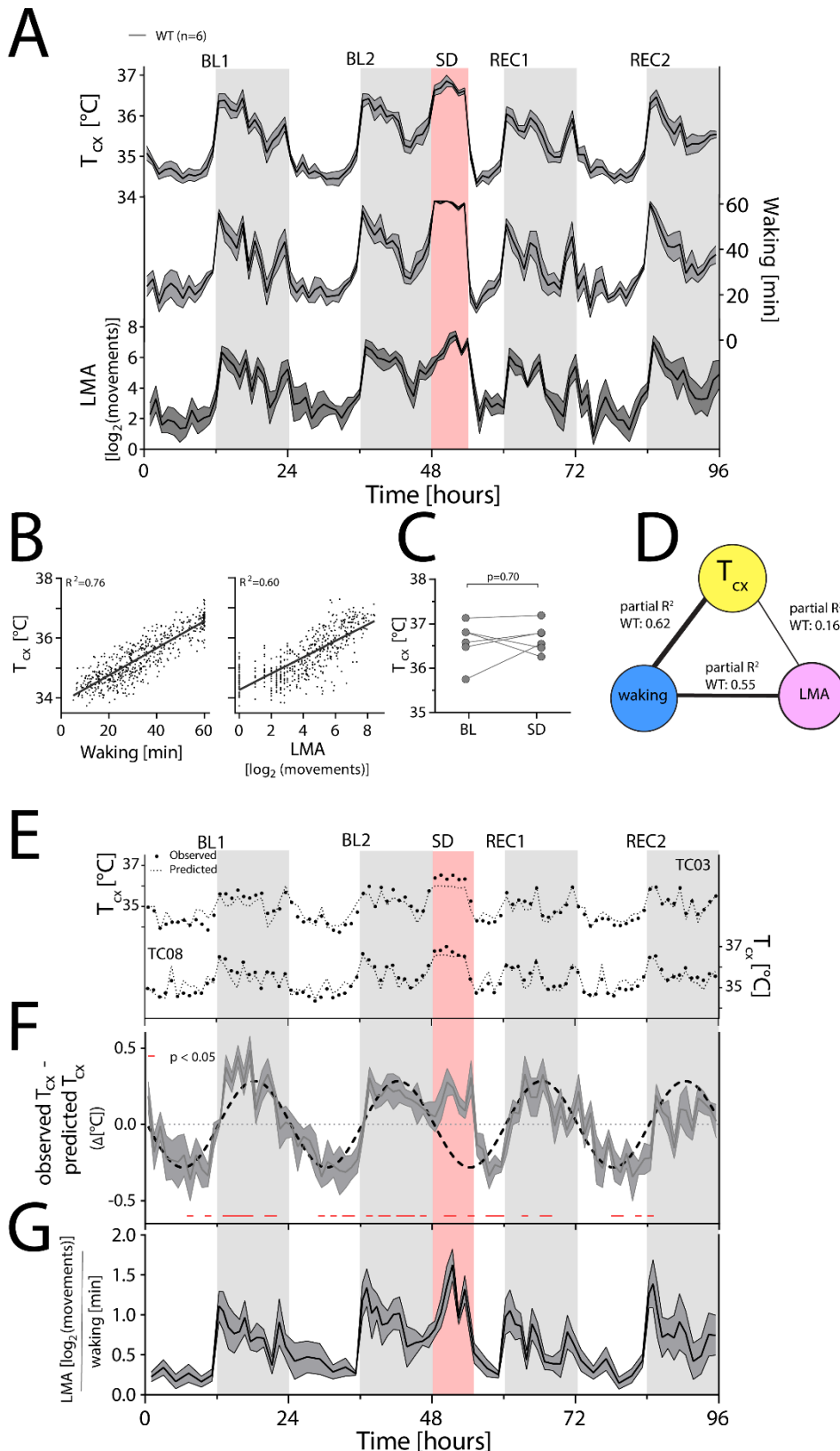


Figure 2 : **Waking is the major determinant of T_{cx} .** (A) Time course of hourly values of T_{cx} , waking and LMA with high T_{cx} , more waking and LMA during the dark phase and during SD. (B) Left graph: Waking correlates with T_{cx} ($n=6$; 96 values per mouse; $R^2=0.76$, $p<0.0001$). Right graph: LMA correlates as well with T_{cx} : $R^2=0.60$, $p<0.0001$. (C) T_{cx} is not significantly different during SD in comparison to long waking bouts during BL ($t(5)=0.41$, $p=0.70$). (D) Waking after correcting for LMA is the major determinant of T_{cx} , as revealed by partial correlation analysis; here performed on the combined hourly values of all WT mice. (E) Two representative examples [TC03 and TC08], with measured T_{cx} (closed circles), and predicted T_{cx} (stippled line) [based on the correlation between T_{cx} and waking]. (F) Based on the amount of waking, higher T_{cx} is expected during the light phase, resulting in negative residuals, and lower T_{cx} during the dark phase and SD, resulting in positive residuals [residuals: observed T_{cx} - predicted T_{cx}] (t-test: data $<> 0$, $p<0.05$). The sinewave was fitted to the residuals during BL. (G) LMA per unit of waking follows a similar pattern as the residuals in figure F.

To determine whether including LMA, in addition to waking, could predict a larger portion of the variance in T_{cx} , we applied three Mixed Linear Models, where LMA was considered by expressing LMA per unit of waking (LMA/Waking). Model₁ explained the variance in T_{cx} based on waking alone, Model₂ also incorporated LMA/Waking, and Model₃ considered additionally the interaction between Waking and LMA/Waking. Indeed, Model₃ predicted best the variance in T_{cx} although in terms of explaining the variance in T_{cx} , the improvement is marginal over the two other models (Model₁: $R^2_c=0.84$; Model₂: $R^2_c=0.85$; Model₃: $R^2_c=0.86$; chi-squared test: Model₁ vs Model₂: $X^2(5)=16.2$; $p<0.0001$; Model₂ vs Model₃: $X^2(6)=25.0$; $p<0.0001$). Thus, the sleep-wake distribution is the most important determinant of T_{cx} but LMA during waking is modestly contributing as well. Nevertheless, also the residuals of this model, depicted in FigS2, still showed a similar pattern like the residuals in Fig.2F, pointing towards either the contribution of another unidentified variable and/or a non-linearity of the association between the contribution of LMA and sleep-wake states to changes in T_{cx} .

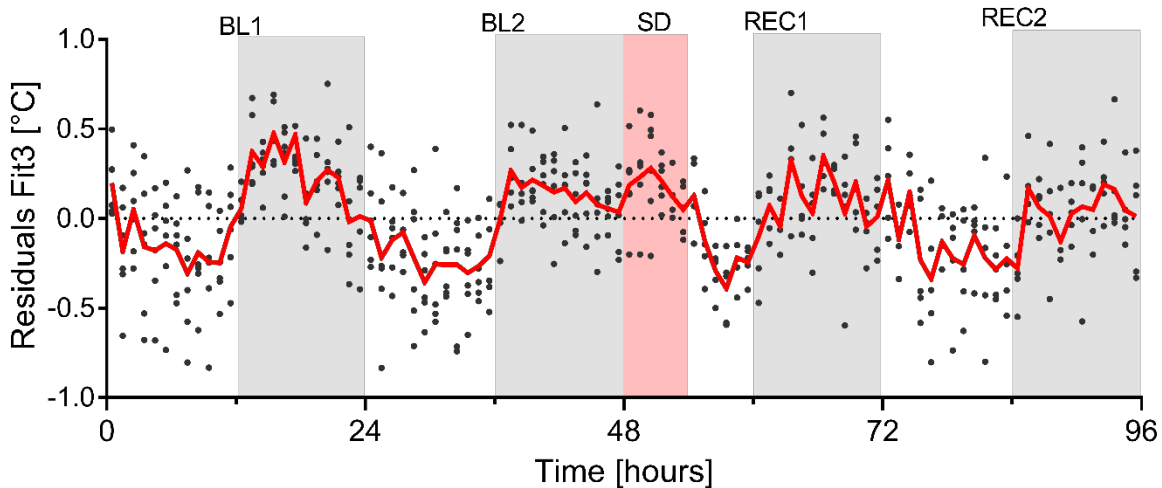


Figure S2. The residuals of the optimized mixed linear model (fit3) still show a pattern alike the residuals in Figure 2-F.

THE INFLUENCE OF SD AND CIRBP ON TRANSCRIPTS IN CORTEX AND LIVER

Our next and main question concerned whether CIRBP participates in linking the effect of SD to clock gene expression. To this end, we quantified 11 transcripts from liver and 15 from cortex before and after SD by RT-qPCR. Genes of interest included transcripts affected by SD (Maret et al., 2007; Mongrain et al., 2010) and/or by the presence of CIRBP (Liu et al., 2013; Morf et al., 2012), with an emphasis on clock genes. Mice were sacrificed before SD at ZTo, or 6 hours later after SD (ZT6-

SD) together with non-sleep deprived control mice that could sleep *ad lib* (ZT6-NSD). Statistics on ZT0 (t-test) and ZT6 (2-way ANOVA) can be found in table S1.

From ZT0 to ZT6 in BL, T_{cx} decreased because during this time mice sleep the most (see Fig 2A), which was accompanied by the expected increase in the cold-induced transcript *Cirbp* expression in WT mice (cortex: $t(8)=3.2$, $p=0.01$; liver: $t(8)=2.7$, $p=0.03$); Fig 5A and SFig3, compare also with SFig 1). In contrast, SD during the same time span, incurred a decrease in cortical and hepatic *Cirbp* relative to non-sleep deprived controls (cortex: Fig 5A; liver: SFig3), consistent with the wake-

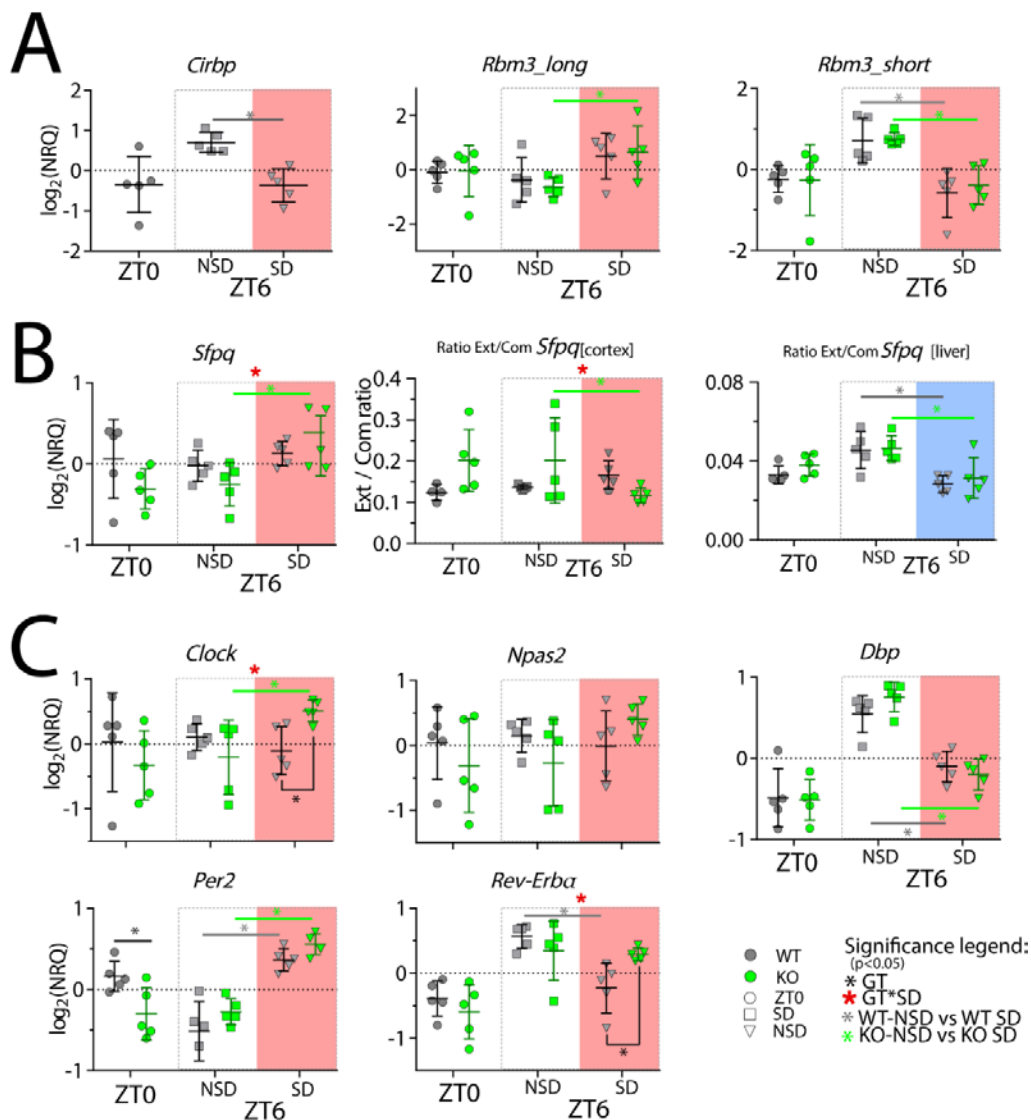
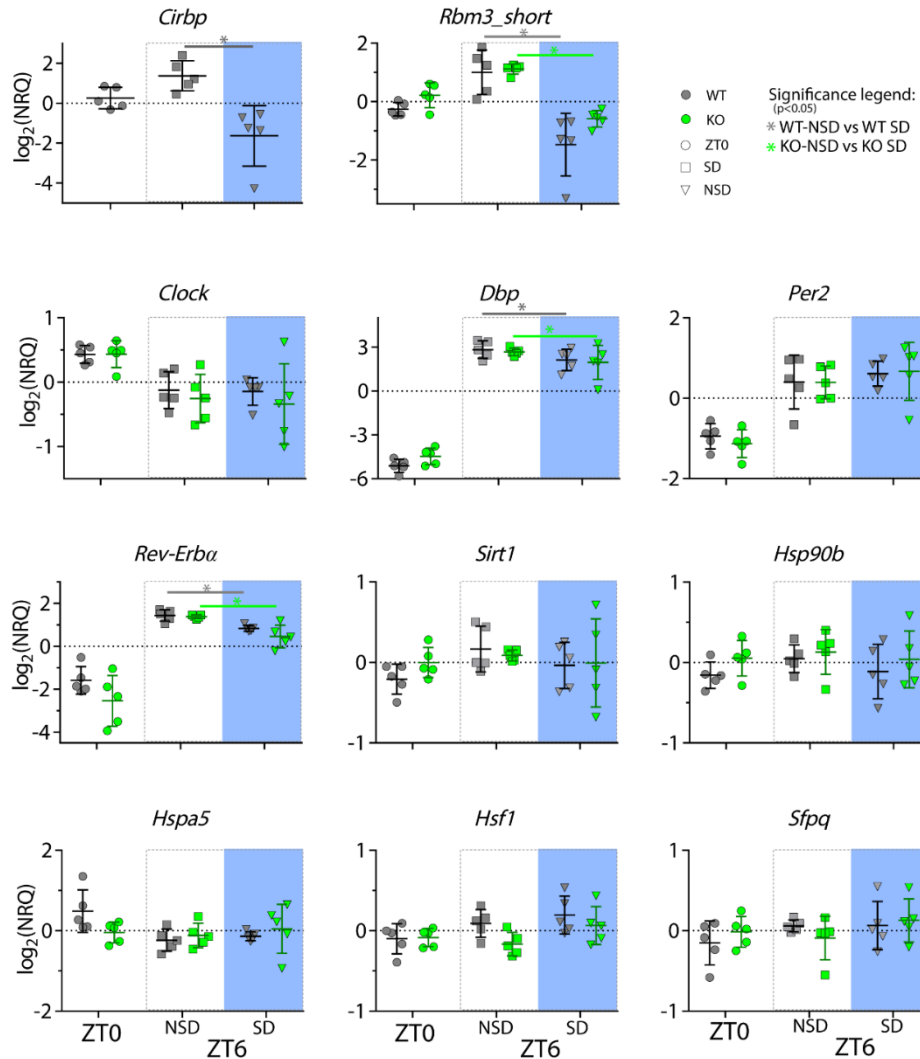


Figure 3 **Cortical expression of several genes is affected by SD and the lack of CIRBP** Mice were sacrificed at ZT0, at ZT6 after sleep deprivation (ZT6-SD) or after sleeping *ad lib* (ZT6-NSD). Statistics are performed separately on ZT0 (factor GT, t-test), and ZT6 (factor GT and SD; 2-W ANOVA). Significant ($p < 0.05$) GT differences are indicated by a black line and *, the effect of SD in WT mice with a grey line and *, and in KO mice with a green line and *. Interaction effects (GTxSD) at ZT6 are indicated by a red *. See table S1 in supplementary data for statistics.

induced increase in T_{cx} during SD. No *Cirbp* mRNA was detected in KO mice.

RBM3 is another cold-inducible RNA Binding Protein and, like CIRBP, mediates temperature into high-amplitude clock gene expression *in vitro* (Liu et al., 2013). A long and a short isoform of *Rbm3* (*Rbm3-long* and *-short*, resp.) that differ in their 3'UTR length, were discovered in the mouse cortex. Although called 'cold-induced', these isoforms exhibit opposite responses to SD (H. Wang et al., 2010), with a decrease in the *short* isoform and an increase in the *long* isoform. We found that the short isoform is far more prevalent than the long isoform which could not be detected in liver (PCR cycle number for all samples pooled: liver: *Rbm3-short*: 28.2 ± 0.2 , *Rbm3-long*: >32 (?); i.e., beyond reliable detection limit; cortex: *Rbm3-short*: 25.6 ± 0.2 , *Rbm3-long*: 29.7 ± 0.1 , amplification efficiency *Rbm3-short*: 2.11 and *Rbm3-long* 2.07). We confirmed that after SD, *Rbm3-short* was



Supplementary Figure-3 **Changes in transcripts incurred by the absence of CIRBP and/or SD in the liver.** Legend same as in Figure 4-5. See Table S1 for statistics.

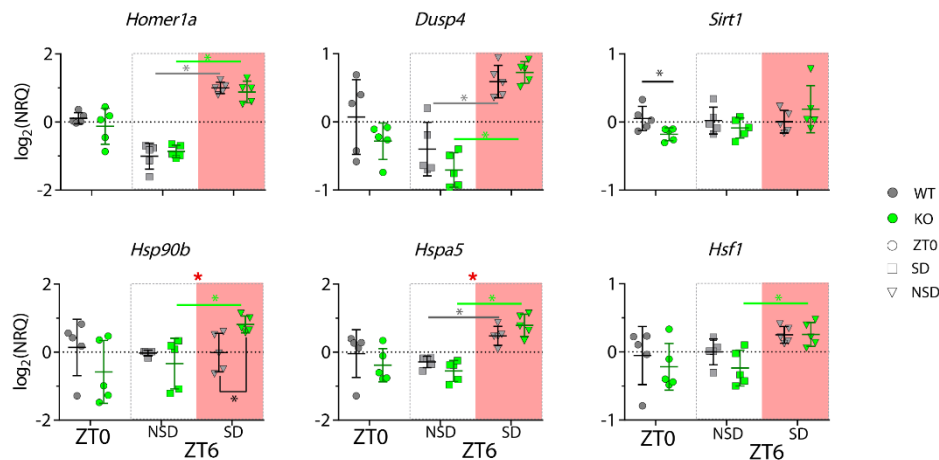
decreased in the cortex (Fig 5A) and liver (SFig3), whereas *Rbm3-long* was increased in cortex. The latter observation reached significance only in the KO mice (Fig-5A).

As anticipated, cortical expression of the activity (and waking)-induced transcripts *Homer1a*, *Dusp4*, *Hspa5/BiP*, *Hsp90b*, and *Hsfi* was increased by SD (SFig4), although post-hoc tests revealed that the latter two were significantly increased only in *Cirbp* KO mice. Furthermore, the effect of SD on the transcripts *Hsp90b* and *Hspa5* was significantly amplified in *Cirbp* KO mice compared to WT mice. Unexpectedly, no changes in the expression of heat shock transcripts incurred by SD or genotype were detected in the liver (SFig3).

The presence of CIRBP and RBM3 is associated with longer 3'UTRs *in vitro*, thereby increasing the ratio of the longer (extended or *ext*) over the shorter (common or *com*) isoform, also known as the *ext/com* ratio (Liu et al., 2013). We aimed to replicate this finding *in vivo* in the cortices and livers of WT and KO mice, and hypothesized that in both tissues i) SD, by suppressing *Cirbp* and *Rbm3*, reduces the *ext/com* ratio and ii) *Cirbp* KO mice have reduced *ext/com* ratio under BL conditions. We selected the transcript splice-factor proline Q (*Sfpq*) for further investigation because it is known to be sleep-wake driven ((Maret et al., 2007); see its supplementary table 5 and GSE9444) and the poly-adenylation site is affected by the presence of CIRBP (((Liu et al., 2013), see also FigS4-S5 of Liu et al., 2013). SD indeed increased the overall levels of the transcript *Sfpq*, although this only reached significance in *Cirbp* KO (Fig3B). As expected, SD significantly decreased the *ext/com* ratio in both genotypes and tissues (Fig 3B; 2-way ANOVA, factor SD: $F(1,16)=20.4$, $p=0.003$), except for the cortical *ext/com* ratio of WT mice. More specifically, we observed an unexpected non-significant increase of this ratio in the cortex of WT mice, leading to a significant GT x SD interaction ($F(1,16)=5.25$, $p=0.036$). The lack of CIRBP in *Cirbp* KO mice under baseline conditions was not associated with differences in the *ext/com* ratio at neither ZTo nor at ZT6 (ZTo (liver: $t(8)=1.55$, $p=0.16$); cortex: $t(7)=2.0$, $p=0.09$; ZT6: liver: $t(8)=0.19$, $p=0.85$, cortex: $t(8)=1.4$, $p=0.20$). Thus, although SD generally led to the expected decrease in *ext/com* ratio, genetic deletion of CIRBP did not. *Si-Cirbp* can, like SD, be considered, as an acute manipulation of *Cirbp* levels and contrasts with the *Cirbp* KO mouse, where CIRBP was never present. This suggest that only the acute presence of the cold-induced proteins CIRBP and RBM3 is critical in adjusting the 3'UTR length of *Sfpq*, whereas chronic absence of CIRBP by genetic deletion does not importantly contribute to the *ext/com* ratio.

Our main question concerned the contribution of CIRBP to sleep-wake induced changes in clock gene expression. Previous studies evaluating the effects of SD on cortical clock transcripts

showed a consistent increase in *Per2* and a decrease in *Dbp* and *Rev-erba*, whereas the response of *Clock* and *Npas2* varied among studies, but if any, tended to increase after SD (reviewed in (Mang & Franken, 2015)). Indeed, in the cortex of WT mice, SD increased cortical *Per2*, decreased *Dbp* and *Rev-erba*, but did not significantly affect *Clock* and *Npas2*. In accordance with our hypothesis, CIRBP attenuated the SD incurred changes of cortical *Rev-erba*, a transcriptional repressor recently implicated in the sleep homeostat (Mang et al., 2016). This observation contrasts with the genotype-



Supplementary Figure-4 Changes in transcripts incurred by the absence of CIRBP and/or SD in the cortex. Legend same as in Figure 4-5. See Table S1 for statistics.

dependent changes in *Per2*. When the lower levels of cortical *Per2* in *Cirbp* KO mice at ZT0 are considered, the effect of SD was larger (2-way ANOVA, ZT0-ZT6[SD], interaction effect GT x SD: $F(1,16)=12.4$, $p=0.0028$). Also, the expression of *Clock* in the cortex was significantly increased by SD in *Cirbp* KO mice. Compared to the cortex, the clock gene expression in the liver appeared more resilient to the effect of SD, as only *Dbp* and *Rev-erba* were significantly affected and not *Per2* (SFig 5). The lack of CIRBP did not interfere with this response, nor did it contribute to genotype dependent changes of other (clock) gene transcripts in the liver.

Taken together, the absence of CIRBP modulated the SD induced changes in the cortical expression of the clock genes *Rev-erba*, *Clock* and *Per2*. Furthermore, the expression of transcripts in the heat shock pathway were also affected by CIRBP.

CIRBP CONTRIBUTES TO SLEEP HOMEOSTASIS

Because *Cirbp* KO mice showed a modulation of the response to SD in three out of five cortical clock gene transcripts, and clock genes importantly partake in the sleep homeostatic process (reviewed in (Franken, 2013)), we hypothesized that *Cirbp* KO mice have an altered sleep-homeostatic process. Sleep-wake states were determined based on EEG and EMG signals (see Methods) in male KO mice and their WT littermates. We also quantified EEG power in the delta band [0.75 – 4.0 Hz] during NREM sleep, which is a proxy of NREM sleep pressure and reflects a homeostatically regulated sleep process, Process S (S. Daan et al., 1984). As a second sleep homeostatic measure, we calculated the amount of NREM and REM sleep recovered after SD relative to baseline sleep.

Baseline characteristics of sleep-wake behavior do not differ between Cirbp KO and WT mice

During the two baseline days, no significant differences in waking, NREM or REM sleep were observed. This was assessed by comparing time spent in these three behavioral states per light and dark phases and by inspecting their average time course during baseline (see Fig.3A and Fig4B).

	WT		KO		Statistics (2-W ANOVA)
	Light	Dark	Light	Dark	Factor GT x Light, Df : 1,35
NREM sleep	389±4	189±10	376±4	170±13	F=0.02, p=0.89
REM sleep	70±2	19±2	66±2	20±2	F=0.83, p=0.37
Total waking	260±4	512±11	277±5	530±14	F=0.02, p=0.9
TDW	45±3	179±12	55±5	192±15	F=0.13, p=0.72
LMA	119±16	817±70	181±26	1370±142	F=7.1, p=0.01

Table 1. Baseline time spent in sleep-wake states (min) and LMA (movements) per 12 hours per genotype. 2-way ANOVA (Factor GT and Light/Dark) on those same 12-hour values. Degrees of freedom for both GT and Light/Dark: Df=1; error term: Df=35.

Sleep homeostatic processes under BL and recovery

The time course of delta power in the two genotypes was overall similar. In the dark phase, when mice spent most of their time awake and thus sleep pressure accumulates, delta power during NREM sleep was highest. This contrasts with the end of the light phase [ZT8-12], where NREM sleep delta power reached its lowest levels of the day due to the high and sustained prevalence of NREM sleep in the preceding hours. Despite the overall similarities in daily changes of NREM delta power, subtle differences were observed: delta power levels were higher during the dark phase in *Cirbp* KO mice compared to WT, and these differences reached significance during the dark periods of recovery (Fig 4A, 2nd graph from top).

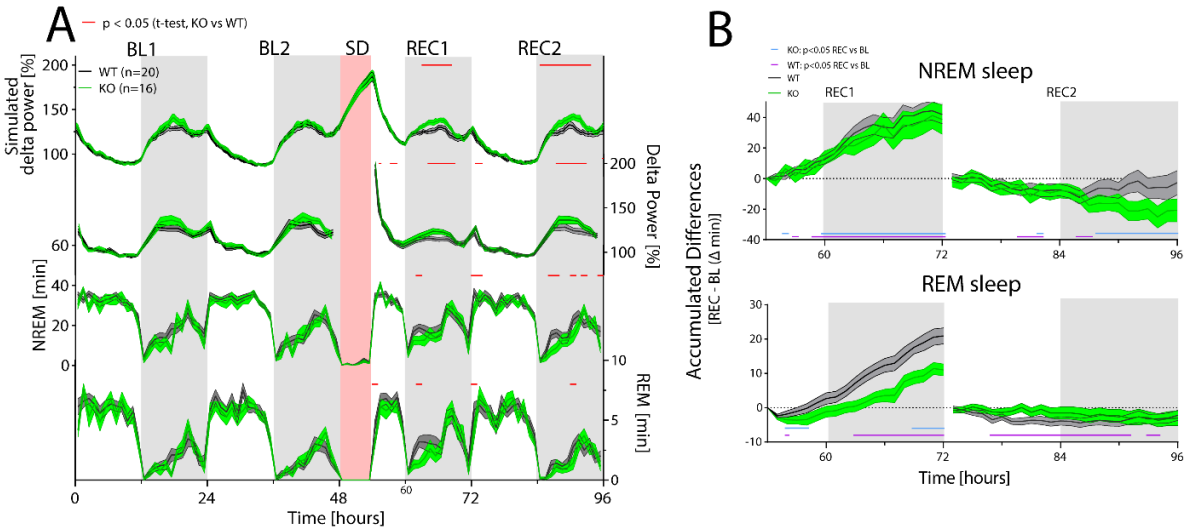


Figure 4 CIRBP affects sleep distribution during the recovery and the REM sleep homeostat. *Cirbp* KO (green lines and areas) and WT (black line, grey areas) mice during BL, SD and REC (areas span ± 1 SEM range) (A) From top to bottom: Simulated delta power (Process S), measured NREM delta power, NREM sleep and REM sleep. During BL, trends, but no significant effect of GT or its interaction with time are detected in the simulation of process S, delta power, NREM sleep or REM sleep. During REC, the simulation predicts increased delta power in *Cirbp* KO mice (GT: $F(1,34)=5.56$, $p=0.024$), based on differences in NREM distribution (GT: $F(1,34)=6.02$, $p=0.0194$) which are also reflected by increased delta power during the dark phase (GT: $F(1,34)=4.65$, $p=0.038$). Genotype effects in REM sleep are also detected during recovery (factor GT: $F(1,34)=5.45$, $p=0.026$). Exact timing of GT differences is indicated by infra-posed red lines (post-hoc t-test, $p < 0.05$). (B) Top: In the second recovery day, less NREM sleep is recovered in KO mice than in WT mice (REC1 at 72Hr: WT: 41.9 ± 6.1 KO: 38.6 ± 9.7 min; t-test: $t(34)=0.30$, $p=0.76$). Bottom: KO mice accumulate less REM sleep during the first recovery day over the baseline day in comparison to WT mice relative to baseline (REC1 at 72Hr, WT: 20.9 ± 2.3 KO: 11.2 ± 2.0 , t-test: $t(35)=3.0$, $p=0.004$).

Differences in delta power can be attributed either to changes in the dynamics of the underlying homeostatic process (Process S) and/or to changes in the sleep-wake distribution. Evidence supporting the latter possibility were observed because *Cirbp* KO mice tended to spend less time in NREM sleep (and more time awake) during the early dark phase compared to WT mice, reaching significance during the recovery (Fig 4A; 3rd graph from top). To test if these changes in the sleep-wake distribution were indeed sufficient to raise NREM delta power above WT levels, we estimated the increase (τ_i) and decrease (τ_d) rate of delta power by a simulation of the underlying Process S based on the sleep-wake distribution. Process S increases exponentially during waking and REM sleep with time constant τ_i and decreases during NREM sleep with τ_d (see Materials and Methods, and (Franken et al., 2001) for more details). This simulation not only captured well the overall dynamics but also the genotype differences in delta power (Fig 4A; top graph, mean square of the differences measured-predicted delta power, mean \pm SEM: WT: 10.1 ± 0.3 , KO: 10.4 ± 0.4). No differences in the time constants of Process S were detected (see Table 2). Hence, the reduction in NREM sleep in *Cirbp* KO mice in the beginning of the dark period causes the higher NREM EEG

delta power values in subsequent hours, underscoring the notion that small differences in NREM sleep time can have large repercussions on delta power when waking prevails and thus Process S increases (Franken et al., 2001).

	WT	KO	t-test, df=34
S_o [%]	128.2 ± 2.4	132.1 ± 2.6	t=1.10, p=0.29
τ_i [h]	13.2 ± 1.2	12.9 ± 1.0	t=-0.16, p=0.87
τ_d [h]	3.0 ± 0.2	2.8 ± 0.2	t=-0.74, p=0.46
LA [%]	45.1 ± 1.4	45.1 ± 1.1	t=-0.02, p=0.98
UA [%]	288.8 ± 3.0	296.6 ± 3.2	t=1.80, p=0.09

Table 2 Time constants for Process S do not differ between *Cirbp* WT and KO mice. Mean time constants (\pm SEM) obtained by the simulation (Process S) with the best fit to the NREM delta power values, where the increase of process S is simulated by τ_i , the decrease by τ_d and the upper- and lower asymptotes by UA and LA, respectively. No significant genotype differences were observed. See material and methods for detailed description of the simulation.

A different aspect of NREM sleep homeostasis concerns the regulation of time spent in this state. This can be quantified by accumulating relative differences in time spent in NREM sleep from corresponding baseline hours over the recovery period. During the first recovery day, both KO and WT mice gained ca. 40 minutes of NREM sleep relative to baseline (Fig 4B).

The amount of REM sleep is also homeostatically defended (Franken, 2002). By the end of REC₁, both WT and KO mice spent more time in REM sleep compared to corresponding baseline hours. However, this increase was significantly attenuated by 46% in *Cirbp* KO mice (Fig 4B). Because no significant differences were detected during baseline in time spent in REM sleep (see also Table 1), this attenuated rebound in REM sleep resulted from less REM sleep during recovery, specifically in the first hours of the dark phase when the genotypic differences were most prominent (Fig 4A, lowest graph).

Thus, although CIRBP did not affect the processes underlying NREM sleep intensity, it did contribute to REM sleep homeostasis by increasing the amount of REM sleep after SD.

An unanticipated waking phenotype in Cirbp KO mice

While quantifying sleep-wake states, we observed unexpectedly that *Cirbp* KO mice were more active than their WT littermates during the dark phase ($t(31)=-2.56$, $p=0.015$, see also Table 1). Especially in the first 6hrs of the dark phase, *Cirbp* KO mice were almost twice as active (movements: WT: 463.8 \pm 60.7, KO: 801.8 \pm 118.4, $t(35)=-2.7$, $p=0.012$). Interestingly, this pronounced increase was not associated with a significant increase in time spent awake (per 12 hrs: $t(35)=1.2$,

$p=0.24$, and see Table 1), and indeed *Cirbp* KO mice are more active per unit of waking (average in the dark phase, LMA [movements/waking(min)], WT: 1.3 ± 0.13 , KO: 2.1 ± 0.28 ; $t(35)=-2.7$, $p=0.01$). Note that also T_{cx} was not significantly increased in *Cirbp* KO mice during the dark phase (t-test, $t(10)=1.3$, $p=0.24$; WT: 35.9 ± 0.1 , KO: 36.1 ± 0.1) despite the increased LMA at this time of the day, further underscoring the minimal contribution of LMA to T_{cx} .

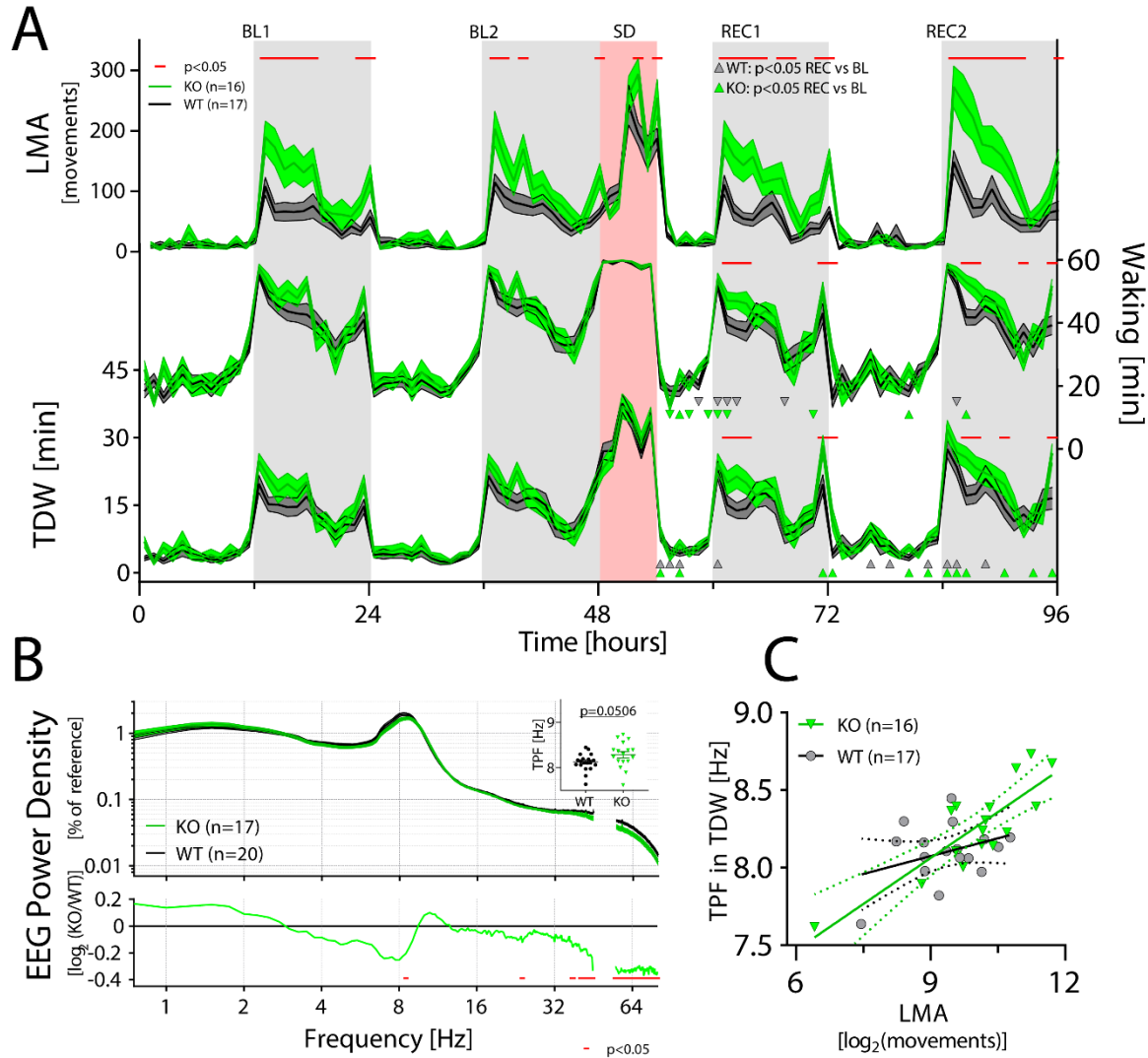
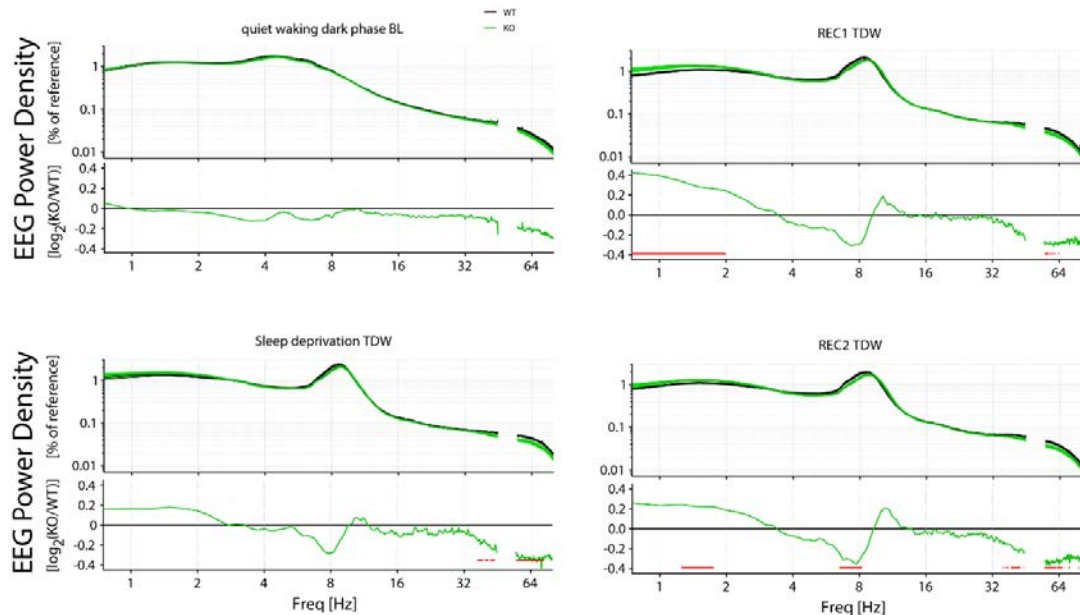


Figure 5 CIRBP suppresses LMA and affects spectral composition during TDW. (A) LMA (top), waking (middle), and TDW (bottom graph) in *Cirbp* KO (green lines and areas) and WT (black line, grey areas) mice during BL and SD per hour (areas span ± 1 SEM range). *Cirbp* KO mice are more active in the dark periods only (BL: GTxTime: $F(47, 1457) = 3.514$, $P < 0.0001$; REC: GTxTime: $F(41, 1271) = 5.241$, $P < 0.001$), and spent more time awake and in TDW during REC compared to WT mice (total waking: BL: GTxTime: $F(47, 1457) = 1.08$, $P = 0.3316$ REC: GTxTime: $F(41, 1271) = 1.912$, $P = 0.0005$; TDW: BL: GTxTime: $F(47, 1457) = 1.067$, $P = 0.3530$; REC: GTxTime: $F(41, 1271) = 1.754$, $P = 0.0025$). Significant GT differences are marked by red lines above the respective graphs (post-hoc t-tests; $p < 0.05$). Δ and ∇ indicate a significant increase and decrease in REC compared to same time in BL, respectively. (B) *Cirbp* KO (green lines and areas) and WT (black line, grey areas) mice (areas span ± 1 SEM range). CIRBP contributes to the spectral composition of TDW in the dark phase (2-way RM ANOVA; GTxFreq: $F(278, 9730) = 2.04$; $p < 0.0001$, red symbols in lower panel: post-hoc t-tests, $p < 0.05$), and KO mice tend to have a faster theta peak frequency (TPF) during TDW in the dark phase ($t(35) = 2.03$; $p = 0.0506$). (C) TPF in the dark phase correlates only in KO mice significantly with LMA (WT: $R^2 = 0.12$, $p = 0.17$, KO: $R^2 = 0.71$, $p < 0.0001$).

CIRBP modulates the spectral composition of the EEG during theta dominated waking

Theta-dominated waking (TDW) is a sub-state of waking that correlates with activity, prevails during the dark phase and SD, and is characterized by the presence of EEG theta-activity (Buzsáki, 2006). We used a previously designed algorithm to determine TDW (see material and methods and (Vassalli & Franken, 2017)). Despite their increased LMA *Cirbp* KO mice did not spend more time in TDW during the dark phase of the BL (see Table 1, $t_{(31)}=-1.22$, $p=0.23$). If not time spent in TDW, does the increased LMA in *Cirbp* KO mice relate to changes in brain activity during dark phase TDW?



Supplementary Figure-5 **Changes in the EEG spectra are observed in TDW, but not in quiet waking.** Spectral composition of *Cirbp* KO (green lines and areas) and WT (black line, grey areas) mice at different times of the experiment (indicated by the title). In each graph, the top panel depicts the spectral composition whereas in the lower panel, the KO spectral composition relative to the WT is shown (ratio KO/WT). Red symbols in lower panel indicate significant different for the frequency bins (post-hoc t-test, $p < 0.05$). **'Quiet' waking baseline dark phase:** No effect of GT or an interaction effect (2w RM ANOVA, $GT * Freq$: $F(278, 9730)=0.81$, $P=0.99$) on the spectral composition of quit waking in the dark phase during the baseline. **Sleep deprivation TDW:** significant interaction between GT and Freq ($F(278, 9730) = 1.722$, $P < 0.0001$). **TDW_REC1:** significant interaction: $F(278, 9730) = 2.984$, $P < 0.0001$; **TDW_REC2:** sign interaction $F(278, 9730)=3.083$, $P < 0.0001$).

Although in both genotypes the TDW EEG showed the characteristic theta activity [6.5-12.0 Hz], subtle differences between genotypes were detected by spectral decomposition of the EEG signal. Slow [32-45Hz] and fast [55-80Hz] gamma power were both reduced during TDW in *Cirbp* KO mice (Fig 3-B) and was present across the whole experiment (Supplementary Figure 5; and see time course Supplementary Figure 6), indicating that these spectral genotype differences are robust across different light conditions, sleep deprivation, and circadian time. In contrast, the spectral composition of the EEG during 'quiet' waking (*i.e.* all waking that is not TDW) was remarkable similar between the two genotypes (Supplementary Figure 5), demonstrating that the changes in

spectral composition of TDW EEG are not the result of a general effect of CIRBP on the waking EEG.

The non-significant decrease in slow and increase in faster theta activity in the TDW EEG of *Cirbp* KO mice points to an acceleration of theta peak frequency (TPF; lower panel in Fig 5B). TPF during TDW in BL was indeed increased in KO mice (Fig 3B; +0.15Hz) although our significance threshold was not met ($t_{(35)}=2.0$, $p=0.0506$). No suggestions for accelerated TPF in REM sleep during BL, the other sleep-wake state characterized by distinct theta oscillations in the EEG, were detected (WT: 7.63 ± 0.05 ; KO: 7.71 ± 0.05 , $t_{(35)}=1.21$, $p=0.23$), indicating that the accelerated TPF in *Cirbp* KO mice was state-specific. Increased LMA is associated with increased TPF (Jeewajee, Barry, O'Keefe, & Burgess, 2008). In accordance with this observation, mean log₂-transformed LMA levels per mouse during the dark phase predicted well the mean TPF observed during TDW at the same time of day (WT and KO combined; $R^2=0.52$, $p<0.0001$), although this relationship was significant in the KO mice only when assessing the two genotypes separately (Fig3C).

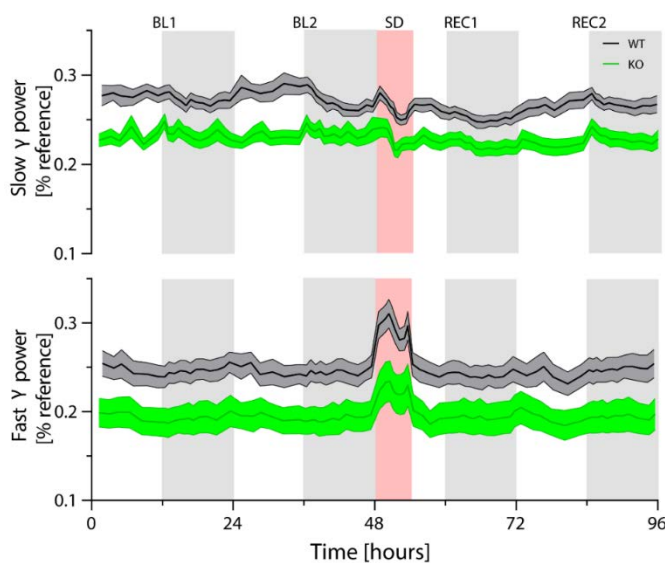
TPF during BL	WT	KO
Light	7.77 ± 0.03	7.64 ± 0.04
Dark	8.13 ± 0.04	8.28 ± 0.07

Table 2: Average TPF during baseline light and dark (mean \pm SEM) in TDW

Because the individual LMA levels can offset the group correlation, the individual correlation between hourly TPF and LMA was assessed. To test if this association between TPF and LMA was light-independent, we analyzed the correlation between TPF and LMA under baseline conditions during the dark and light phase separately (*i.e.* 24 values per mouse). In the dark phase, this correlation was in all but one mouse (KO) significant, and both the slope as well the predictive power of this correlation did not significantly differ between genotypes (slope: WT: 0.15 ± 0.01 , KO: 0.14 ± 0.01 , $t_{(31)}=0.37$, $p=0.72$; R^2 : WT: 0.81 ± 0.03 ; KO: 0.79 ± 0.04 , t-test on the Fisher Z-transformed R^2 -values: $t_{(31)}=-0.49$, $p=0.62$). During the light phase, this association is weakened (paired t-test: slope: $t_{(32)}=7.8$, $p<0.0001$; Fisher Z-transformed R^2 -values of all genotypes grouped: $t_{(32)}=5.9$, $p<0.0001$), but not differently between genotypes (WT: 0.07 ± 0.01 , KO: 0.09 ± 0.01 , $t_{(31)}=1.2$, $p=0.23$; R^2 : WT: 0.59 ± 0.04 ; KO: 0.67 ± 0.05 , t-test on the Fisher Z-transformed R^2 -values: $t_{(31)}=1.2$, $p=0.23$), whereas the non-significant associations were more prevalent at this time of day when LMA and TDW are substantially reduced and estimates of TPF during TDW are less precise (KO: 3/ 16; WT: 3/ 17 mice). Altogether, these results provide further evidence that LMA drives TPF, and suggests also that CIRBP through its effects on LMA, suppresses this correlation.

The SD induced changes in the distribution of waking during the recovery relative to BL (3-way RM ANOVA, factor SD: REC1: $F(1,558)=252.51$, $p<0.0001$; REC2: $F(1,1514)=543.9$, $p<0.0001$; see triangles in REC1 and REC2, Fig3-A). Interestingly and opposite to overall waking, we observed several hourly intervals where TDW is increased during the recovery for both genotypes compared to its baseline values (3-way RM ANOVA, factor SD: REC1: $F(1,558)=13.9$, $p=0.0002$; REC2: $F(1,1514)=233.8$, $p<0.0001$; Fig3-A, upwards pointing triangles). During the dark phase of the recovery, *Cirbp* KO mice spent more time awake and in TDW than WT mice (Fig3-A; see post-hoc tests indicated by red line), as if SD amplified the (non-significant) genotype differences during BL (3-way RM ANOVA on hourly values: factor GTxTimexSD: total waking: $F(41,1271)=1.4$, $p=0.04$; TDW: ($F(41,1271)=1.4$, $p=0.0562$), but not in LMA ($F(41,1271)=1.0$, $p=0.48$).

The EEG spectra during TDW in REC1 and REC2 showed similar profiles as during BL (see FigureS5), although there are some changes that reach significance such as the increase in the delta power band. Along those lines, the suggested increase in TPF in *Cirbp* KO mice during the dark phase under baseline conditions, becomes significantly different in the dark phases of both recovery days (REC1: WT: 8.1 ± 0.05 , KO: 8.4 ± 0.07 , $t(35)=2.7$, $p=0.01$; REC2: WT: 8.2 ± 0.05 , KO: 8.5 ± 0.08 , $t(35)=2.6$, $p=0.01$). Also, under baseline conditions, the slope between TPF and LMA, based on mean \log_2 -transformed LMA and TPF during the dark phase, almost reached significance, (ANCOVA, $F(1,29)=3.8$, $p=0.059$), whereas after SD, this association becomes significantly different between genotypes ($F(1,29)=5.8$, $p=0.02$), providing further evidence that the suggestive genotype differences under baseline conditions do reach significance levels after a challenge of the sleep homeostat.



Supplementary Figure 6 **Slow and fast gamma power over the course of the experiment.** *Cirbp* KO (green lines and areas) and WT (black line, grey areas) mice (areas span ± 1 SEM range). The accumulated power in both slow [32-45Hz] and fast [55-80Hz] gamma is significantly reduced over the course of the experiment in *Cirbp* KO mice (2-way ANOVA: factor GT: slow gamma: $F(1,34)=11.9$, $p=0.002$; fast gamma: $F(1,33)=6.6$, $p=0.01$). Like the analysis of delta power, power in the gamma bands is calculated based on intervals to ensure an equal contribution of epochs to each time point: 6 intervals in the light phase, 12 in the dark periods, 8 in the sleep deprivation and 4 during the recovery light period.

Taken together, we unexpectedly observed that *Cirbp* KO mice are more active during the dark phase, which partly explains the faster TPF. Moreover, KO mice had less power in the gamma band of TDW, and the 6-hour SD strengthened genotype differences in the sleep-wake distribution and EEG activity.

Discussion

In this study, we showed that, like in other rodents, the sleep-wake distribution is the major determinant of T_{cx} in the mouse. Because of the well-established link between temperature and levels of CIRBP, it is therefore likely that the equally well-known sleep-wake driven changes in *Cirbp* expression in the brain (see also FigS1) are driven through the sleep-wake driven changes in brain temperature. As predicted, the SD incurred changes in the expression of clock genes, which was modulated by the presence of CIRBP. However, only for *Rev-Erba* did we observe the anticipated attenuated response to SD in *Cirbp* KO mice, whereas the expression of *Per2* and *Clock* was amplified. Although these altered molecular responses to SD in *Cirbp* KO mice were accompanied by changes in the sleep-wake distribution, the dynamics of EEG delta power during NREM sleep were unaffected. On the other hand, we did discover evidence of altered dynamics of the process regulating time spent in REM sleep. Finally, and unexpectedly, we observed that *Cirbp* KO mice exhibit differences in waking quality during the dark phase with a prominent increase in levels of LMA and changes in the spectral composition of the EEG during TDW.

CHANGES IN CORTICAL TEMPERATURE ARE SLEEP-WAKE DRIVEN

When sleep and waking occur at their expected circadian times, the rhythm of both brain and body temperature has a clear 24-hour rhythm and therefore appears as being controlled directly by the circadian clock. However, several lines of evidence indicate that sleep-wake cycles contribute significantly to both the daily changes in body and brain temperature.

Regarding core body temperature (CBT), an early study describing spontaneous desynchrony in humans under constant conditions, observed two CBT rhythms; one CBT rhythm had a period close to the free-running circadian rhythm of 24-hours, whereas the other CBT rhythm was associated with that of activity and rest (and presumably, wakefulness and sleep), oscillating with a period distinct from 24hrs (Wever, 1979). Subsequent experimental studies in humans took advantage of forced desynchrony and constant routine protocols where sleep was controlled for across the circadian cycle, thereby leaving all circadian rhythmicity in CBT to be attributed to the clock. The

amplitude of the CBT rhythm measured during these protocols is reduced while the phase and period is maintained (Refinetti, 2010). It was estimated that ‘masking’ effects of rest-activity and sleep-wake cycles contributed between 30% and 50% to the amplitude of the circadian CBT rhythm (Hiddinga, Beersma, & Van den Hoofdakker, 1997) (Dijk et al., 2000). This is further supported by a study where enforced wakefulness during the night led to a reduction in amplitude of CBT from 0.31°C to 0.10°C (Barrett, Lack, & Morris, 1993). Not only in humans but also in smaller animals like rats, a circadian and rest-activity component contribute to the circadian fluctuations in CBT (Cambras et al., 2007). Thus, although the phase of CBT is informative as a phase marker of circadian time (Dijk & Czeisler, 1995), the circadian amplitude is amplified when wake and sleep occur in phase with the circadian clock.

On the other hand, brain temperature in the rat is for more than 80% determined by the sleep-wake distribution (Franken et al., 1992b). Likewise, the sleep-wake driven changes in brain temperature are still intact in circadian arrhythmic animals (F. C. Baker et al., 2005; Edgar et al., 1993), pointing to a more sleep-wake dependency of T_{cx} in comparison to CBT. Consistent with the rat findings, we found that also in the mouse 80% of the variation in T_{cx} can be explained by the sleep-wake distribution alone. This was confirmed at a high time resolution (seconds) by inspecting temperature changes at transitions between sleep-wake states, and across the day, by investigating hourly dynamics. We also estimated the contribution of LMA to changes in T_{cx} and found that waking with higher LMA is associated with higher T_{cx} . Although significant, the contribution of LMA to the daily changes in T_{cx} was modest and explained only 2% more of the variance. However, important to consider is that these models assumed a linear relationship between the variables and T_{cx} , whereas it is to be expected that these variables have a non-linear association. For example, the prediction of T_{cx} in the rat based on the sleep-wake distribution was performed with a non-linear simulation. This model was further optimized by assuming a circadian modulation of the upper and lower asymptotes between which T_{cx} fluctuated (Franken et al., 1992b). Also in our current study, the residuals from the correlation between waking and T_{cx} appeared to follow a circadian distribution, which possibly reflects the circadian modulation of the homeostatic setpoint of T_{cx} . However, this is not reflected in the residuals during the SD, which remain increased, in a similar fashion that compares with the residuals during the dark-phase. Optimization of the model by assuming non-linearity between waking and T_{cx} could improve further the prediction of T_{cx} based on waking.

The observation that T_{cx} changed when transitioning between sleep-wake states and that SD increased T_{cx} at a time of day when this normally would be low, argue strongly against a direct involvement of the circadian clock in determining T_{cx} . It is nevertheless important to bear in mind that by timing sleep and wake, the circadian clock indirectly contributes to the daily changes in T_{cx} . Moreover, the literature suggests that the contribution of the circadian clock and the sleep-wake distribution also differs among species, as well as where temperature is measured (*e.g.* core body temperature versus brain), as discussed above. Lastly, the contribution of LMA to changes in T_{cx} was in our experiment very modest relative to sleep-wake driven changes, but this is likely to be affected by the type of activity; *e.g.* exercise is known to increase both peripheral and (proxies) of brain temperature in men (Nybo, Secher, & Nielsen, 2002).

CIRBP ADJUSTS CLOCK GENE EXPRESSION AND REM SLEEP RECOVERY FOLLOWING SD

CIRBP modulated the response to SD in the expression of some clock genes. As anticipated, the SD incurred decrease in cortical *Rev-erb α* was attenuated in *Cirbp* KO mice. *Rev-erb α* (also known as Nr1d1) protein acts as a transcriptional repressor of positive clock elements such as BMAL1 (Preitner et al., 2002). Furthermore, KO of both *Rev-erb α* and its homolog *Rev-erb β* in mice, has profound effects on circadian rhythms at the behavioral and metabolic level (Cho et al., 2012). We recently established that *Rev-erb α* also partakes in several aspects of sleep homeostasis: *Rev-erb α* KO mice accumulated at a slower rate NREM sleep need and had reduced efficiency of REM sleep recovery in the first hours after SD, making the observation that *Cirbp* KO had an attenuated response of *Rev-erb α* to SD especially relevant.

The response to SD of other clock genes was also modulated in the absence of CIRBP. *Clock* expression was only significantly increased after SD in *Cirbp* KO mice, and the expression of *Per2* was amplified. These findings suggest that parts of the core clock are sensitive to the presence of CIRBP in response to SD. Given the role of clock genes in sleep homeostasis (Franken, 2013), the affected clock gene expression in response to SD in KO mice could have contributed to the changes in sleep-wake distribution during the recovery.

Because several studies showed that mutations in clock genes incurred a loss in REM sleep amount recovered after SD [*i.e.* CLOCK (Naylor et al., 2000), PER3 (Hasan et al., 2011), or impacted the initial efficiency of REM sleep recovery [*i.e.* DBP (Franken et al., 2000) and REV-ERB α (Mang et al., 2016)], the changes in clock gene expression in *Cirbp* KO mice could link to the REM sleep homeostat phenotype. Although REM sleep is primarily regulated through its time spent (Franken,

2002), its timing is largely dependent on circadian time (Czeisler, Zimmerman, Ronda, Moore-Ede, & Weitzman, 1980). Further studies need to address if disturbed clock gene expression in KO mice acts through this circadian modulation of REM sleep – although we indeed do not find evidence in any such direction.

OTHER MECHANISMS LINKING SLEEP-WAKE STATE TO CLOCK GENE EXPRESSION

The SD incurred changes in clock gene expression did not depend as much on CIRBP as hypothesized *a priori*. This finding suggests that more than one pathway contributes to the SD-incurred changes in clock gene expression (reviewed in (Franken, 2013)). A few suggestions for such pathways, based on our data and the literature, will be discussed here, starting with temperature sensitive mechanisms.

Rbm3 (RNA Binding Motif Protein 3) is another cold-inducible transcript which is closely related to CIRBP and conveys also temperature information into high amplitude clock gene *in vitro* expression (Liu et al., 2013). Thus, RBM3 might be another mechanism through which changes in sleep-wake state are linked to changes in clock gene expression. Therefore, we anticipated that RBM3 may have acted as a compensatory mechanism in *Cirbp* KO mice. However, our measures at the RNA-level do not convincingly show that *Rbm3* expression is upregulated in *Cirbp* KO mice. It therefore appears unlikely that *Rbm3* acts as a compensatory mechanism in *Cirbp* KO mice.

Not only cold-inducible transcripts but also transcripts of the heat shock pathway are sensitive to changes in temperature, of which heat shock factor 1 (*Hsfi*) is capable of resetting the clock in response to temperature signals (Buhr et al., 2010). Two of the three cortical heat shock pathway transcripts (*Hsp90b* and *Hspa5/BiP*) that we have quantified, showed a significant *Cirbp* KO specific SD incurred amplification. Because the SD incurred increase in *Hsfi* was significant only in *Cirbp* KO mice, and *Hsfi* can bind to heat shock elements upstream of *Per2* (Reinke et al., 2008), it is tempting to speculate that the amplified expression of *Per2* in *Cirbp* KO mice is due to the increased expression of *Hsfi*. This idea is further supported by the genotype dependent increase in the expression of *Hsp90b* and *Hspa5* after SD, which like *Per2*, have a heat shock element in their promotor region and whose expression can therefore be initiated by HSF1 (Reinke et al., 2008). Thus, HSF1 might have compensated for the absence of *Cirbp*, thereby masking the contribution of CIRBP to SD incurred changes in clock gene expression.

Beyond temperature, many other physiological changes occur during prolonged wakefulness that can subsequently affect clock gene expression. One of these other mechanisms, the surge in

corticosterone during SD, has been experimentally addressed by adrenalectomizing mice. This study showed that the SD induced changes in expression of some, but not all, clock genes is modulated by corticosterone (Mongrain et al., 2010).

Further studies will address the contribution of other pathways, such as changes in redox state, light exposure and oxygen consumption, to changes in clock gene expression.

A last factor to be considered is that there might be already aberrant behavior in the core molecular clock under baseline conditions in *Cirbp* KO mice, which modulates the SD incurred changes in clock gene transcripts. Although our molecular data cannot test if *Cirbp* KO mice differ in their molecular clock (for this, an around-the-clock quantification would be necessary), it would be reasonable to assume decreased clock gene amplitude based on the *in vitro* data. Hence, a parallel can be drawn between *Cirbp* KO mice and circadian clock gene KO mice. Because clock gene KO mice do not only have differential regulation of sleep and wake, but also respond differently at the molecular level to sleep deprivation (e.g. *Npas2* KO mice have a reduced increase in *Per2* expression in the forebrain after SD (Franken et al., 2006)), this could also have contributed to the observed changes in clock gene expression after SD in *Cirbp* KO mice.

TISSUE SPECIFICITY AND REPRODUCIBILITY

In our study, the transcripts we studied where in the cortex more sensitive to SD compared to the liver (effect of SD: cortex: 12/15 [80%]; liver: 4/11 [36%]). Mixed reports about differential tissue sensitivity to SD have been published. Our previous micro-array study found that after SD the liver exhibited three times more transcriptional changes compared to whole brain (Maret et al., 2007), whereas one of our recent studies, using RNA-seq, showed that 78% of all expressed genes were affected by SD in cortex, but only 60% in liver (Diessler et al., 2018). The discrepancy of the results between these two studies could be due to the increased dynamic range in RNA-seq compared to micro-array, enabling to capture smaller changes (Z. Wang, Gerstein, & Snyder, 2009).

Like the study from (Diessler et al., 2018), we also observed that the cortex was more sensitive than the liver to SD for the relative few transcripts quantified. However, when comparing the SD incurred changes in our transcripts with the same transcripts in the Maret et al., 2007 and Diessler et al., 2018 study, we did not corroborate the hepatic increase in the heat shock transcripts that they reported on (*Hsfi*, *Hsp90b* and *Hspa5*) and *Per2*. On the other hand, we did observe the previously reported effects of SD on *Cirbp*, *Rbm3-short*, *Dbp* and *Rev-erba*. If this is due to technical differences is at this point unknown.

FROM *IN VITRO* TO *IN VIVO*: A (TOO) BIG LEAP?

Two studies using different models and techniques (different temperature cycles; different mRNA quantification techniques; immortalized mouse embryonic stem cells and immortalized NIH3T3 cells, (Liu et al., 2013) and (Morf et al., 2012), resp.) showed that CIRBP (and RBM3) are necessary to translate temperature information into high amplitude clock gene expression *in vitro*. Although the expression of clock genes was modulated by in the absence of CIRBP, we did not observe the hypothesized widespread CIRBP-dependent SD induced change in clock gene expression. Two factors can be considered when explaining the absence of this observation.

First, a caveat of our experimental design is that the hypothesis emerged from studies performed in a relatively simple biological system, immortalized cell lines, where *Cirbp* was acutely suppressed by silencing its RNA. We applied the conclusions of these studies to a far more complex system: hepatic and cortical tissue of adult male mice. Already *in vitro* studies find differences between cell lines from different origins and age with respect to circadian characteristics (for examples, see (Kaeffer & Pardini, 2005) and Fig6 in (Saini et al., 2012)). Thus, it is likely that other uncontrolled factors differed between the *in vitro* studies on which we based our hypothesis and the *in vivo* study we performed.

Secondly, our hypothesis is built on the idea that T_{cx} is changing with waking whereas many other variables also change with waking. Some of these waking associated factors interact with CIRBP and could potentially show a compensatory response in its absence, as discussed above.

LMA-DEPENDENT AND INDEPENDENT CHANGES IN WAKING CHARACTERISTICS

Little is known about the role of CIRBP in neuronal and behavioral functioning. It was therefore unanticipated that *Cirbp* KO mice had increased LMA during the dark phase. Neither were the changes in neuronal oscillations expected during TDW: a reduction in low- and high γ power and an increase in TPF. The latter observation could partly be explained by the increase in LMA, as previously observed (Jeevajee et al., 2008). This is in contrast with the general decrease in γ power and its relation to LMA, which is not as well described in the literature. Some studies have found that increased speed of LMA relates to increased power in the gamma band (Furth et al., 2017; Niell & Stryker, 2010; Vinck, Batista-Brito, Knoblich, & Cardin, 2015), whereas another study found that this association depends on the frequency band (Zheng, Bieri, Trettel, & Colgin, 2015). However, a direct relationship between the decreased power in the gamma bands of *Cirbp* KO mice and their

increased LMA seems unlikely, because their spectral phenotype was also present during the light phase, when LMA did not differ.

On the other hand, prolonged running wheel activity, referred to as ‘stereotypic behavior’, is associated with a reduction in cortical firing rate compared to exploratory behavior (Fisher et al., 2016), suggesting that *Cirbp* KO mice may move more, but that this behavior is non-goal directed. Moreover, a body of literature suggests coupling of theta-phase and gamma-activity in the hippocampus, which have been postulated to function in higher cognitive functions (for review see (Colgin, 2015)). Because of CIRBPs role in slowing down theta peak frequency and increasing power in the gamma bands, further analyses and experiments can address if *Cirbp* KO mice have indeed altered phase coherence between these two frequency bands. Together with a possible increase in non-goal directed behavior in *Cirbp* KO mice, it would be interesting to assess if lack of CIRBP is related to cognitive consequences.

Several aspects of waking that appeared to differ between *Cirbp* KO and WT mice but were non-significant under baseline conditions, reached significance during the recovery, as if SD amplified the genotypic differences. Sleep disturbance, like SD, has been identified as a risk factor for disease progression; for example, it can amplify molecular and behavioral phenotypes of Alzheimers’ mouse models (for review, see (Musiek, Xiong, & Holtzman, 2015)) as well sensitivity to pain (Sutton & Opp, 2014). It would be of interest to see if a similar phenomenon occurs in *Cirbp* KO mice, where a single 6-hr SD can unlock the genotypic differences, and to what extent these changes are reversible.

CONCLUSION

This hypothesis-driven study explored if the SD incurred changes in clock gene expression are linked by the cold-induced transcript CIRBP. After SD, the cortical expression of *Rev-erba*, which we recently identified as a player in the sleep homeostat, was as hypothesized, attenuated in *Cirbp* KO mice. Furthermore, the expression of two other clock genes, *Per2* and *Clock*, was modulated.

Sleeping at the wrong time of the day and sleeping too little are both associated with disturbed metabolism and can subsequently lead to metabolic disorders like type two diabetes mellitus (Copinschi, Leproult, & Spiegel, 2014; Panda, 2016). The expression of clock genes, which regulates those downstream metabolic pathways (Panda, 2016), is also in humans modulated by sleep-wake state (Archer et al., 2014). Furthermore, genetic disruption of clock genes can exacerbate the development of metabolic disorders (e.g. (Rudic et al., 2004)). Hence, disturbances in clock gene

expression could underly the observation that both sleep curtailment and circadian disturbances have metabolic consequences. Because impaired sleep has been suggested to accelerate the development of metabolic pathologies, it is of uttermost importance to understand further via which pathways a disturbed sleep-wake distribution, may it be by sleeping too little or at the wrong time of the day, modulates clock gene expression.

Acknowledgements

We would like to thank Maxime Jan for his help in constructing the linear mixed model; our colleagues for assistance with the sleep deprivations and Hannes Richter from the Genomic Technology Facility, UNIL for his support when setting up the RT-qPCR.

Material and Methods

MICE AND HOUSING CONDITIONS

Cirbp KO mice, kindly provided by Prof Jun Fujita (Kyoto University, Japan), were maintained on a C57BL6/J background. In these mice, exon 1 to 6 were replaced by a TK-neo gene through homologous recombination in D3 embryonic stem cells, resulting in the absence of the *Cirbp* transcript and protein (Masuda et al., 2012). Breeding couples or trios consisted of heterozygous male and female mice. WT littermates were used as controls. Throughout the experiment, mice were individually housed in polycarbonate cages (31×18×18 cm) with food and water *ad libitum* and exposed to a 12 h light/12 h dark cycle (70–90 lux). All experiments were approved by the Ethical Committee of the State of Vaud Veterinary Office Switzerland under license VD2743.

EEG/EMG IMPLANTATION

At the age of 9 to 13 weeks, 17 KO and 20 WT male mice were implanted with electroencephalogram (EEG) and electromyogram (EMG) electrodes. The surgery took place under deep xylazine/ ketamine anesthesia complemented with isoflurane (1%) when necessary; for details see (Mang & Franken, 2012). Briefly, six gold-plated screws (diameter 1.1 mm) were screwed bilaterally into the skull, over the frontal and parietal cortices. Two screws served as EEG electrodes and the remaining four anchored the electrode connector assembly. As EMG electrodes, two gold wires were inserted into the neck musculature. Of all EEG/EMG implanted mice, 8 KO and 9 WT mice were additionally implanted with a thermistor (serie P20AAA102M, General Electrics (currently Thermometrics), Northridge, California, USA) which was placed on top of the right

cortex (2.5 mm lateral to the midline, 2.5 mm posterior to bregma). The EEG and EMG electrodes and thermistor were soldered to a connector and cemented to the skull. Mice recovered from surgery during 5–7 days before they were connected to the recording cables in their home cage for habituation, which was at least 6 days prior to the experiment. In total no less than 11 days were scheduled between surgery and start of experiment.

EXPERIMENTAL PROTOCOL AND DATA ACQUISITION

EEG and EMG signals, T_{cx} and LMA were recorded continuously for 96 h. The recording started at light onset; i.e., Zeitgeber Time (ZT)0. During the first 48 h (days BL1 and BL2), mice were left undisturbed to establish a baseline. Starting at ZT0 of day 3, mice were sleep deprived by gentle handling for 6 hours (ZT0–6), as described in (Mang & Franken, 2012). The remaining 18 h of day 3 and the entire day 4 were considered as recovery (days REC1 and REC2, respectively). The analog EEG and EMG signals were amplified (2,000 \times), digitized at 2 kHz and subsequently down sampled to 200 Hz and stored. The EEG was subjected to a discrete Fourier transformation yielding power spectra (range: 0–100 Hz; frequency resolution: 0.25 Hz; time resolution: consecutive 4-sec epochs; window function: Hamming). Thermistors were supplied with a constant measuring current ($I_{const} = 100$ microA) and voltage (V) was measured at 10 Hz which was subsequently used to calculate the median resistance (R_t) per 4-s epoch as in eq. (1).

$$(1) R_t = \frac{V}{I_{const}}$$

Each thermistor has an individual material constant, β . The resistance was measured at 25°C ($R_{25^\circ C}$) and 37°C ($R_{37^\circ C}$) by the manufacturer, and used to determine β as in eq.(2), with T values in Kelvin ($^\circ C + 273.15$).

$$(2) \beta = \frac{T_{25} * T_{37}}{T_{25} - T_{37}} * \ln \frac{R_{37^\circ C}}{R_{25^\circ C}}$$

Following on eq. (2), the temperature (t) in $^\circ C$ can be calculated as described in eq. (3).

$$(3) t(^\circ C) = \left[\frac{1}{\beta} * \log \left[\frac{R_t}{R_{25^\circ C}} \right] + \frac{1}{T_{25^\circ C}} \right]^{-1} - 273.15$$

The EEG, EMG, and voltage across the thermistor were recorded with Hardware (EMBLA) and software (Somnologica-3) purchased from Medcare Flaga (EMBLA, Thornton, USA). LMA was monitored with passive infrared sensors (ClockLab, ActiMetrics, Wilmette, Illinois, USA).

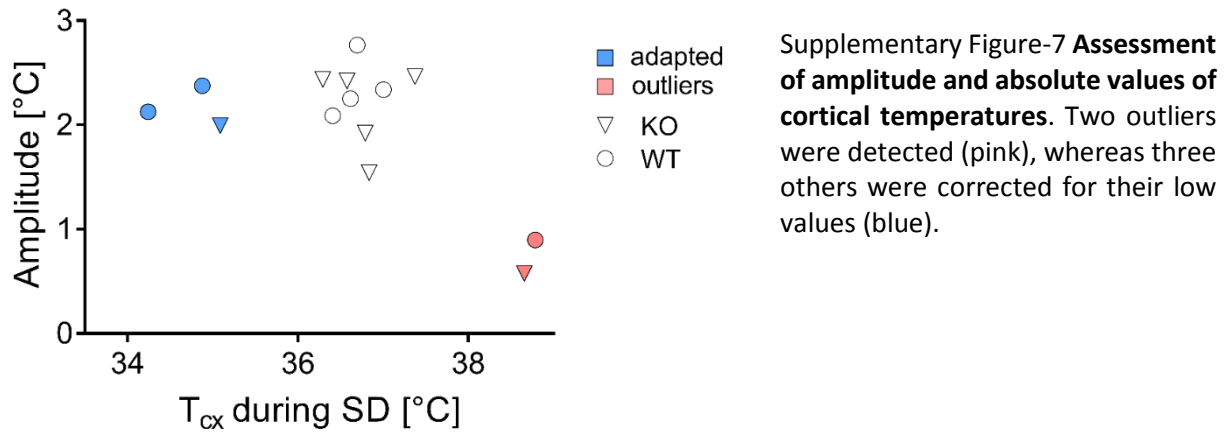
DETERMINATION OF BEHAVIORAL STATES

Offline, the mouse's behavior was visually classified as 'Wakefulness', 'REM sleep', or 'NREM sleep' for consecutive 4-sec epochs based on the EEG and EMG signals as previously described (Mang & Franken, 2012). Wakefulness was characterized by EEG activity of mixed frequency and low amplitude and variable muscle tone. NREM sleep was defined by synchronous activity in the delta frequency (1–4 Hz) and low and stable muscle tone. REM sleep was characterized by regular theta oscillations (6–9 Hz) with low EMG activity. Waking was further differentiated into 'quiet waking' and 'theta-dominated waking' (TDW), with TDW determined as described in (Vassalli & Franken, 2017) based on the relative importance of power in the 6.5 to 12.0 Hz range to the overall power in the EEG during artefact-free 4-sec scored as wakefulness. We refer to waking that is not classified as TDW as 'quiet' waking. 4-sec epochs containing EEG artefacts were marked according to the state in which they occurred and excluded from EEG spectral analysis but included in the sleep-wake distribution analyses. During the four day recording, $7.0 \pm 0.9\%$, $2.1 \pm 0.3\%$ and $2.5 \pm 0.2\%$ of the epochs was scored as an artefact in waking, NREM, and REM sleep, respectively, and this did not differ between genotypes (two sample t-tests, $t(35)=1.77$, $p=0.09$; $t(35)=0.64$, $p=0.53$; $t(35)=0.99$, $p=0.33$).

ANALYSIS OF CORTICAL TEMPERATURE

The raw T_{cx} data showed unexpected variation. Therefore, we inspected the inter-individual variation in daily amplitude and absolute T_{cx} levels. The latter was determined in two ways: i) by averaging T_{cx} during the last five hours of SD, thus minimizing the sleep-wake state incurred differences in T_{cx} , and ii) by averaging T_{cx} during the 12h baseline light phase. These measures were highly correlated ($R^2=0.99$; $p<0.0001$). Variation in the daily amplitude was quantified by averaging the difference between the highest and lowest hourly mean of T_{cx} of each of the two baseline days. No effect of genotype on absolute average T_{cx} or amplitude was detected (t-test, $t(12)=0.61$, $p=0.55$; $t(12)=-0.63$, $p=0.54$, respectively). Two mice (one of each genotype) exhibited a ca. 2-fold reduction in amplitude together with 2°C higher values during the SD relative to the other mice (Supplementary data, SFig2, pink symbols). Therefore, we excluded these two mice from subsequent T_{cx} analysis. Three other mice (2 WT and 1 KO) showed normal amplitude but overall lower absolute values (Supplementary data, SFig2, blue symbols). We corrected for this difference by raising their T_{cx} values by the difference between the T_{cx} reached in each of these 3 mice during the sleep deprivation to the average T_{cx} reached over the same recording period in the remaining 9

mice. Of note, most of our T_{cx} analysis focuses on its relative sleep-wake dependent changes, which are not affected by differences in absolute T_{cx} values. Finally, the baseline T_{cx} data was based on 6 WT and 6 KO mice. In the recovery, one KO mice was excluded due to aberrant high T_{cx} that could not be accounted for by the sleep-wake distribution, leaving 6 WT and 5 KO mice for analyses involving REC1 and REC2.



To aid visualization of sleep-wake states and T_{cx} in Figure 1, these variables were averaged per minute, thereby visually underrepresenting REM sleep, because this stage occurs less and in shorter bouts than waking and NREM sleep.

We determined the T_{cx} dynamics before and after a sleep-wake state transition in baseline. Selected transitions lasted at least 8 epochs (*i.e.* ≥ 32 sec) before and after the transition. In each mouse, a minimum of 10 transitions contributed to the mean change in T_{cx} per sleep-wake state transition. Thus, the closer to the sleep-wake state transition, the more epochs contributed to the mean individual T_{cx} . With these criteria, we detected an average of 38 wake to NREM sleep, 101 NREM sleep to REM sleep, 28 REM sleep to wake and 32 NREM sleep to wake transitions per mouse during the two baseline days.

The residuals of the correlation between waking and T_{cx} exhibited a circadian pattern under BL conditions. We quantified this further by fitting a sinewave through the data (Prism, non-linear regression; sine-wave with non-zero baseline; least squares fit).

ANALYSIS OF LMA

To inspect the time course of LMA corrected for time-spent-awake, raw LMA was expressed per unit of waking in percentiles to which an equal amount of time-spent-awake contributed (Figure

2G). The number of percentiles per recording period were chosen according to the prevalence of wakefulness, where 6 percentiles were used during the light phase and 12 during the dark phase, with the exception for 6 sections during the SD and 3 sections during the remaining 6hrs of the light phase of REC1. To assess genotype differences in LMA (Figure 3), the absolute number of movements were inspected. The LMA recordings of four mice (3 WT, 1 KO) were interrupted due to technical problems during the experiment and therefore excluded, leaving data from 17 WT and 16 KO mice for analyses involving LMA.

GENE EXPRESSION IN LIVER AND BRAIN

Five mice of each genotype (n=15 per genotype in total) were sacrificed either prior to SD (ZTo), at ZT6 without SD (ZT6-NSD), or at ZT6 after 6h SD (ZT6-SD) to quantify the effects of genotype on gene expression in cortex and liver. Genes of interest included transcripts affected by SD (Maret et al., 2007; Mongrain et al., 2010) and/or by the presence of CIRBP (Liu et al., 2013; Morf et al., 2012) with a special interest for clock genes. To quantify mRNA expression, specific forward and reverse primers and Taqman probes were designed (see Supplementary data, Table S2).

Upon sacrifice, both the cerebral cortex and liver were extracted and immediately flash frozen in liquid nitrogen. Samples were stored at -80°C. RNA from cortex was extracted and purified using the RNeasy Lipid Tissue Mini Kit 50 (QIAGEN, Hombrechtikon, Switzerland); RNA from liver was extracted and purified using the RNeasy Plus Mini Kit 50 (QIAGEN, Hombrechtikon, Switzerland), according to manufacturer's instructions. RNA quantity (NanoDrop ND-1000 spectrophotometer; Thermo Scientific, Wilmington, NC, USA) and integrity (Fragment Analyzer, Advanced Analytical, Ankeny, IA, USA) was measured and verified for each sample. 1000 ng of purified total RNA was reverse-transcribed in 20µL using a mix of First-strand buffer, DTT 0.1M, random primers 0.25µg/µL, dNTP 10mM, RNAzin Plus RNase Inhibitor and Superscript II reverse transcriptase (Invitrogen, Life Technologies, Zug, Switzerland) according to manufacturers' procedures. The cDNA was diluted 10 times in Tris 10 mM pH 8.0, and 2µL of the template dilution was amplified in a 10µL TaqMan reaction in technical triplicates on an ABI PRISM HT 7900 detection system (Applied Biosystems, Life Technologies, Zug, Switzerland). Cyclor conditions were: 2 min at 50°C, 10 min at 95°C followed by 45 cycles at 95°C for 15 s and 60°C for 1 min. Standard curves were calculated to determine the amplification efficiency (E). A sample maximization strategy was used where all biological replicates of one tissue were amplified for two genes per plate. Gene expression levels were normalized to two reference genes (cortex: *Eef1a* and *Gapdh*: M=0.23, CV=0.09 and liver: *Gadph* and

Tbp; M=0.32, CV=0.11) using QbasePLUS software (Biogazelle, Zwijnaarde, Belgium). To correct post-hoc a suboptimal primer design, *Rbm3* isoforms were in a separate run quantified in liver and cortex, again with their housekeeping genes (same as previously; cortex: M=0.22, and CV=0.08; liver: M=0.13, CV=0.05). Transcripts with an average Ct-value>30 were omitted from analysis (in KO and WT livers: *Rbm3*, *Dusp4*, *Homer1a*, and *Npas2*; in cortex and liver of KO mice: *Cirbp*). Results are expressed as normalized relative quantity (NRQ) which is indicative of gene expression and based on the overall mean expression per gene, which was set at 1.0 (Hellemans, Mortier, De Paepe, Speleman, & Vandesompele, 2007).

CIRBP affects the poly-adenylation sites of several transcripts (Liu et al., 2013). We explored if this newly discovered role of CIRBP could be corroborated in our study by focusing on the transcript Splicing factor, proline and glutamine rich, *Sfpq* which exhibits CIRBP-dependent alternative poly-adenylation (APA) ((Liu et al., 2013), see their Supplemental Fig4-5). We calculated the ratio of the prevalence of the distal/external 3'UTR region over the common region according to eq. (6),

$$(4) \text{Ratio}_{ext / comm} = \frac{E^{-Ct_{ext}}}{E^{-Ct_{comm}}}$$

where E is the amplification efficiency and Ct_{ext} and Ct_{comm} the number of cycles for the detection of the distal and common isoform, respectively.

ANALYSIS OF EEG BASED ON BEHAVIORAL STATE

Unless otherwise stated in the methods section, all mice (20 WT and 17 KO) were included in the analyses based on the EEG data. Spectral content of the EEG within sleep-wake states was calculated as follows. To account for inter-individual differences in overall EEG power, EEG spectra were expressed as a percentage of an individual reference value calculated as the total EEG power across 0.75-45 Hz and all sleep-wake states in the 48h baseline. This reference value was weighted so that for all mice the relative contribution of the three sleep-wake states to this reference value was equal.

Theta peak frequency (TPF) in TDW and in REM sleep was calculated by determining the frequency at which power density peaks in the 6.5 to 12.0 Hz band per 4-s epoch and subsequently averaged per individual.

Time course analysis of EEG delta power (*i.e.*, the mean EEG power density in the 0.75-4.0 Hz range in NREM sleep) during baseline and after SD was performed as described previously (Franken, Malafosse, & Tafti, 1999), similar to the analysis of LMA per unit of waking. The light periods of BL₁, BL₂, and REC₂ were divided into 12 percentiles, the REC₁ light period (ZT6-12) into

8 sections, and all dark periods into 6 sections, and was based on the prevalence of NREM sleep like explained for wakefulness above. EEG delta power values in NREM sleep were averaged within each percentile and then expressed relative to the mean value reached in the last 4hr of the two main rest periods in baseline between ZT8–12. This reference was selected because delta power values reach lowest values here, that are least influenced by differences in prior history of sleep and wakefulness (see also (Franken et al., 1999)).

The effect of 6hr SD on subsequent time spent in NREM and REM sleep was assessed by calculating the recovery-baseline difference in sleep time per 1hr intervals.

SIMULATING NREM EEG DELTA POWER [PROCESS S]

We applied a computational method to predict the change in delta power during NREM sleep based on the sleep-wake distribution as described before (Franken et al., 2001). Process S is exponentially increasing with time constant τ_i during waking and REM sleep, and exponentially decreasing τ_d during NREM sleep (eq. (4) and (5), respectively).

$$(5) S_{t+1} = UA - (UA - S_t) * e^{-\frac{dt}{\tau_i}}$$

$$(6) S_{t+1} = LA + (S_t - LA) * e^{-\frac{dt}{\tau_d}}$$

In these simulations, UA represents the upper asymptote, LA the lower asymptote and dt the time step of the iteration (4 seconds). The upper and lower asymptotes were based on the 99% level of the relative frequency distribution of delta power reached in all 4s epochs scored as NREM sleep in the 4-day recording and the intersection of these values with the relative frequency distribution of REM delta power, respectively. At the start of the simulation, an iteration through the first 24-hr (BL1) was performed with $S_0=150$ at $t=0$. The value reached after 24-hrs is independent of S_0 at $t=0$ and reflects Process S at the start of the baseline.

The fit was optimized by minimizing the mean squared difference of simulated and observed NREM delta power for a range of T_i : 1-25 h, step size 0.125h; T_d : 0.1-5.0 h, step size 0.025h; *i.e.* the simulation was run for all 38'021 combinations of T_i and T_d for each mouse. The combination of T_i and T_d giving the best fit was used to assess differences in process S between genotypes.

We noted a subtle but consistent linear discrepancy in the alignment of simulation process S to the measured NREM delta power values at the end of the light phase on BL1, BL2 and REC2 (Pearson correlation, slope \neq 0: 1 sample t-test; $t(35)=-4.38$, $p=0.0001$). This change correlated well with the

day-to-day changes in total spectral power in the EEG calculated across all sleep-wake states in BL₁, BL₂, and REC₂ (Pearson correlation: $R^2=0.70$, $p<0.0001$; $n=36$). We attributed these linear changes to be of non-biological origin and detrended the measured NREM delta power values before optimizing the fit between observed and simulated delta power. There was no effect of genotype on slope (Δ delta power %/h; students' t-test; $t(34)=0.62$; $p=0.54$; WT: -0.086 ± 0.027 ; KO: -0.065 ± 0.021) or intercept ($t(34)=-0.88$; $p=0.38$; WT: 101.5 ± 0.62 ; KO: 100.7 ± 0.56 ; WT: $n=20$, KO: $n=17$).

STATISTICS

Statistics were performed in R (version 3.3.2) and Prism (version 7.0). The threshold of significance was set at $p=0.05$. Deviations from the mean are representing standard error of the mean. The distribution of the LMA data was normalized by a \log_2 transformation on the hourly values, allowing for subsequent parametric analyses on the relationship between T_{cx} and LMA as in Figure 2.

Time course data were analyzed by 1- and 2-way repeated measures (RM) analysis of variance (ANOVA) with as factors 'time' and 'genotype' (GT). Upon significance, t-tests were computed. Differences between BL and REC values within genotype were computed by paired t-tests. EEG spectra were also analyzed by 1- and 2-way RM ANOVA with as factors 'time' or 'frequency' and 'GT'. When GT or its interaction with time or frequency reached significance, post-hoc t-tests were computed. The above-mentioned analyses were all performed in Prism.

In the time course of NREM delta power, one mouse (KO) demonstrated a strong decrease over the course of the experiment which could not be attributed to changes in the sleep-wake distribution. 9 out of the 12 delta power values during the light phase of REC₂ in this mouse were outliers (MAD outlier test, consult (Leys, Ley, Klein, Bernard, & Licata, 2013) for details). This mouse was excluded from the analysis involving hourly and accumulated time-spent-in NREM sleep, resulting in 20 WT mice and 16 KO for these analyses (Fig4-A and Fig4-B).

Correlation coefficients of linear regression were calculated in Prism over all hourly values of LMA, T_{cx} and waking per genotype (96 per mice). To understand if slopes of regression lines differed between genotypes, an ANCOVA was applied based on (Zar, 1984) and run in Prism. To quantify the contribution of waking and LMA independent from each other to T_{cx} , a partial correlation was performed (R software; package 'ppcor', function `pcor.test`). Mixed model analysis was performed with factors LMA (\log_2 transformed), waking, and genotype (R packages 'lme4', 'lmer', 'lmerTest',

and 'MuMIn'). Model₁ quantified the predictive power of waking to T_{cx} , Model₂ of waking and LMA per unit of waking (LMA/Waking) and Model₃ of waking, LMA/Waking and its interaction to predict T_{cx} . Predictive power of models was compared with Chi-squared tests by assessing the statistical significance in the reduction of residual sum of squares between two models ordered by complexity; *i.e.* Model₁ was compared to Model₂, and upon significance, Model₂ was compared to Model₃. Goodness-of-fit was assessed by the marginal R-squared (R^2_m) which explains the effect of the fixed factors only, and the conditional R-squared (R^2_c), which considers the individual variance as well and is therefore more biological relevant. Hence, in the results section only the R^2_c values are reported.

For the molecular data, the qPCR NRQ values were \log_2 -transformed to normalize the distribution. Genotype differences at ZTo were tested with a t-test. The effect of SD and genotype at ZT6 was assessed by 2-way ANOVA with post-hoc Fisher LSD tests upon significance. One outlier (WT, cortex) in the *ext/com* ratio analyses was detected by the Grubbs outliers test ($\alpha < 0.05$).

Supplementary Table 1: sequences of the forward and reverse primer and probe used for the RT-qPCR

GeneName	FwdPrimer	RevPrimer	Probe
<i>Cirbp</i>	AGGGTTCTCCAGAGGAGGAG	CCGGCTGGCATAGTAGTCTC	CGCTTTGAGTCCCGAGTGGG
<i>Clock</i>	CGAGAAAGATGGACAAGTCTACTG	TCCAGTCTGTGCAATCTCA	TGCGCAAACATAAAGAGACCACTGCA
<i>Dbp</i>	CGTGGAGGTGCTTAATGACCTTT	CATGGCCTGGAATGCTTGA	AACCTGATCCCGCTGATCTCGC
<i>Dusp4</i>	GTTTCATGGAAGCCATCGAGT	CCGCTTCTTCATCATCAGGT	TCCCGATCAGCCACCACTCTGC
<i>Eef1a</i>	CCTGGCAAGCCCATGTGT	TCATGTCACGAACAGCAAAGC	TGAGAGCTTCTCTGACTACCCTCCACTTGGT
<i>Gadph</i>	TCCATGACAACCTTGCCATTG	CAGTCTTCTGGGTGGCAGTGA	AAGGGCTCATGACCACAGTCCATGC
<i>Homer1a</i>	GCATTGCCATTTCCACATAGG	ATGAACTCCATATTTATCCACCTTACTT	ACA5ATT5AATT5AG5AATCATGA (*)
<i>Hsf1</i>	CAACAACATGGCTAGCTTCG	CTCGGTGTCTCTCTCAGG	TGAGCAGGGTGGCCTGGTCA
<i>Hsp90b1</i>	TGTACCCACATCTGCACCTC	TTGGGCATCATATCATGGAA	CGCCGCTATTTCATCAGATGA
<i>Hspa5/Bip</i>	CACTTGAATGACCCTTCG	GTTTGCCACCTCCAATATC	TGGCAAGAAGTGTGCTCCTGCTGC
<i>Npas2</i>	AGGAAAGGACGTCTGCTTCA	CCAAGCTATGCCTCGAAGTG	CCTGGCAACCCCGCAGTCTTA
<i>Per2</i>	ATGCTCGCATCCACAAGA	GCGGAATCGAATGGGAGAAT	ATCCTACAGGCCGGTGGACAGCC
<i>Rbm3Long</i>	TGATGCTGTCTTCAGGATGC	GGCCCAACACAAGTAAAGGA	TCAAGGATGAGGTAAGTATGCTATCCTTGAGC
<i>Rbm3Short</i>	GGCTATGACCGCTACTCAGG	CAGCAATTTGCAAGGACGAT	TGAGATGGGGCATGCACACA
<i>Nr1d1 / reverb-α</i>	AGGGCACAAAGCAACATTACC	CAGGCGTCACTCCATAGT	AGGCCACGTCCCCACACACC
<i>Sfpq</i>	GCATTTGAAAGATGCAGTGAA	CAGGAAGACCATCTTCGTCA	TCGCCAGTCATTGTGGAACCA
<i>Sfpq_Comm</i>	TGGATGTTAGCAGTTTATTGACC	GCACAAGGTACTGTCATT	TGTAATGGCCTGTTTGGGCAGG
<i>Sfpq_Ext</i>	TGCTTCTCCACCATAAG	TTGCTCTAACGAAAGGAAATTC	TGGGGATGTTTGTGATGTCAGTTCA
<i>Sirt1</i>	TTGTGAAGCTGTTCTGTTGAG	CTCATCAGTGGGCACCTA	TTTTAATCAGGTAGTTCCTCGGTGCC
<i>Tbp</i>	TTGACCTAAAGACCATTCACCTTC	TTCTCATGATGACTGCAGCAA	TGCAAGAAATGCTGAATATAATCCCAAGCG

(*) 5 = propynyl-dC ; increases the melting temperature of the probe

Supplementary Table 2: statistics on RT-qPCR results

Transcript	Cortex				Liver			
	ZT0 (#)	ZT6 SD/NSD(*)	GT (*)	Interaction (*)	ZT0 (#)	ZT6 SD/NSD (*)	GT (*)	Interaction (*)
<i>Cirbp</i>	X	t(8)=4.9, p=0.001	X	X	X	t(8)=4.0, p=0.004	X	X
<i>Clock</i>	t=0.86; p=0.21	F=2.38 p=0.14	F=0.85; p=0.37	F=8.02; p=0.01	t=0.03; p=0.98	F=0.09; p=0.77	F=0.81; p=0.38	F=0.03; p=0.87
<i>Dbp</i>	t= 0.13; p=0.90	F=82.0; p<0.0001	F=0.39; p=0.54	F=3.06; p=0.10	t=1.99 p=0.08	F= 4.37; p=0.05	F=0.23; p=0.64	F=0.0002; p=0.99
<i>Dusp4</i>	t=1.29; p=0.23	F=97.55; p<0.0001	F=0.50; p=0.49	F=3.24; p=0.09	X	X	X	X
<i>Homer1a</i>	t=0.96; p=0.36	F=228.8; p<0.0001	F=0.005; p=0.94	F=1.08; p=0.31	X	X	X	X
<i>Hsf1</i>	t=0.67; p=0.52	F=18.22; p=0.0006	F=1.79; p=0.20	F=1.9; p=0.18	t=0.14; p=0.89	F=3.43; p=0.08	F=4.63; p=0.05	F=0.48 p=0.50
<i>Hsp90b</i>	t=1.29; p=0.23	F=7.18; p=0.0164	F=1.40; p=0.25	F=6.86; p=0.02	t=1.71; p=0.12	F=0.93; p=0.35	F=0.80; p=0.38	F=0.07; p=0.80
<i>Hspa5</i>	t=0.89; p=0.40	F=72.03; p<0.0001	F=0.03; p=0.86	F=5.32; p=0.03	t=2.02; p=0.08	F=0.62; p=0.44	F=0.84; p=0.37	F=0.04; p=0.86
<i>Npas2</i>	t=0.86; p=0.41	F=1.56; p=0.2298	F=0.0008; p=0.98	F=3.99; p=0.06	X	X	X	X
<i>Per2</i>	t=2.78; p=0.02	F=75.22; p<0.0001	F=4.78; p=0.04	F=0.06; p=0.80	t=0.90; p=0.40	F=0.95; p=0.34	F=0.01; p=0.92	F=0.02; p=0.90
<i>Rbm3-short</i>	t=0.05; p=0.96	F=32.04; p<0.001	F=0.31, p=0.59	F=0.13, p=0.73	t=2.23, p=0.06	F=47.6, p<0.0001	F=2.7, p=0.12	F=1.6, p=0.22
<i>Rbm3-long</i>	t=0.10, p=0.92	F=9.49, p=0.007	F=0.03, p=0.86	F=0.32, p=0.58	X	X	X	X
<i>Rev-erba</i>	t=0.91; p=0.39	F=8.95; p=0.009	F=1.09; p=0.31	F=6.80; p=0.02	t=1.59; p=0.15	F=31.13; p<0.0001	F=2.41; p=0.14	F=1.37; p=0.26
<i>Sfpq</i>	t=1.51; p=0.17	F=11.61; p=0.004	F=0.017; p=0.90	F=4.44; p=0.05	t=0.93; p=0.38	F=1.26; p=0.28	F=2.78; p=0.11	F<0.001; p=0.98
<i>Sirt1</i>	t=2.56; p=0.04	F=1.61; p=0.22	F=0.14; p=0.72	F=2.07; p=0.17	t=1.75; p=0.12	F=0.94; p=0.35	F=0.03; p=0.87	F=0.12; p=0.73

GT: genotype, SD/NSD: Sleep deprived / non-sleep deprived (control)

ZT0: t-test, degrees of freedom: 8

ZT6: two-way ANOVA (factors SD and GT), df=1 for both factors SD, GT and its interaction; error df=16

X: Ct>30 or undetected

Green: significant increase

Red: significant decrease

Purple: significant interaction

Significance level: $\alpha \leq 0.05$

“Scientific objectivity is not the absence of initial bias.
It is attained by frank confession of it.”

Mortimer J. Adler

Chapter 5 General Discussion

In this chapter, the results and conclusions of the two projects are discussed in the broader context of sleep, circadian rhythms and clock genes. The points raised go beyond the specific considerations brought up in the discussion sections of the experimental chapters.

PER₂ ENCOMPASSES CIRCADIAN TIME AND SLEEP PRESSURE

It is known for more than fifteen years that sleep deprivation affects clock gene expression (Wisor et al., 2002). However, our study is the first to report on a relationship between sleep-wake state and PER₂ bioluminescence in a freely behaving mouse. Our read-outs are based on undisturbed measurements thereby overcoming potential confounding factors that are associated with sleep deprivation. This experimental set up provided two more advantages: i) we did not have to sacrifice mice at each time-point, thereby tremendously decreasing the number of animals, and ii) mice were functioning as their own control, thereby overcoming inter-individual variation and thus strengthening the experimental design. Our most important finding, however, is that also under undisturbed conditions, it appears that PER₂ bioluminescence functions as an output of the sleep-wake distribution, instead of the clock.

Changes in PER₂ bioluminescence were occurring on a relatively short time scale as a function of spontaneous sleep-wake state. We assume that these changes reflect differences in PER₂ protein, but do they? If this is the case, changes at the transcriptional and/or translation level need to occur fast as well. There are only a handful experiments that addressed the induction of period-genes at a time-scale comparable to ours.

Experiments supporting rapid changes at the level of transcription revealed that light pulses delivered from CT16 to CT16.5 can induce an increase in *Per1* in the SCN within ten minutes after light onset (Shigeyoshi et al., 1997). A light pulse at CT13.5 and CT20 also elicits increased expression of *Per1* and *Per2* in the SCN within 30 minutes after the light pulse (Moriya, Horikawa, Akiyama, & Shibata, 2000).

At the translational level, the production of PERIOD-proteins can be induced fast too. Exposing mouse embryonic fibroblasts to horse serum induces an increase in PER₁ and PER₂ within 30 minutes (R. Cao et al., 2015). Moreover, an acute stressor (forced swim test) induced significant increases in PER₁ levels in several areas of the rat brain within one-hour (Al-Safadi et al., 2014).

Thus, the changes in PER2 bioluminescence that we observed around sleep-wake state transitions could reflect rapid changes in PER2 protein levels. The aforementioned studies used western blot and immunohistochemistry, respectively, to estimate Period-protein levels, even though these techniques are considered semi-quantitative. To detect PER2 changes at the time-scale we are interested in, a sensitive protein quantification method needs to be deployed.

PER2 and delta power: correlates of sleep pressure?

There is cross-talk occurring between the circadian and sleep homeostatic components of the two-process model (Borbely, Daan, Wirz-Justice, & Deboer, 2016). For example, feelings of sleepiness are the result of the interaction between time spent awake and circadian time (Akerstedt et al., 2014). *Per2*, although considered a clock gene, also encompasses both time spent awake and circadian time (Curie et al., 2013). Manipulating the core clock in mouse models affects sleep deprivation incurred changes in the cortical *Per2* response and the NREM sleep homeostatic process (*i.e.* delta power): an amplified increase of delta power correlated with increased levels of *Per2* (Wisor et al., 2008). Furthermore, a lower build-up rate of NREM sleep pressure, and lower NREM delta power after spontaneous wake bouts, was associated with an attenuated increase in cortical *Per2* ((Franken et al., 2006) and (Vassalli & Franken, 2017), respectively).

Given *Per2*'s correlation with NREM delta power, this gene could be expected to be causally involved in the NREM sleep homeostat as well. This was addressed in studies where the function of the *Per2* gene was impaired or removed by genetic mutations. The first study found that *Per2*-mutant mice slept more during the recovery of the 6hr sleep deprivation compared to WT (wild-type) mice. Moreover, the increase in delta power immediately after sleep deprivation was attenuated in *Per2*-mutant mice (Kopp et al., 2002). The second study, using a different mutation on a different genetic background, found that after sleep deprivation *Per2* mutant mice also recovered more NREM sleep. However, this study did not specifically address genotype differences in delta power after sleep deprivation (Shiromani et al., 2004). The third study is work in progress from our lab and demonstrated that sleep deprivation did not increase NREM delta power differently between WT and *Per2* knock-out mice. However, *Per2* knock-out mice did recover significantly less NREM sleep compared to their WT-littermates (Spada, 2013). All together, these results suggest that *Per2* is implicated in different aspects of sleep homeostasis, but the differences in experimental design and analysis make it challenging to compare the results between studies directly.

Thus, further studies will need to identify the source of variation and assess if PER2 is functionally implicated in the sleep-wake distribution, or merely reflects time-spent-awake and circadian time.

Considering sleep-wake state in clock gene expression: the caveat of food

Like body temperature, clock gene expression is considered a phase marker of circadian rhythms. However, the expression of clock genes (*e.g. Per1-3, Dbp, Rev-erb α*) outside the SCN is affected by sleep-wake state and should thus be used with caution when informing about time of day. Knowing that sleep-wake state affects clock gene expression can support understanding in other circadian-related phenomena's, such as food anticipatory activity. Offering food to mice at restricted times of the day induces food-entrained behavior: mice anticipate the arrival of food, as if there was a clock informing them when food is available. This food-entrained behavior is associated with phase shifts of clock gene expression in the periphery and functions independently of the SCN (reviewed in (Escobar, Cailotto, Angeles-Castellanos, Delgado, & Buijs, 2009)). The underlying substrate of this food-entrainable oscillator remains mysterious but has, amongst others, shown to be dependent on the presence of functional core clock genes such as *Npas2* (Dudley et al., 2003).

By extending this 'circadian' view on food driven changes in peripheral clock gene expression, it could be argued that the effect of sleep deprivation on clock gene expression is mediated by increased food intake too. Two studies from our lab addressed the importance of food in the sleep deprivation induced changes in clock gene expression (unpublished observations). First, we found that mice do not eat significantly more during the sleep deprivation (ZT0-ZT6) in comparison to the same time of the day when they can sleep *ad lib*. This observation is in corroboration with the circadian modulation of food intake measured during the 2hOn/Off experiment (this thesis). Secondly, we demonstrated that food availability does not modulate the sleep deprivation induced changes in cortical clock gene expression (Spada, 2013).

Therefore, the interpretation that the 'food entrainable oscillator' is driving changes in clock gene expression might be inaccurate: instead, it could be the consequence of being awake, with all the associated wake-driven physiological changes in for example temperature and corticosterone (personal communication, P. Franken). However, distinguishing between being awake and food intake is not straightforward, as one needs to be awake to eat. Therefore, an experiment should be designed where food intake is dissociated from the need to wake up. For example, a technique could

be used where food is constantly infused into the stomach (as described here: (Ueno et al., 2012)). This constant food supply can then be combined with a daily occurring arousing event thereby mimicking the waking that is associated with food anticipatory activity.

How do clock genes contribute to the sleep homeostat?

To narrow down the question, we could first ask *where* clock genes contribute to the sleep homeostat by quantifying where sleep deprivation affects clock gene expression. This phenomenon occurs in varying degrees, but in all organs and fluids quantified (reviewed in (Archer & Oster, 2015)). Importantly, an exception are the SCN, which are not affected by sleep deprivation in terms of PER2 protein levels (Curie et al., 2015), although the electrophysiological properties of the SCN are sensitive to changes in sleep-wake state (Deboer, Vansteensel, Detari, & Meijer, 2003). Moreover, no intact SCN in terms of tissue (Trachsel, Edgar, Seidel, Heller, & Dement, 1992) or molecular clock is necessary for an intact sleep homeostat (P. Franken, personal communication). Taking together, this suggests that clock gene expression outside the SCN is participating in the sleep homeostatic process.

Most clock gene mutant studies investigated the importance of clock genes in the sleep homeostat by using full body mutant mice models. For example, full body KO *Bmal1* mice sleep much more than their WT littermates (Laposky et al., 2005). A follow-up study assessed in which tissue *Bmal1* contributes to this sleep homeostatic phenotype. Surprisingly, the loss of sleep in full *Bmal1* KO mice could be partly by reinstating *Bmal1* rhythmicity in the muscle, but not in the brain (Ehlen et al., 2017). To my knowledge, this is the only study so far that experimentally established a functional link between peripheral clock gene expression and overt sleep-wake behavior.

Follow-up questions could address which signals are conveyed from the muscle to induce sleep at the level of brain activity. It might be through metabolic pathways that these changes occur, because: i) clock gene mutations affect metabolism (reviewed in (Panda, 2016)) and ii) changes in metabolic state affect sleep; for example, a high fat diet in rats reduces the time spent awake and promotes wake fragmentation (Luppi et al., 2014). To investigate this possible pathway further, mice with a specific *Bmal1*-arrest in the liver (Kornmann et al., 2007; Lamia, Storch, & Weitz, 2008) can be sleep phenotyped. If these mice exhibit an *Bmal1* KO sleep phenotype at the level of the brain, this might be conveyed through changes in metabolism. Overlapping the blood transcriptome and metabolome profile of the liver-arrest *Bmal1* mouse with the full *Bmal1* KO mouse can provide clues on sleep signaling molecules, thereby unravelling how clock genes contribute to sleep homeostasis.

Conclusions and perspectives

Sleep deprivation affects clock gene expression. Our results show that PER2 bioluminescence is not only driven as a function of the circadian clock but as well by sleep-wake state. These insights are of importance. Acknowledging the intimate crosstalk between metabolism, clock genes and its link to pathologies (Bass & Takahashi, 2010) while ignoring the importance of the sleep-wake distribution hampers the development of treatments aiming to ameliorate circadian (or sleep!)-associated pathologies.

CIRBPS' CONTRIBUTION TO WAKE-DRIVEN CHANGES IN CLOCK GENE EXPRESSION

In the second experimental chapter, a mechanism underlying the sleep-wake induced changes in clock gene expression is investigated. The hypothesis of this work was based on the results of two *in vitro* studies showing that the rhythmic expression of CIRBP (Morf et al., 2012), and CIRBP and RBM3 independently (Liu et al., 2013) facilitates high amplitude clock gene expression in temperature synchronized conditions. Therefore, we hypothesized that the increase in brain temperature incurred by sleep deprivation affects CIRBP levels which in turn mediates the changes in clock gene expression. However, the sleep-wake dependent changes in clock gene expression were only for *Rev-erba* attenuated in *Cirbp* KO mice, whereas the effect of sleep deprivation on the clock genes *Per2* and *Clock* was amplified in *Cirbp* KO mice. Thus, the sleep deprivation incurred changes in clock gene expression were not as widespread dependent on CIRBP as hypothesized. In hindsight, did we overlook some factors?

The observation that CIRBP is necessary for high amplitude clock gene expression *in vitro* appears robust because two independent studies using different methods (different temperature cycles; different mRNA quantification techniques; immortalized mouse embryonic stem cells and immortalized NIH3T3 cells, respectively by (Liu et al., 2013) and (Morf et al., 2012)). However, a decrease in clock gene expression amplitude can be due to its reduction in each individual cell, or be the resultant of individual cells gradually become desynchronized from each other (Nagoshi et al., 2004). Hence, cyclic changes in CIRBP could facilitate synchronization between cells, whereas in its complete absence, promote desynchronization of cells, appearing as a reduction in amplitude. However, Morf et al. discovered the postulated mechanism at the individual cell level through which CIRBP drives high amplitude clock gene expression, advocating against a synchronizing role

of CIRBP. Nevertheless, further experiments still need to address if this mechanism still holds at the group level.

Our presented results raise another question: Could RBM3 have compensated for the lack of CIRBP? Two arguments can be raised against this suggestion: i) both above mentioned *in vitro* studies reported that CIRBP alone (Morf et al., 2012) or CIRBP and RBM3 separately (Liu et al., 2013) are necessary for high amplitude clock gene expression and ii) no compensatory response in terms of *Rbm3* transcript levels was observed. Therefore, it appears unlikely that RBM3 could – completely- rescue our *Cirbp* KO phenotype.

One possible caveat of our experimental design to consider is that the hypothesis emerged from studies performed in a relatively simple biological system, immortalized cell lines, where *Cirbp* was acutely suppressed by silencing its RNA. We applied their conclusions to a very complex system: hepatic and cortical tissue of adult male mice. Already *in vitro* studies find discrepancies of circadian features between cell lines from different origins and age (for examples, see (Kaeffer & Pardini, 2005) and Fig6 in (Saini et al., 2012)). Moreover, our hypothesis is built on the idea that cortical temperature changes with waking whereas many other variables also change with waking (see for examples (Franken, 2013)). Some of these waking associated factors interact with CIRBP and could potentially show a compensatory response in its absence. For example, two of the three quantified cortical heat shock pathway transcripts (*Hsp90b* and *Hspa5/BiP*) showed a significant genotype-dependent sleep deprivation incurred amplification in our study. Interestingly, heat-shock factor 1 (HSF1) has, like CIRBP, been identified as a component mediating the effect of temperature to clock gene expression (Saini et al., 2012). HSF1 drives the expression of other heat shock proteins and the circadian expression of *Per2* by acting as a transcription factor (Reinke et al., 2008). The sleep deprivation incurred increase in *Hsf1* was only significant in *Cirbp* KO mice. Therefore, it is tempting to speculate that the amplified expression of *Per2* in *Cirbp* KO mice underlies a compensatory effect by HSF1-driven *Per2* transcription. This idea is further supported by the genotype dependent increase after sleep deprivation of *Hsp90b* and *Hspa5*, whose expression is also mediated by HSF1. Thus, HSF1 might have compensated for the absence of *Cirbp* in our study.

Another argument considering the step from *in vitro* to *in vivo* stems from the (absence of) reports on a circadian phenotype of overt behavior of *Cirbp* and *Rbm3* mutant mice. Because of the absence of those reports, it might be that *Cirbp* and/or *Rbm3* mutant mice have not a clear circadian phenotype and therefore the data has not been published (*i.e.* the ‘file drawer problem’). The results of our locomotor activity experiments showed that *Cirbp* KO mice are more active during the dark

(*i.e.* increased amplitude), which is counterintuitive regarding the *in vitro* studies where *si-Cirbp* led to reduced amplitude clock gene expression.

Conclusions and perspectives

Altogether, by taking the results from the *in vitro* studies to our *in vivo* experiments, we might have oversimplified our model for the questions asked. I would like to discuss briefly how this explanation of our results can be tested. The amplitude of clock gene expression can be quantified in *Cirbp* KO mice under baseline conditions to test if it is reduced like *in vitro*. If the amplitude is not reduced in KO mice, this supports the notion that the *in vitro* work is not directly translatable to the *in vivo* work. We could then reverse the approach and start with the simplest model; *i.e.* *in vitro* immortalized cell lines. First, we would reproduce that high amplitude clock gene expression is impaired in temperature synchronized cells upon *si-Cirbp*, and then add increasing levels of complexity. For example, by taking primary fibroblasts instead of immortalized cell lines, and incrementally add *in vitro* waking-associated agents to mimic more our *in vivo* system. When the effect of *si-Cirbp* on the amplitude of clock gene expression disappears, this points towards an underlying compensatory mechanism.

OTHER CONSIDERATIONS

Throughout the course of my scientific training, I expanded my knowledge on designing and conducting scientific experiments. The insights I gained through this learning process provided me with tools to better reflect on our work and understand its' shortcomings. Therefore, I would like to spend a few words on this here.

Sleep regulation beyond Process S and C

A study that motivated me to learn more about neuroscience showed that cage enrichment prevents rodents from addiction (Alexander, Beyerstein, Hadaway, & Coombs, 1981). Or, to put it the other way around, deprivation from cage enrichment facilitates addiction. Hence, one might wonder if such a complex behavior as sleep is affected by housing conditions. For logistic reasons, sleep studies in rodents have been performed mainly under environmentally deprived conditions. However, recently studies started to investigate the importance of housing conditions and indeed found that social housing affects baseline sleep (Febinger, George, Priestley, Toth, & Opp, 2014; Kaushal, Nair, Gozal, & Ramesh, 2012), the response to sleep deprivation (Kaushal et al., 2012) and

sleep after a stressful event (DaSilva et al., 2017; DaSilva et al., 2011; Meerlo, de Bruin, Strijkstra, & Daan, 2001). Also, the type of sleep deprivation (continuous cage change versus gentle handling) modulates sleep latency (Suzuki, Sinton, Greene, & Yanagisawa, 2013). Thus, environmental factors can modulate sleep. It remains to be determined if this also affects the build-up and decay rate of process S. However, there are indications that an aroused state of waking increases sleep pressure faster (Vassalli & Franken, 2017).

These insights should be considered when interpreting the results of the relationship between peripheral PER2 bioluminescence and sleep-wake state, because the mice were housed solitary deprived of environmental enrichment. Further studies need to address the impact of this environmental factor as soon as the technology is available.

Sex differences

Another example, which I did not specifically address in the two studies of this thesis, concerns sex differences. There is a large body of evidence demonstrating a significant contribution of sex in both circadian rhythms and sleep-wake behavior (for reviews see (Bailey & Silver, 2014) and (Mong & Cusmano, 2016)). In general, female mice spend less time asleep and exhibit higher NREM delta power, which is dependent on sex steroids (Mong & Cusmano, 2016). Furthermore, modelling of NREM sleep pressure based on the sleep wake distribution demonstrated that sleep pressure accumulated at a much slower rate in females than males (Franken et al., 2006). There are only a few studies that considered the relationship between clock genes and sleep regulation while controlling for sex. First, sex did not affect the increase in PER2 protein levels after sleep deprivation (Curie et al., 2015). Knocking out *Npas2* from the mouse's genome leads to a sex dependent genotype effect on the sleep-homeostatic process (Franken et al., 2006). Another study mentioned that both sexes were investigated but did not report on any specific sex differences afterwards (He et al., 2009). Understanding the contribution of sex to sleep-wake regulation could not only expand our knowledge further on sex differences in sleep, but can also provide clues towards mechanisms underlying sleep regulation in general.

How to implement the perfect design in a world with limited resources

Thus, sex differences and environmental enrichment are two examples of supposedly 'confounding factors' that, once we understand their mechanisms better, could expand our knowledge of sleep. In general, a different research question is posed in the same model under the

same conditions, whereas understanding the importance of the above-mentioned factors requires addressing the same question in a different model under different conditions. There are many logistic reasons why the first approach is dominating in (murine) research: *e.g.* there are/were many more (genetic) tools available in mice compared to any other (rodent) species; the housing conditions are required to meet certain standards; and funding is easier to obtain for a novel observation in the same model than to replicate a previously obtained finding in a different model.

Still, incorporating the extra variation can make our conclusions more general, or if not, more precise and thereby even providing clues about underlying mechanisms. Embracing this kind of change in experimental design needs to emerge from both the scientific communities and the funding agencies. Since 2017, the NIH has imposed sex as a biological variable, which hopefully also comes with the financial support to pursue these experiments in duplicate.

References

- Abel, T., Havekes, R., Saletin, J. M., & Walker, M. P. (2013). Sleep, plasticity and memory from molecules to whole-brain networks. *Curr Biol*, *23*(17), R774-788. doi:10.1016/j.cub.2013.07.025
- Ackermann, S., & Rasch, B. (2014). Differential effects of non-REM and REM sleep on memory consolidation? *Curr Neurol Neurosci Rep*, *14*(2), 430. doi:10.1007/s11910-013-0430-8
- Adamovich, Y., Ladeux, B., Golik, M., Koeners, M. P., & Asher, G. (2017). Rhythmic Oxygen Levels Reset Circadian Clocks through HIF1alpha. *Cell Metab*, *25*(1), 93-101. doi:10.1016/j.cmet.2016.09.014
- Akerstedt, T., Anund, A., Axelsson, J., & Kecklund, G. (2014). Subjective sleepiness is a sensitive indicator of insufficient sleep and impaired waking function. *J Sleep Res*, *23*(3), 240-252. doi:10.1111/jsr.12158
- Akhtar, R. A., Reddy, A. B., Maywood, E. S., Clayton, J. D., King, V. M., Smith, A. G., . . . Kyriacou, C. P. (2002). Circadian cycling of the mouse liver transcriptome, as revealed by cDNA microarray, is driven by the suprachiasmatic nucleus. *Curr Biol*, *12*(7), 540-550.
- Al-Fageeh, M. B., & Smales, C. M. (2009). Cold-inducible RNA binding protein (CIRP) expression is modulated by alternative mRNAs. *RNA*, *15*(6), 1164-1176. doi:10.1261/rna.1179109
- Al-Fageeh, M. B., & Smales, C. M. (2013). Alternative promoters regulate cold inducible RNA-binding (CIRP) gene expression and enhance transgene expression in mammalian cells. *Mol Biotechnol*, *54*(2), 238-249. doi:10.1007/s12033-013-9649-5
- Al-Safadi, S., Al-Safadi, A., Branchaud, M., Rutherford, S., Dayanandan, A., Robinson, B., & Amir, S. (2014). Stress-induced changes in the expression of the clock protein PERIOD1 in the rat limbic forebrain and hypothalamus: role of stress type, time of day, and predictability. *PLoS One*, *9*(10), e111166. doi:10.1371/journal.pone.0111166
- Alexander, B. K., Beyerstein, B. L., Hadaway, P. F., & Coombs, R. B. (1981). Effect of early and later colony housing on oral ingestion of morphine in rats. *Pharmacol Biochem Behav*, *15*(4), 571-576.
- Alfoldi, P., Rubicsek, G., Cserni, G., & Obal, F., Jr. (1990). Brain and core temperatures and peripheral vasomotion during sleep and wakefulness at various ambient temperatures in the rat. *Pflugers Arch*, *417*(3), 336-341.
- Antle, M. C., & Mistlberger, R. E. (2000). Circadian clock resetting by sleep deprivation without exercise in the Syrian hamster. *J Neurosci*, *20*(24), 9326-9332.
- Archer, S. N., Laing, E. E., Moller-Levet, C. S., van der Veen, D. R., Bucca, G., Lazar, A. S., . . . Dijk, D. J. (2014). Mistimed sleep disrupts circadian regulation of the human transcriptome. *Proc Natl Acad Sci U S A*, *111*(6), E682-691. doi:10.1073/pnas.1316335111
- Archer, S. N., & Oster, H. (2015). How sleep and wakefulness influence circadian rhythmicity: effects of insufficient and mistimed sleep on the animal and human transcriptome. *J Sleep Res*, *24*(5), 476-493. doi:10.1111/jsr.12307
- Archer, S. N., Robilliard, D. L., Skene, D. J., Smits, M., Williams, A., Arendt, J., & von Schantz, M. (2003). A length polymorphism in the circadian clock gene Per3 is linked to delayed sleep phase syndrome and extreme diurnal preference. *Sleep*, *26*(4), 413-415.
- Arendt, T., & Bullmann, T. (2013). Neuronal plasticity in hibernation and the proposed role of the microtubule-associated protein tau as a "master switch" regulating synaptic gain in neuronal networks. *Am J Physiol Regul Integr Comp Physiol*, *305*(5), R478-489. doi:10.1152/ajpregu.00117.2013
- Aryal, R. P., Kwak, P. B., Tamayo, A. G., Gebert, M., Chiu, P. L., Walz, T., & Weitz, C. J. (2017). Macromolecular Assemblies of the Mammalian Circadian Clock. *Mol Cell*, *67*(5), 770-782.e776. doi:10.1016/j.molcel.2017.07.017

- Bagni, C., & Oostra, B. A. (2013). Fragile X syndrome: From protein function to therapy. *Am J Med Genet A*, *161A*(11), 2809-2821. doi:10.1002/ajmg.a.36241
- Bailey, M., & Silver, R. (2014). Sex differences in circadian timing systems: implications for disease. *Front Neuroendocrinol*, *35*(1), 111-139. doi:10.1016/j.yfrne.2013.11.003
- Bainier, C., Mateo, M., Felder-Schmittbuhl, M. P., & Mendoza, J. (2017). Circadian rhythms of hedonic drinking behavior in mice. *Neuroscience*, *349*, 229-238. doi:10.1016/j.neuroscience.2017.03.002
- Baker, F. C., Angara, C., Szymusiak, R., & McGinty, D. (2005). Persistence of sleep-temperature coupling after suprachiasmatic nuclei lesions in rats. *Am J Physiol Regul Integr Comp Physiol*, *289*(3), R827-838. doi:10.1152/ajpregu.00093.2005
- Baker, M. A., & Hayward, J. N. (1968). The influence of the nasal mucosa and the carotid rete upon hypothalamic temperature in sheep. *J Physiol*, *198*(3), 561-579.
- Barrett, J., Lack, L., & Morris, M. (1993). The sleep-evoked decrease of body temperature. *Sleep*, *16*(2), 93-99.
- Bass, J., & Takahashi, J. S. (2010). Circadian integration of metabolism and energetics. *Science*, *330*(6009), 1349-1354. doi:10.1126/science.1195027
- Bastide, A., Peretti, D., Knight, J. R., Grosso, S., Spriggs, R. V., Pichon, X., . . . Willis, A. E. (2017). RTN3 Is a Novel Cold-Induced Protein and Mediates Neuroprotective Effects of RBM3. *Curr Biol*, *27*(5), 638-650. doi:10.1016/j.cub.2017.01.047
- Bellesi, M., de Vivo, L., Tononi, G., & Cirelli, C. (2015). Effects of sleep and wake on astrocytes: clues from molecular and ultrastructural studies. *BMC Biol*, *13*, 66. doi:10.1186/s12915-015-0176-7
- Benington, J. H., & Heller, H. C. (1995). Restoration of brain energy metabolism as the function of sleep. *Prog Neurobiol*, *45*(4), 347-360.
- Berger, R. J., & Phillips, N. H. (1995). Energy conservation and sleep. *Behav Brain Res*, *69*(1-2), 65-73.
- Bhadra, U., Thakkar, N., Das, P., & Pal Bhadra, M. (2017). Evolution of circadian rhythms: from bacteria to human. *Sleep Med*, *35*, 49-61. doi:10.1016/j.sleep.2017.04.008
- Borbely, A. A., Achermann, P., Trachsel, L., & Tobler, I. (1989). Sleep initiation and initial sleep intensity: interactions of homeostatic and circadian mechanisms. *J Biol Rhythms*, *4*(2), 149-160.
- Borbely, A. A., Daan, S., Wirz-Justice, A., & Deboer, T. (2016). The two-process model of sleep regulation: a reappraisal. *J Sleep Res*, *25*(2), 131-143. doi:10.1111/jsr.12371
- Borbely, A. A., & Neuhaus, H. U. (1979). SLEEP-DEPRIVATION - EFFECTS ON SLEEP AND EEG IN THE RAT. *Journal of Comparative Physiology*, *133*(1), 71-87. doi:10.1007/bf00663111
- Boyce, R., Williams, S., & Adamantidis, A. (2017). REM sleep and memory. *Curr Opin Neurobiol*, *44*, 167-177. doi:10.1016/j.conb.2017.05.001
- Braun, A. R., Balkin, T. J., Wesenten, N. J., Carson, R. E., Varga, M., Baldwin, P., . . . Herscovitch, P. (1997). Regional cerebral blood flow throughout the sleep-wake cycle. An H₂(15)O PET study. *Brain*, *120* (Pt 7), 1173-1197.
- Buhr, E. D., Yoo, S. H., & Takahashi, J. S. (2010). Temperature as a universal resetting cue for mammalian circadian oscillators. *Science*, *330*(6002), 379-385. doi:10.1126/science.1195262
- Buzsáki, G. (2006). *Rhythms of the brain*. England: Oxford University Press.
- Cambras, T., Weller, J. R., Angles-Pujoras, M., Lee, M. L., Christopher, A., Diez-Noguera, A., . . . de la Iglesia, H. O. (2007). Circadian desynchronization of core body temperature and sleep stages in the rat. *Proc Natl Acad Sci U S A*, *104*(18), 7634-7639. doi:10.1073/pnas.0702424104
- Campbell, S. S., & Tobler, I. (1984). Animal sleep: a review of sleep duration across phylogeny. *Neurosci Biobehav Rev*, *8*(3), 269-300.
- Cao, R., Gkogkas, C. G., de Zavalía, N., Blum, I. D., Yanagiya, A., Tsukumo, Y., . . . Sonenberg, N. (2015). Light-regulated translational control of circadian behavior by eIF4E phosphorylation. *Nat Neurosci*, *18*(6), 855-862. doi:10.1038/nn.4010

- Cao, Y. A., Wagers, A. J., Beilhack, A., Dusich, J., Bachmann, M. H., Negrin, R. S., . . . Contag, C. H. (2004). Shifting foci of hematopoiesis during reconstitution from single stem cells. *Proc Natl Acad Sci U S A*, *101*(1), 221-226. doi:10.1073/pnas.2637010100
- Chappell, S. A., Owens, G. C., & Mauro, V. P. (2001). A 5' Leader of Rbm3, a Cold Stress-induced mRNA, Mediates Internal Initiation of Translation with Increased Efficiency under Conditions of Mild Hypothermia. *J Biol Chem*, *276*(40), 36917-36922. doi:10.1074/jbc.M106008200
- Cheeseman, J. F., Winnebeck, E. C., Millar, C. D., Kirkland, L. S., Sleigh, J., Goodwin, M., . . . Warman, G. R. (2012). General anesthesia alters time perception by phase shifting the circadian clock. *Proc Natl Acad Sci U S A*, *109*(18), 7061-7066. doi:10.1073/pnas.1201734109
- Chip, S., Zelmer, A., Ogunshola, O. O., Felderhoff-Mueser, U., Nitsch, C., Buhner, C., & Wellmann, S. (2011). The RNA-binding protein RBM3 is involved in hypothermia induced neuroprotection. *Neurobiol Dis*, *43*(2), 388-396. doi:10.1016/j.nbd.2011.04.010
- Cho, H., Zhao, X., Hatori, M., Yu, R. T., Barish, G. D., Lam, M. T., . . . Evans, R. M. (2012). Regulation of circadian behaviour and metabolism by REV-ERB-alpha and REV-ERB-beta. *Nature*, *485*(7396), 123-127. doi:10.1038/nature11048
- Cirelli, C. (2017). Sleep, synaptic homeostasis and neuronal firing rates. *Curr Opin Neurobiol*, *44*, 72-79. doi:10.1016/j.conb.2017.03.016
- Cirelli, C., & Tononi, G. (2015). Cortical development, electroencephalogram rhythms, and the sleep/wake cycle. *Biol Psychiatry*, *77*(12), 1071-1078. doi:10.1016/j.biopsych.2014.12.017
- Colgin, L. L. (2015). Theta-gamma coupling in the entorhinal-hippocampal system. *Curr Opin Neurobiol*, *31*, 45-50. doi:10.1016/j.conb.2014.08.001
- Cooper, T. A., Wan, L., & Dreyfuss, G. (2009). RNA and disease. *Cell*, *136*(4), 777-793. doi:10.1016/j.cell.2009.02.011
- Copinschi, G., Leproult, R., & Spiegel, K. (2014). The important role of sleep in metabolism. *Front Horm Res*, *42*, 59-72. doi:10.1159/000358858
- Curie, T., Maret, S., Emmenegger, Y., & Franken, P. (2015). In Vivo Imaging of the Central and Peripheral Effects of Sleep Deprivation and Suprachiasmatic Nuclei Lesion on PERIOD-2 Protein in Mice. *Sleep*, *38*(9), 1381-1394. doi:10.5665/sleep.4974
- Curie, T., Mongrain, V., Dorsaz, S., Mang, G. M., Emmenegger, Y., & Franken, P. (2013). Homeostatic and circadian contribution to EEG and molecular state variables of sleep regulation. *Sleep*, *36*(3), 311-323. doi:10.5665/sleep.2440
- Czeisler, C. A., Zimmerman, J. C., Ronda, J. M., Moore-Ede, M. C., & Weitzman, E. D. (1980). Timing of REM sleep is coupled to the circadian rhythm of body temperature in man. *Sleep*, *2*(3), 329-346.
- Daan, S., Barnes, B. M., & Strijkstra, A. M. (1991). Warming up for sleep? Ground squirrels sleep during arousals from hibernation. *Neurosci Lett*, *128*(2), 265-268.
- Daan, S., Beersma, D. G., & Borbely, A. A. (1984). Timing of human sleep: recovery process gated by a circadian pacemaker. *Am J Physiol*, *246*(2 Pt 2), R161-183.
- Daan, S., & Pittendrigh, C. S. (1976). A Functional analysis of circadian pacemakers in nocturnal rodents. *Journal of Comparative Physiology*, *106*(3), 253-266. doi:10.1007/bf01417857
- Danno, S., Nishiyama, H., Higashitsuji, H., Yokoi, H., Xue, J. H., Itoh, K., . . . Fujita, J. (1997). Increased transcript level of RBM3, a member of the glycine-rich RNA-binding protein family, in human cells in response to cold stress. *Biochem Biophys Res Commun*, *236*(3), 804-807. doi:10.1006/bbrc.1997.7059
- Darnell, R. B. (2013). RNA protein interaction in neurons. *Annu Rev Neurosci*, *36*, 243-270. doi:10.1146/annurev-neuro-062912-114322
- DaSilva, J. K., Husain, E., Lei, Y., Mann, G. L., Morrison, A. R., & Tejani-Butt, S. (2017). Social partnering alters sleep in fear-conditioned Wistar rats. *PLoS One*, *12*(10), e0186017. doi:10.1371/journal.pone.0186017

- DaSilva, J. K., Husain, E., Lei, Y., Mann, G. L., Tejani-Butt, S., & Morrison, A. R. (2011). Social partnering significantly reduced rapid eye movement sleep fragmentation in fear-conditioned, stress-sensitive Wistar-Kyoto rats. *Neuroscience*, *199*, 193-204. doi:10.1016/j.neuroscience.2011.09.066
- Deboer, T., Detari, L., & Meijer, J. H. (2007). Long term effects of sleep deprivation on the mammalian circadian pacemaker. *Sleep*, *30*(3), 257-262.
- Deboer, T., Franken, P., & Tobler, I. (1994). Sleep and cortical temperature in the Djungarian hamster under baseline conditions and after sleep deprivation. *J Comp Physiol A*, *174*(2), 145-155.
- Deboer, T., Vansteensel, M. J., Detari, L., & Meijer, J. H. (2003). Sleep states alter activity of suprachiasmatic nucleus neurons. *Nat Neurosci*, *6*(10), 1086-1090. doi:10.1038/nn1122
- Diering, G. H., Nirujogi, R. S., Roth, R. H., Worley, P. F., Pandey, A., & Huganir, R. L. (2017). Homer1a drives homeostatic scaling-down of excitatory synapses during sleep. *Science*, *355*(6324), 511-515. doi:10.1126/science.aai8355
- Diessler, S., Jan, M., Emmenegger, Y., Guex, N., Middleton, B., Skene, D. J., . . . Franken, P. (2018). A systems genetics resource and analysis of sleep regulation in the mouse. *PLoS Biol*, *16*(8), e2005750. doi:10.1371/journal.pbio.2005750
- Dietrich, W. D., Atkins, C. M., & Bramlett, H. M. (2009). Protection in animal models of brain and spinal cord injury with mild to moderate hypothermia. *J Neurotrauma*, *26*(3), 301-312. doi:10.1089/neu.2008.0806
- Dijk, D. J., & Czeisler, C. A. (1995). Contribution of the circadian pacemaker and the sleep homeostat to sleep propensity, sleep structure, electroencephalographic slow waves, and sleep spindle activity in humans. *J Neurosci*, *15*(5 Pt 1), 3526-3538.
- Dijk, D. J., Duffy, J. F., & Czeisler, C. A. (2000). Contribution of circadian physiology and sleep homeostasis to age-related changes in human sleep. *Chronobiol Int*, *17*(3), 285-311.
- DiNuzzo, M., & Nedergaard, M. (2017). Brain energetics during the sleep-wake cycle. *Curr Opin Neurobiol*, *47*, 65-72. doi:10.1016/j.conb.2017.09.010
- Doran, S. M., Van Dongen, H. P., & Dinges, D. F. (2001). Sustained attention performance during sleep deprivation: evidence of state instability. *Arch Ital Biol*, *139*(3), 253-267.
- Dresios, J., Aschrafi, A., Owens, G. C., Vanderklish, P. W., Edelman, G. M., & Mauro, V. P. (2005). Cold stress-induced protein Rbm3 binds 60S ribosomal subunits, alters microRNA levels, and enhances global protein synthesis. *Proc Natl Acad Sci U S A*, *102*(6), 1865-1870. doi:10.1073/pnas.0409764102
- Dudley, C. A., Erbel-Sieler, C., Estill, S. J., Reick, M., Franken, P., Pitts, S., & McKnight, S. L. (2003). Altered patterns of sleep and behavioral adaptability in NPAS2-deficient mice. *Science*, *301*(5631), 379-383. doi:10.1126/science.1082795
- Duong, H. A., Robles, M. S., Knutti, D., & Weitz, C. J. (2011). A molecular mechanism for circadian clock negative feedback. *Science*, *332*(6036), 1436-1439. doi:10.1126/science.1196766
- Edgar, D. M., Dement, W. C., & Fuller, C. A. (1993). Effect of SCN lesions on sleep in squirrel monkeys: evidence for opponent processes in sleep-wake regulation. *J Neurosci*, *13*(3), 1065-1079.
- Ehlen, J. C., Brager, A. J., Baggs, J., Pinckney, L., Gray, C. L., DeBruyne, J. P., . . . Paul, K. N. (2017). Bmal1 function in skeletal muscle regulates sleep. *Elife*, *6*. doi:10.7554/eLife.26557
- Epperson, L. E., Dahl, T. A., & Martin, S. L. (2004). Quantitative analysis of liver protein expression during hibernation in the golden-mantled ground squirrel. *Mol Cell Proteomics*, *3*(9), 920-933. doi:10.1074/mcp.M400042-MCP200
- Erson-Bensan, A. E. (2016). Alternative polyadenylation and RNA-binding proteins. *J Mol Endocrinol*, *57*(2), F29-34. doi:10.1530/jme-16-0070

- Escobar, C., Cailotto, C., Angeles-Castellanos, M., Delgado, R. S., & Buijs, R. M. (2009). Peripheral oscillators: the driving force for food-anticipatory activity. *Eur J Neurosci*, *30*(9), 1665-1675. doi:10.1111/j.1460-9568.2009.06972.x
- Evans, M. S., Chaurette, J. P., Adams, S. T., Jr., Reddy, G. R., Paley, M. A., Aronin, N., . . . Miller, S. C. (2014). A synthetic luciferin improves bioluminescence imaging in live mice. *Nat Methods*, *11*(4), 393-395. doi:10.1038/nmeth.2839
- Febinger, H. Y., George, A., Priestley, J., Toth, L. A., & Opp, M. R. (2014). Effects of housing condition and cage change on characteristics of sleep in mice. *J Am Assoc Lab Anim Sci*, *53*(1), 29-37.
- Fedorov, V. B., Goropashnaya, A. V., Toien, O., Stewart, N. C., Chang, C., Wang, H., . . . Barnes, B. M. (2011). Modulation of gene expression in heart and liver of hibernating black bears (*Ursus americanus*). *BMC Genomics*, *12*, 171. doi:10.1186/1471-2164-12-171
- Finelli, L. A., Baumann, H., Borbely, A. A., & Achermann, P. (2000). Dual electroencephalogram markers of human sleep homeostasis: correlation between theta activity in waking and slow-wave activity in sleep. *Neuroscience*, *101*(3), 523-529.
- Fisher, S. P., Cui, N., McKillop, L. E., Gemignani, J., Bannerman, D. M., Oliver, P. L., . . . Vyazovskiy, V. V. (2016). Stereotypic wheel running decreases cortical activity in mice. *Nat Commun*, *7*, 13138. doi:10.1038/ncomms13138
- Fossat, N., Tourle, K., Radziewicz, T., Barratt, K., Liebhold, D., Studdert, J. B., . . . Tam, P. P. (2014). C to U RNA editing mediated by APOBEC1 requires RNA-binding protein RBM47. *EMBO Rep*, *15*(8), 903-910. doi:10.15252/embr.201438450
- Frank, M. G., & Cantera, R. (2014). Sleep, clocks, and synaptic plasticity. *Trends Neurosci*, *37*(9), 491-501. doi:10.1016/j.tins.2014.06.005
- Franken, P. (2002). Long-term vs. short-term processes regulating REM sleep. *J Sleep Res*, *11*(1), 17-28.
- Franken, P. (2013). A role for clock genes in sleep homeostasis. *Curr Opin Neurobiol*, *23*(5), 864-872. doi:10.1016/j.conb.2013.05.002
- Franken, P., Chollet, D., & Tafti, M. (2001). The homeostatic regulation of sleep need is under genetic control. *J Neurosci*, *21*(8), 2610-2621.
- Franken, P., Dudley, C. A., Estill, S. J., Barakat, M., Thomason, R., O'Hara, B. F., & McKnight, S. L. (2006). NPAS2 as a transcriptional regulator of non-rapid eye movement sleep: genotype and sex interactions. *Proc Natl Acad Sci U S A*, *103*(18), 7118-7123. doi:10.1073/pnas.0602006103
- Franken, P., Lopez-Molina, L., Marcacci, L., Schibler, U., & Tafti, M. (2000). The transcription factor DBP affects circadian sleep consolidation and rhythmic EEG activity. *J Neurosci*, *20*(2), 617-625.
- Franken, P., Malafosse, A., & Tafti, M. (1999). Genetic determinants of sleep regulation in inbred mice. *Sleep*, *22*(2), 155-169.
- Franken, P., Thomason, R., Heller, H. C., & O'Hara, B. F. (2007). A non-circadian role for clock-genes in sleep homeostasis: a strain comparison. *BMC Neurosci*, *8*, 87. doi:10.1186/1471-2202-8-87
- Franken, P., Tobler, I., & Borbely, A. A. (1992a). Cortical temperature and EEG slow-wave activity in the rat: analysis of vigilance state related changes. *Pflugers Arch*, *420*(5-6), 500-507.
- Franken, P., Tobler, I., & Borbely, A. A. (1992b). Sleep and waking have a major effect on the 24-hr rhythm of cortical temperature in the rat. *J Biol Rhythms*, *7*(4), 341-352. doi:10.1177/074873049200700407
- Fu, X. D., & Ares, M., Jr. (2014). Context-dependent control of alternative splicing by RNA-binding proteins. *Nat Rev Genet*, *15*(10), 689-701. doi:10.1038/nrg3778
- Fujita, T., Higashitsuji, H., Higashitsuji, H., Liu, Y., Itoh, K., Sakurai, T., . . . Fujita, J. (2017). TRPV4-dependent induction of a novel mammalian cold-inducible protein SRSF5 as well as CIRP and RBM3. *Sci Rep*, *7*(1), 2295. doi:10.1038/s41598-017-02473-x

- Fujita, T., Liu, Y., Higashitsuji, H., Itoh, K., Shibasaki, K., Fujita, J., & Nishiyama, H. (2018). Involvement of TRPV3 and TRPM8 ion channel proteins in induction of mammalian cold-inducible proteins. *Biochem Biophys Res Commun*, *495*(1), 935-940. doi:10.1016/j.bbrc.2017.11.136
- Furth, K. E., McCoy, A. J., Dodge, C., Walters, J. R., Buonanno, A., & Delaville, C. (2017). Neuronal correlates of ketamine and walking induced gamma oscillations in the medial prefrontal cortex and mediodorsal thalamus. *PLoS One*, *12*(11), e0186732. doi:10.1371/journal.pone.0186732
- Gekakis, N., Staknis, D., Nguyen, H. B., Davis, F. C., Wilsbacher, L. D., King, D. P., . . . Weitz, C. J. (1998). Role of the CLOCK protein in the mammalian circadian mechanism. *Science*, *280*(5369), 1564-1569.
- Glisovic, T., Bachorik, J. L., Yong, J., & Dreyfuss, G. (2008). RNA-binding proteins and post-transcriptional gene regulation. *FEBS Lett*, *582*(14), 1977-1986. doi:10.1016/j.febslet.2008.03.004
- Gotic, I., Omid, S., Fleury-Olela, F., Molina, N., Naef, F., & Schibler, U. (2016). Temperature regulates splicing efficiency of the cold-inducible RNA-binding protein gene *Cirbp*. *Genes Dev*, *30*(17), 2005-2017. doi:10.1101/gad.287094.116
- Groch, S., Zinke, K., Wilhelm, I., & Born, J. (2015). Dissociating the contributions of slow-wave sleep and rapid eye movement sleep to emotional item and source memory. *Neurobiol Learn Mem*, *122*, 122-130. doi:10.1016/j.nlm.2014.08.013
- Hamada, T., Sutherland, K., Ishikawa, M., Miyamoto, N., Honma, S., Shirato, H., & Honma, K. (2016). In vivo imaging of clock gene expression in multiple tissues of freely moving mice. *Nat Commun*, *7*, 11705. doi:10.1038/ncomms11705
- Hasan, S., van der Veen, D. R., Winsky-Sommerer, R., Dijk, D. J., & Archer, S. N. (2011). Altered sleep and behavioral activity phenotypes in PER3-deficient mice. *Am J Physiol Regul Integr Comp Physiol*, *301*(6), R1821-1830. doi:10.1152/ajpregu.00260.2011
- Hasan, S., van der Veen, D. R., Winsky-Sommerer, R., Hogben, A., Laing, E. E., Koentgen, F., . . . Archer, S. N. (2014). A human sleep homeostasis phenotype in mice expressing a primate-specific PER3 variable-number tandem-repeat coding-region polymorphism. *FASEB J*, *28*(6), 2441-2454. doi:10.1096/fj.13-240135
- Hastings, J. W., & Sweeney, B. M. (1957). ON THE MECHANISM OF TEMPERATURE INDEPENDENCE IN A BIOLOGICAL CLOCK. *Proc Natl Acad Sci U S A*, *43*(9), 804-811.
- Hastings, M. H., Duffield, G. E., Ebling, F. J., Kidd, A., Maywood, E. S., & Schurov, I. (1997). Non-photoc signalling in the suprachiasmatic nucleus. *Biol Cell*, *89*(8), 495-503.
- Hayward, J. N., & Baker, M. A. (1968). Role of cerebral arterial blood in the regulation of brain temperature in the monkey. *Am J Physiol*, *215*(2), 389-403.
- He, Y., Jones, C. R., Fujiki, N., Xu, Y., Guo, B., Holder, J. L., Jr., . . . Fu, Y. H. (2009). The transcriptional repressor DEC2 regulates sleep length in mammals. *Science*, *325*(5942), 866-870. doi:10.1126/science.1174443
- Hellemans, J., Mortier, G., De Paepe, A., Speleman, F., & Vandesompele, J. (2007). qBase relative quantification framework and software for management and automated analysis of real-time quantitative PCR data. *Genome Biol*, *8*(2), R19. doi:10.1186/gb-2007-8-2-r19
- Hiddinga, A. E., Beersma, D. G., & Van den Hoofdakker, R. H. (1997). Endogenous and exogenous components in the circadian variation of core body temperature in humans. *J Sleep Res*, *6*(3), 156-163.
- Hirano, A., Fu, Y. H., & Ptacek, L. J. (2016). The intricate dance of post-translational modifications in the rhythm of life. *Nat Struct Mol Biol*, *23*(12), 1053-1060. doi:10.1038/nsmb.3326
- Izumo, M., Johnson, C. H., & Yamazaki, S. (2003). Circadian gene expression in mammalian fibroblasts revealed by real-time luminescence reporting: temperature compensation and damping. *Proc Natl Acad Sci U S A*, *100*(26), 16089-16094. doi:10.1073/pnas.2536313100

- Jeewajee, A., Barry, C., O'Keefe, J., & Burgess, N. (2008). Grid cells and theta as oscillatory interference: electrophysiological data from freely moving rats. *Hippocampus*, *18*(12), 1175-1185. doi:10.1002/hipo.20510
- Jessen, N. A., Munk, A. S., Lundgaard, I., & Nedergaard, M. (2015). The Glymphatic System: A Beginner's Guide. *Neurochem Res*, *40*(12), 2583-2599. doi:10.1007/s11064-015-1581-6
- Joiner, W. J. (2016). Unraveling the Evolutionary Determinants of Sleep. *Curr Biol*, *26*(20), R1073-r1087. doi:10.1016/j.cub.2016.08.068
- Jones, S., Pfister-Genskow, M., Benca, R. M., & Cirelli, C. (2008). Molecular correlates of sleep and wakefulness in the brain of the white-crowned sparrow. *J Neurochem*, *105*(1), 46-62. doi:10.1111/j.1471-4159.2007.05089.x
- Jud, C., Schmutz, I., Hampp, G., Oster, H., & Albrecht, U. (2005). A guideline for analyzing circadian wheel-running behavior in rodents under different lighting conditions. *Biol Proced Online*, *7*, 101-116. doi:10.1251/bpo109
- Jung, C. M., Melanson, E. L., Frydendall, E. J., Perreault, L., Eckel, R. H., & Wright, K. P. (2011). Energy expenditure during sleep, sleep deprivation and sleep following sleep deprivation in adult humans. *J Physiol*, *589*(Pt 1), 235-244. doi:10.1113/jphysiol.2010.197517
- Kaeffer, B., & Pardini, L. (2005). Clock genes of Mammalian cells: practical implications in tissue culture. *In Vitro Cell Dev Biol Anim*, *41*(10), 311-320. doi:10.1007/s11626-005-0001-7
- Kaushal, N., Nair, D., Gozal, D., & Ramesh, V. (2012). Socially isolated mice exhibit a blunted homeostatic sleep response to acute sleep deprivation compared to socially paired mice. *Brain Res*, *1454*, 65-79. doi:10.1016/j.brainres.2012.03.019
- Kidd, P. B., Young, M. W., & Siggia, E. D. (2015). Temperature compensation and temperature sensation in the circadian clock. *Proc Natl Acad Sci U S A*, *112*(46), E6284-6292. doi:10.1073/pnas.1511215112
- Koike, N., Yoo, S. H., Huang, H. C., Kumar, V., Lee, C., Kim, T. K., & Takahashi, J. S. (2012). Transcriptional architecture and chromatin landscape of the core circadian clock in mammals. *Science*, *338*(6105), 349-354. doi:10.1126/science.1226339
- Konopka, R. J., & Benzer, S. (1971). Clock mutants of *Drosophila melanogaster*. *Proc Natl Acad Sci U S A*, *68*(9), 2112-2116.
- Kopp, C., Albrecht, U., Zheng, B., & Tobler, I. (2002). Homeostatic sleep regulation is preserved in mPer1 and mPer2 mutant mice. *Eur J Neurosci*, *16*(6), 1099-1106.
- Kornmann, B., Schaad, O., Bujard, H., Takahashi, J. S., & Schibler, U. (2007). System-driven and oscillator-dependent circadian transcription in mice with a conditionally active liver clock. *PLoS Biol*, *5*(2), e34. doi:10.1371/journal.pbio.0050034
- Kurosawa, G., & Iwasa, Y. (2005). Temperature compensation in circadian clock models. *J Theor Biol*, *233*(4), 453-468. doi:10.1016/j.jtbi.2004.10.012
- Lamia, K. A., Storch, K. F., & Weitz, C. J. (2008). Physiological significance of a peripheral tissue circadian clock. *Proc Natl Acad Sci U S A*, *105*(39), 15172-15177. doi:10.1073/pnas.0806717105
- Laposky, A., Easton, A., Dugovic, C., Walisser, J., Bradfield, C., & Turek, F. (2005). Deletion of the mammalian circadian clock gene BMAL1/Mop3 alters baseline sleep architecture and the response to sleep deprivation. *Sleep*, *28*(4), 395-409.
- Lazar, A. S., Lazar, Z. I., & Dijk, D. J. (2015). Circadian regulation of slow waves in human sleep: Topographical aspects. *Neuroimage*, *116*, 123-134. doi:10.1016/j.neuroimage.2015.05.012
- LeGates, T. A., Fernandez, D. C., & Hattar, S. (2014). Light as a central modulator of circadian rhythms, sleep and affect. *Nat Rev Neurosci*, *15*(7), 443-454. doi:10.1038/nrn3743
- Leys, C., Ley, C., Klein, O., Bernard, P., & Licata, L. (2013). Detecting outliers: Do not use standard deviation around the mean, use absolute deviation around the median. *Journal of Experimental Social Psychology*, *49*(4), 764-766. doi:<https://doi.org/10.1016/j.jesp.2013.03.013>

- Li, J. D., Hu, W. P., & Zhou, Q. Y. (2012). The circadian output signals from the suprachiasmatic nuclei. *Prog Brain Res*, 199, 119-127. doi:10.1016/b978-0-444-59427-3.00028-9
- Li, S., Zhang, Z., Xue, J., Liu, A., & Zhang, H. (2012). Cold-inducible RNA binding protein inhibits H(2)O(2)-induced apoptosis in rat cortical neurons. *Brain Res*, 1441, 47-52. doi:10.1016/j.brainres.2011.12.053
- Li, W., Ma, L., Yang, G., & Gan, W. B. (2017). REM sleep selectively prunes and maintains new synapses in development and learning. *Nat Neurosci*, 20(3), 427-437. doi:10.1038/nn.4479
- Liu, Y., Hu, W., Murakawa, Y., Yin, J., Wang, G., Landthaler, M., & Yan, J. (2013). Cold-induced RNA-binding proteins regulate circadian gene expression by controlling alternative polyadenylation. *Sci Rep*, 3, 2054. doi:10.1038/srep02054
- Lowrey, P. L., Shimomura, K., Antoch, M. P., Yamazaki, S., Zemenides, P. D., Ralph, M. R., . . . Takahashi, J. S. (2000). Positional syntenic cloning and functional characterization of the mammalian circadian mutation tau. *Science*, 288(5465), 483-492.
- Lowrey, P. L., & Takahashi, J. S. (2011). Genetics of circadian rhythms in Mammalian model organisms. *Adv Genet*, 74, 175-230. doi:10.1016/b978-0-12-387690-4.00006-4
- Lukong, K. E., Chang, K. W., Khandjian, E. W., & Richard, S. (2008). RNA-binding proteins in human genetic disease. *Trends Genet*, 24(8), 416-425. doi:10.1016/j.tig.2008.05.004
- Luppi, M., Cerri, M., Martelli, D., Tupone, D., Del Vecchio, F., Di Cristoforo, A., . . . Amici, R. (2014). Waking and sleeping in the rat made obese through a high-fat hypercaloric diet. *Behav Brain Res*, 258, 145-152. doi:10.1016/j.bbr.2013.10.014
- Madsen, P. L., & Vorstrup, S. (1991). Cerebral blood flow and metabolism during sleep. *Cerebrovasc Brain Metab Rev*, 3(4), 281-296.
- Majercak, J., Sidote, D., Hardin, P. E., & Edery, I. (1999). How a circadian clock adapts to seasonal decreases in temperature and day length. *Neuron*, 24(1), 219-230.
- Mang, G. M., & Franken, P. (2012). Sleep and EEG Phenotyping in Mice. *Curr Protoc Mouse Biol*, 2(1), 55-74. doi:10.1002/9780470942390.mo110126
- Mang, G. M., & Franken, P. (2015). Genetic dissection of sleep homeostasis. *Curr Top Behav Neurosci*, 25, 25-63. doi:10.1007/7854_2013_270
- Mang, G. M., La Spada, F., Emmenegger, Y., Chappuis, S., Ripperger, J. A., Albrecht, U., & Franken, P. (2016). Altered Sleep Homeostasis in Rev-erbalpha Knockout Mice. *Sleep*, 39(3), 589-601. doi:10.5665/sleep.5534
- Marchant, E. G., & Mistlberger, R. E. (1997). Anticipation and entrainment to feeding time in intact and SCN-ablated C57BL/6j mice. *Brain Res*, 765(2), 273-282.
- Maret, S., Dorsaz, S., Gurcel, L., Pradervand, S., Petit, B., Pfister, C., . . . Tafti, M. (2007). Homer1a is a core brain molecular correlate of sleep loss. *Proc Natl Acad Sci U S A*, 104(50), 20090-20095. doi:10.1073/pnas.0710131104
- Masuda, T., Itoh, K., Higashitsuji, H., Higashitsuji, H., Nakazawa, N., Sakurai, T., . . . Fujita, J. (2012). Cold-inducible RNA-binding protein (Cirp) interacts with Dyrk1b/Mirk and promotes proliferation of immature male germ cells in mice. *Proc Natl Acad Sci U S A*, 109(27), 10885-10890. doi:10.1073/pnas.1121524109
- McGinty, D., & Szymusiak, R. (1990). Keeping cool: a hypothesis about the mechanisms and functions of slow-wave sleep. *Trends Neurosci*, 13(12), 480-487.
- McGinty, D., Szymusiak, R., & Thomson, D. (1994). Preoptic/anterior hypothalamic warming increases EEG delta frequency activity within non-rapid eye movement sleep. *Brain Res*, 667(2), 273-277.
- Meerlo, P., de Bruin, E. A., Strijkstra, A. M., & Daan, S. (2001). A social conflict increases EEG slow-wave activity during subsequent sleep. *Physiol Behav*, 73(3), 331-335.

- Mei, L., Fan, Y., Lv, X., Welsh, D. K., Zhan, C., & Zhang, E. E. (2018). Long-term in vivo recording of circadian rhythms in brains of freely moving mice. *Proc Natl Acad Sci U S A*. doi:10.1073/pnas.1717735115
- Menet, J. S., Rodriguez, J., Abruzzi, K. C., & Rosbash, M. (2012). Nascent-Seq reveals novel features of mouse circadian transcriptional regulation. *Elife*, *1*, e00011. doi:10.7554/eLife.00011
- Mitsui, S., Yamaguchi, S., Matsuo, T., Ishida, Y., & Okamura, H. (2001). Antagonistic role of E4BP4 and PAR proteins in the circadian oscillatory mechanism. *Genes Dev*, *15*(8), 995-1006. doi:10.1101/gad.873501
- Mong, J. A., & Cusmano, D. M. (2016). Sex differences in sleep: impact of biological sex and sex steroids. *Philos Trans R Soc Lond B Biol Sci*, *371*(1688), 20150110. doi:10.1098/rstb.2015.0110
- Mongrain, V., Hernandez, S. A., Pradervand, S., Dorsaz, S., Curie, T., Hagiwara, G., . . . Franken, P. (2010). Separating the contribution of glucocorticoids and wakefulness to the molecular and electrophysiological correlates of sleep homeostasis. *Sleep*, *33*(9), 1147-1157.
- Mongrain, V., La Spada, F., Curie, T., & Franken, P. (2011). Sleep loss reduces the DNA-binding of BMAL1, CLOCK, and NPAS2 to specific clock genes in the mouse cerebral cortex. *PLoS One*, *6*(10), e26622. doi:10.1371/journal.pone.0026622
- Moore, R. Y., & Eichler, V. B. (1972). Loss of a circadian adrenal corticosterone rhythm following suprachiasmatic lesions in the rat. *Brain Res*, *42*(1), 201-206.
- Morf, J., Rey, G., Schneider, K., Stratmann, M., Fujita, J., Naef, F., & Schibler, U. (2012). Cold-inducible RNA-binding protein modulates circadian gene expression posttranscriptionally. *Science*, *338*(6105), 379-383. doi:10.1126/science.1217726
- Morf, J., & Schibler, U. (2013). Body temperature cycles: gatekeepers of circadian clocks. *Cell Cycle*, *12*(4), 539-540. doi:10.4161/cc.23670
- Moriya, T., Horikawa, K., Akiyama, M., & Shibata, S. (2000). Correlative association between N-methyl-D-aspartate receptor-mediated expression of period genes in the suprachiasmatic nucleus and phase shifts in behavior with photic entrainment of clock in hamsters. *Mol Pharmacol*, *58*(6), 1554-1562.
- Mure, L. S., Le, H. D., Benegiamo, G., Chang, M. W., Rios, L., Jillani, N., . . . Panda, S. (2018). Diurnal transcriptome atlas of a primate across major neural and peripheral tissues. *Science*, *359*(6381). doi:10.1126/science.aao0318
- Musiek, E. S., Xiong, D. D., & Holtzman, D. M. (2015). Sleep, circadian rhythms, and the pathogenesis of Alzheimer disease. *Exp Mol Med*, *47*, e148. doi:10.1038/emm.2014.121
- Muto, V., Jaspar, M., Meyer, C., Kusse, C., Chellappa, S. L., Degueldre, C., . . . Maquet, P. (2016). Local modulation of human brain responses by circadian rhythmicity and sleep debt. *Science*, *353*(6300), 687-690. doi:10.1126/science.aad2993
- Nagoshi, E., Saini, C., Bauer, C., Laroche, T., Naef, F., & Schibler, U. (2004). Circadian gene expression in individual fibroblasts: cell-autonomous and self-sustained oscillators pass time to daughter cells. *Cell*, *119*(5), 693-705. doi:10.1016/j.cell.2004.11.015
- Naidoo, N., Ferber, M., Galante, R. J., McShane, B., Hu, J. H., Zimmerman, J., . . . Pack, A. I. (2012). Role of Homer proteins in the maintenance of sleep-wake states. *PLoS One*, *7*(4), e35174. doi:10.1371/journal.pone.0035174
- Naylor, E., Bergmann, B. M., Krauski, K., Zee, P. C., Takahashi, J. S., Vitaterna, M. H., & Turek, F. W. (2000). The circadian clock mutation alters sleep homeostasis in the mouse. *J Neurosci*, *20*(21), 8138-8143.
- Niell, C. M., & Stryker, M. P. (2010). Modulation of visual responses by behavioral state in mouse visual cortex. *Neuron*, *65*(4), 472-479. doi:10.1016/j.neuron.2010.01.033

- Nishiyama, H., Itoh, K., Kaneko, Y., Kishishita, M., Yoshida, O., & Fujita, J. (1997). A glycine-rich RNA-binding protein mediating cold-inducible suppression of mammalian cell growth. *J Cell Biol*, *137*(4), 899-908.
- Nishiyama, H., Xue, J. H., Sato, T., Fukuyama, H., Mizuno, N., Houtani, T., . . . Fujita, J. (1998). Diurnal change of the cold-inducible RNA-binding protein (Circp) expression in mouse brain. *Biochem Biophys Res Commun*, *245*(2), 534-538. doi:10.1006/bbrc.1998.8482
- NobelPrize.org. (2017). https://www.nobelprize.org/nobel_prizes/medicine/laureates/2017/press.html.
- Nybo, L., Secher, N. H., & Nielsen, B. (2002). Inadequate heat release from the human brain during prolonged exercise with hyperthermia. *J Physiol*, *545*(Pt 2), 697-704.
- O'Donnell, J., Zeppenfeld, D., McConnell, E., Pena, S., & Nedergaard, M. (2012). Norepinephrine: a neuromodulator that boosts the function of multiple cell types to optimize CNS performance. *Neurochem Res*, *37*(11), 2496-2512. doi:10.1007/s11064-012-0818-x
- Ono, D., Honma, K., & Honma, S. (2015). Circadian and ultradian rhythms of clock gene expression in the suprachiasmatic nucleus of freely moving mice. *Sci Rep*, *5*, 12310. doi:10.1038/srep12310
- Panda, S. (2016). Circadian physiology of metabolism. *Science*, *354*(6315), 1008-1015. doi:10.1126/science.aah4967
- Peretti, D., Bastide, A., Radford, H., Verity, N., Molloy, C., Martin, M. G., . . . Mallucci, G. R. (2015). RBM3 mediates structural plasticity and protective effects of cooling in neurodegeneration. *Nature*, *518*(7538), 236-239. doi:10.1038/nature14142
- Pilotte, J., Cunningham, B. A., Edelman, G. M., & Vanderklish, P. W. (2009). Developmentally regulated expression of the cold-inducible RNA-binding motif protein 3 in euthermic rat brain. *Brain Res*, *1258*, 12-24. doi:10.1016/j.brainres.2008.12.050
- Pilotte, J., Dupont-Versteegden, E. E., & Vanderklish, P. W. (2011). Widespread regulation of miRNA biogenesis at the Dicer step by the cold-inducible RNA-binding protein, RBM3. *PLoS One*, *6*(12), e28446. doi:10.1371/journal.pone.0028446
- Pittendrigh, C. S. (1954). ON TEMPERATURE INDEPENDENCE IN THE CLOCK SYSTEM CONTROLLING EMERGENCE TIME IN DROSOPHILA. *Proc Natl Acad Sci U S A*, *40*(10), 1018-1029.
- Pittendrigh, C. S. (1960). Circadian rhythms and the circadian organization of living systems. *Cold Spring Harb Symp Quant Biol*, *25*, 159-184.
- Porkka-Heiskanen, T., & Kalinchuk, A. V. (2011). Adenosine, energy metabolism and sleep homeostasis. *Sleep Med Rev*, *15*(2), 123-135. doi:10.1016/j.smrv.2010.06.005
- Preitner, N., Damiola, F., Lopez-Molina, L., Zakany, J., Duboule, D., Albrecht, U., & Schibler, U. (2002). The orphan nuclear receptor REV-ERB α controls circadian transcription within the positive limb of the mammalian circadian oscillator. *Cell*, *110*(2), 251-260.
- Preussner, M., & Heyd, F. (2016). Post-transcriptional control of the mammalian circadian clock: implications for health and disease. *Pflugers Arch*, *468*(6), 983-991. doi:10.1007/s00424-016-1820-y
- Rasch, B., & Born, J. (2013). About sleep's role in memory. *Physiol Rev*, *93*(2), 681-766. doi:10.1152/physrev.00032.2012
- Refinetti, R. (2010). The circadian rhythm of body temperature. *Front Biosci (Landmark Ed)*, *15*, 564-594.
- Reick, M., Garcia, J. A., Dudley, C., & McKnight, S. L. (2001). NPAS2: an analog of clock operative in the mammalian forebrain. *Science*, *293*(5529), 506-509. doi:10.1126/science.1060699
- Reinke, H., Saini, C., Fleury-Olela, F., Dibner, C., Benjamin, I. J., & Schibler, U. (2008). Differential display of DNA-binding proteins reveals heat-shock factor 1 as a circadian transcription factor. *Genes Dev*, *22*(3), 331-345. doi:10.1101/gad.453808
- Reyes, B. A., Pendergast, J. S., & Yamazaki, S. (2008). Mammalian peripheral circadian oscillators are temperature compensated. *J Biol Rhythms*, *23*(1), 95-98. doi:10.1177/0748730407311855

- Rudic, R. D., McNamara, P., Curtis, A. M., Boston, R. C., Panda, S., Hogenesch, J. B., & Fitzgerald, G. A. (2004). BMAL1 and CLOCK, two essential components of the circadian clock, are involved in glucose homeostasis. *PLoS Biol*, 2(11), e377. doi:10.1371/journal.pbio.0020377
- Saini, C., Liani, A., Curie, T., Gos, P., Kreppel, F., Emmenegger, Y., . . . Schibler, U. (2013). Real-time recording of circadian liver gene expression in freely moving mice reveals the phase-setting behavior of hepatocyte clocks. *Genes Dev*, 27(13), 1526-1536. doi:10.1101/gad.221374.113
- Saini, C., Morf, J., Stratmann, M., Gos, P., & Schibler, U. (2012). Simulated body temperature rhythms reveal the phase-shifting behavior and plasticity of mammalian circadian oscillators. *Genes Dev*, 26(6), 567-580. doi:10.1101/gad.183251.111
- Saito, K., Fukuda, N., Matsumoto, T., Iribe, Y., Tsunemi, A., Kazama, T., . . . Hayashi, N. (2010). Moderate low temperature preserves the stemness of neural stem cells and suppresses apoptosis of the cells via activation of the cold-inducible RNA binding protein. *Brain Res*, 1358, 20-29. doi:10.1016/j.brainres.2010.08.048
- Sakaguchi, S., Glotzbach, S. F., & Heller, H. C. (1979). Influence of hypothalamic and ambient temperatures on sleep in kangaroo rats. *Am J Physiol*, 237(1), R80-88.
- Sangoram, A. M., Saez, L., Antoch, M. P., Gekakis, N., Staknis, D., Whiteley, A., . . . Takahashi, J. S. (1998). Mammalian circadian autoregulatory loop: a timeless ortholog and mPer1 interact and negatively regulate CLOCK-BMAL1-induced transcription. *Neuron*, 21(5), 1101-1113.
- Sano, Y., Shiina, T., Naitou, K., Nakamori, H., & Shimizu, Y. (2015). Hibernation-specific alternative splicing of the mRNA encoding cold-inducible RNA-binding protein in the hearts of hamsters. *Biochem Biophys Res Commun*, 462(4), 322-325. doi:10.1016/j.bbrc.2015.04.135
- Sato, T. K., Panda, S., Miraglia, L. J., Reyes, T. M., Rudic, R. D., McNamara, P., . . . Hogenesch, J. B. (2004). A functional genomics strategy reveals Rora as a component of the mammalian circadian clock. *Neuron*, 43(4), 527-537. doi:10.1016/j.neuron.2004.07.018
- Schibler, U. (2014). Presentation at CIG symposium.
- Schmidt, M. H. (2014). The energy allocation function of sleep: a unifying theory of sleep, torpor, and continuous wakefulness. *Neurosci Biobehav Rev*, 47, 122-153. doi:10.1016/j.neubiorev.2014.08.001
- Shao, C., Liu, Y., Ruan, H., Li, Y., Wang, H., Kohl, F., . . . Yan, J. (2010). Shotgun proteomics analysis of hibernating arctic ground squirrels. *Mol Cell Proteomics*, 9(2), 313-326. doi:10.1074/mcp.M900260-MCP200
- Shatz, C. J. (1992). The developing brain. *Sci Am*, 267(3), 60-67.
- Shaw, P. J., Tononi, G., Greenspan, R. J., & Robinson, D. F. (2002). Stress response genes protect against lethal effects of sleep deprivation in *Drosophila*. *Nature*, 417(6886), 287-291. doi:10.1038/417287a
- Sheikh, M. S., Carrier, F., Papathanasiou, M. A., Hollander, M. C., Zhan, Q., Yu, K., & Fornace, A. J., Jr. (1997). Identification of several human homologs of hamster DNA damage-inducible transcripts. Cloning and characterization of a novel UV-inducible cDNA that codes for a putative RNA-binding protein. *J Biol Chem*, 272(42), 26720-26726.
- Shigeyoshi, Y., Taguchi, K., Yamamoto, S., Takekida, S., Yan, L., Tei, H., . . . Okamura, H. (1997). Light-induced resetting of a mammalian circadian clock is associated with rapid induction of the mPer1 transcript. *Cell*, 91(7), 1043-1053.
- Shiromani, P. J., Xu, M., Winston, E. M., Shiromani, S. N., Gerashchenko, D., & Weaver, D. R. (2004). Sleep rhythmicity and homeostasis in mice with targeted disruption of mPeriod genes. *Am J Physiol Regul Integr Comp Physiol*, 287(1), R47-57. doi:10.1152/ajpregu.00138.2004
- Smart, F., Aschrafi, A., Atkins, A., Owens, G. C., Pilotte, J., Cunningham, B. A., & Vanderklish, P. W. (2007). Two isoforms of the cold-inducible mRNA-binding protein RBM3 localize to dendrites

- and promote translation. *J Neurochem*, 101(5), 1367-1379. doi:10.1111/j.1471-4159.2007.04521.x
- Spada, F. L. (2013). On the role of period-2 in the circadian and homeostatic regulation of sleep. *Thesis LNDS*.
- Stephan, F. K., & Zucker, I. (1972). Circadian rhythms in drinking behavior and locomotor activity of rats are eliminated by hypothalamic lesions. *Proc Natl Acad Sci U S A*, 69(6), 1583-1586.
- Sumitomo, Y., Higashitsuji, H., Higashitsuji, H., Liu, Y., Fujita, T., Sakurai, T., . . . Fujita, J. (2012). Identification of a novel enhancer that binds Sp1 and contributes to induction of cold-inducible RNA-binding protein (cirp) expression in mammalian cells. *BMC Biotechnol*, 12, 72. doi:10.1186/1472-6750-12-72
- Sutton, B. C., & Opp, M. R. (2014). Sleep fragmentation exacerbates mechanical hypersensitivity and alters subsequent sleep-wake behavior in a mouse model of musculoskeletal sensitization. *Sleep*, 37(3), 515-524. doi:10.5665/sleep.3488
- Suzuki, A., Sinton, C. M., Greene, R. W., & Yanagisawa, M. (2013). Behavioral and biochemical dissociation of arousal and homeostatic sleep need influenced by prior wakeful experience in mice. *Proc Natl Acad Sci U S A*, 110(25), 10288-10293. doi:10.1073/pnas.1308295110
- Tahara, Y., Kuroda, H., Saito, K., Nakajima, Y., Kubo, Y., Ohnishi, N., . . . Shibata, S. (2012). In vivo monitoring of peripheral circadian clocks in the mouse. *Curr Biol*, 22(11), 1029-1034. doi:10.1016/j.cub.2012.04.009
- Takahashi, J. S. (2017). Transcriptional architecture of the mammalian circadian clock. *Nat Rev Genet*, 18(3), 164-179. doi:10.1038/nrg.2016.150
- Toh, K. L., Jones, C. R., He, Y., Eide, E. J., Hinz, W. A., Virshup, D. M., . . . Fu, Y. H. (2001). An hPer2 phosphorylation site mutation in familial advanced sleep phase syndrome. *Science*, 291(5506), 1040-1043.
- Tononi, G., & Cirelli, C. (2012). Time to be SHY? Some comments on sleep and synaptic homeostasis. *Neural Plast*, 2012, 415250. doi:10.1155/2012/415250
- Trachsel, L., Edgar, D. M., & Heller, H. C. (1991). Are ground squirrels sleep deprived during hibernation? *Am J Physiol*, 260(6 Pt 2), R1123-1129.
- Trachsel, L., Edgar, D. M., Seidel, W. F., Heller, H. C., & Dement, W. C. (1992). Sleep homeostasis in suprachiasmatic nuclei-lesioned rats: effects of sleep deprivation and triazolam administration. *Brain Res*, 589(2), 253-261.
- Turrigiano, G. G. (2008). The self-tuning neuron: synaptic scaling of excitatory synapses. *Cell*, 135(3), 422-435. doi:10.1016/j.cell.2008.10.008
- Ueno, A., Lazaro, R., Wang, P. Y., Higashiyama, R., Machida, K., & Tsukamoto, H. (2012). Mouse intragastric infusion (iG) model. *Nat Protoc*, 7(4), 771-781. doi:10.1038/nprot.2012.014
- Vassalli, A., & Franken, P. (2017). Hypocretin (orexin) is critical in sustaining theta/gamma-rich waking behaviors that drive sleep need. *Proc Natl Acad Sci U S A*, 114(27), E5464-E5473. doi:10.1073/pnas.1700983114
- Vecsey, C. G., Peixoto, L., Choi, J. H., Wimmer, M., Jaganath, D., Hernandez, P. J., . . . Abel, T. (2012). Genomic analysis of sleep deprivation reveals translational regulation in the hippocampus. *Physiol Genomics*, 44(20), 981-991. doi:10.1152/physiolgenomics.00084.2012
- Vinck, M., Batista-Brito, R., Knoblich, U., & Cardin, J. A. (2015). Arousal and locomotion make distinct contributions to cortical activity patterns and visual encoding. *Neuron*, 86(3), 740-754. doi:10.1016/j.neuron.2015.03.028
- Viola, A. U., Archer, S. N., James, L. M., Groeger, J. A., Lo, J. C., Skene, D. J., . . . Dijk, D. J. (2007). PER3 polymorphism predicts sleep structure and waking performance. *Curr Biol*, 17(7), 613-618. doi:10.1016/j.cub.2007.01.073

- Vitaterna, M. H., King, D. P., Chang, A. M., Kornhauser, J. M., Lowrey, P. L., McDonald, J. D., . . . Takahashi, J. S. (1994). Mutagenesis and mapping of a mouse gene, Clock, essential for circadian behavior. *Science*, *264*(5159), 719-725.
- Vyazovskiy, V. V., & Tobler, I. (2005). Theta activity in the waking EEG is a marker of sleep propensity in the rat. *Brain Res*, *1050*(1-2), 64-71. doi:10.1016/j.brainres.2005.05.022
- Wang, G., Zhang, J. N., Guo, J. K., Cai, Y., Sun, H. S., Dong, K., & Wu, C. G. (2016). Neuroprotective effects of cold-inducible RNA-binding protein during mild hypothermia on traumatic brain injury. *Neural Regen Res*, *11*(5), 771-778. doi:10.4103/1673-5374.182704
- Wang, H., Liu, Y., Briesemann, M., & Yan, J. (2010). Computational analysis of gene regulation in animal sleep deprivation. *Physiol Genomics*, *42*(3), 427-436. doi:10.1152/physiolgenomics.00205.2009
- Wang, Z., Gerstein, M., & Snyder, M. (2009). RNA-Seq: a revolutionary tool for transcriptomics. *Nat Rev Genet*, *10*(1), 57-63. doi:10.1038/nrg2484
- Williams, D. R., Epperson, L. E., Li, W., Hughes, M. A., Taylor, R., Rogers, J., . . . Gracey, A. Y. (2005). Seasonally hibernating phenotype assessed through transcript screening. *Physiol Genomics*, *24*(1), 13-22. doi:10.1152/physiolgenomics.00301.2004
- Wisor, J. P., O'Hara, B. F., Terao, A., Selby, C. P., Kilduff, T. S., Sancar, A., . . . Franken, P. (2002). A role for cryptochromes in sleep regulation. *BMC Neurosci*, *3*, 20.
- Wisor, J. P., Pasumarthi, R. K., Gerashchenko, D., Thompson, C. L., Pathak, S., Sancar, A., . . . Kilduff, T. S. (2008). Sleep deprivation effects on circadian clock gene expression in the cerebral cortex parallel electroencephalographic differences among mouse strains. *J Neurosci*, *28*(28), 7193-7201. doi:10.1523/jneurosci.1150-08.2008
- Xie, L., Kang, H., Xu, Q., Chen, M. J., Liao, Y., Thiyagarajan, M., . . . Nedergaard, M. (2013). Sleep drives metabolite clearance from the adult brain. *Science*, *342*(6156), 373-377. doi:10.1126/science.1241224
- Xie, X., Dumas, T., Tang, L., Brennan, T., Reeder, T., Thomas, W., . . . Franken, P. (2005). Lack of the alanine-serine-cysteine transporter 1 causes tremors, seizures, and early postnatal death in mice. *Brain Res*, *1052*(2), 212-221. doi:10.1016/j.brainres.2005.06.039
- Yamaguchi, S., Kobayashi, M., Mitsui, S., Ishida, Y., van der Horst, G. T., Suzuki, M., . . . Okamura, H. (2001). View of a mouse clock gene ticking. *Nature*, *409*(6821), 684. doi:10.1038/35055628
- Yamaguchi, Y., Okada, K., Mizuno, T., Ota, T., Yamada, H., Doi, M., . . . Okamura, H. (2016). Real-Time Recording of Circadian Per1 and Per2 Expression in the Suprachiasmatic Nucleus of Freely Moving Rats. *J Biol Rhythms*, *31*(1), 108-111. doi:10.1177/0748730415621412
- Yan, J., Barnes, B. M., Kohl, F., & Marr, T. G. (2008). Modulation of gene expression in hibernating arctic ground squirrels. *Physiol Genomics*, *32*(2), 170-181. doi:10.1152/physiolgenomics.00075.2007
- Yasenkov, R., & Deboer, T. (2010). Circadian regulation of sleep and the sleep EEG under constant sleep pressure in the rat. *Sleep*, *33*(5), 631-641.
- Yasumoto, Y., Nakao, R., & Oishi, K. (2015). Free access to a running-wheel advances the phase of behavioral and physiological circadian rhythms and peripheral molecular clocks in mice. *PLoS One*, *10*(1), e0116476. doi:10.1371/journal.pone.0116476
- Yoo, S. H., Yamazaki, S., Lowrey, P. L., Shimomura, K., Ko, C. H., Buhr, E. D., . . . Takahashi, J. S. (2004). PERIOD2::LUCIFERASE real-time reporting of circadian dynamics reveals persistent circadian oscillations in mouse peripheral tissues. *Proc Natl Acad Sci U S A*, *101*(15), 5339-5346. doi:10.1073/pnas.0308709101
- Zar, J. H. (1984). *Biostatistical Analysis* Prentice Hall.
- Zhang, R., Lahens, N. F., Ballance, H. I., Hughes, M. E., & Hogenesch, J. B. (2014). A circadian gene expression atlas in mammals: implications for biology and medicine. *Proc Natl Acad Sci U S A*, *111*(45), 16219-16224. doi:10.1073/pnas.1408886111

- Zhao, Z. D., Yang, W. Z., Gao, C., Fu, X., Zhang, W., Zhou, Q., . . . Shen, W. L. (2017). A hypothalamic circuit that controls body temperature. *Proc Natl Acad Sci U S A*, *114*(8), 2042-2047. doi:10.1073/pnas.1616255114
- Zheng, C., Bieri, K. W., Trettel, S. G., & Colgin, L. L. (2015). The relationship between gamma frequency and running speed differs for slow and fast gamma rhythms in freely behaving rats. *Hippocampus*, *25*(8), 924-938. doi:10.1002/hipo.22415
- Zhou, M., Kim, J. K., Eng, G. W., Forger, D. B., & Virshup, D. M. (2015). A Period2 Phosphoswitch Regulates and Temperature Compensates Circadian Period. *Mol Cell*, *60*(1), 77-88. doi:10.1016/j.molcel.2015.08.022
- Zhu, X., Buhner, C., & Wellmann, S. (2016). Cold-inducible proteins CIRP and RBM3, a unique couple with activities far beyond the cold. *Cell Mol Life Sci*, *73*(20), 3839-3859. doi:10.1007/s00018-016-2253-7

'Put quotes in your thesis, because that is what everybody else does'

Paul Franken, 2018